NTNU

Norwegian University of
Science and Technology

Further development of a Network Solver with gas lift optimization

Vemund Flatebakken

Norwegian University of Science and Technology
Department of Geoscience and Petroleum

Abstract

The present Master's Thesis describes a further development of a Network Solver that checks if a certain oil rate is feasible for a given reservoir pressure. Reservoir pressure and surface formation rates (q_o, q_w and q_g) are the inputs to the Solver. These inputs may be generated from software (Eclipse or similar) or tables. In the "main.m" script of the Solver all inputs and properties of the fluids (at surface), the reservoir and the network may be specified by the user.

If the production rate cannot be attained with the given input data, the Solver tries to find a gas lift rate that will make the production feasible. If the maximum gas lift rate is exceeded, the formation rate will be lowered until a feasible solution is found. Economics is not part of this Solver yet, thus instead of comparing oil- and gas prices to find the optimal solution, the Solver assumes that "oil is more valuable than gas". Therefore, once the maximum gas lift rate is exceeded, the gas lift rate will be kept at maximum while the Solver is trying to find the highest formation rate possible.

The Network Solver consists of two main parts: A simulator that, based on mathematical correlations, calculates pressure values in the entire network for the given inputs, and an Optimizer that tries to find the best, feasible formation- and lift rates. Only the Network Simulator is further developed in this master thesis project, the Network Optimizer is unchanged.

Four additions have been made to the Network Solver: A mechanistic approach for pressure drop calculations have been included as an alternative to the Beggs and Brill method, heat transfer calculation and temperature drop have been included in the pipes, a Compositional Model has been included as an alternative to the the black oil model, and a simple reservoir Material Balance Model has been added.

The mechanistic pressure drop calculations are shown to be more accurate than the Beggs and Brill method. The calculated pressure and temperature profiles correspond well with commercial software used in industry. The Compositional Model provides accurate calculations of local fluid properties, but the runtime is slow compared to the black oil model. The Material Balance Model is a simple, but useful addition to the software suite. It has its limitations, but works well together with the Network Solver.

The Network Solver developed may be further improved by including an economical aspect, by improving the runtime of the Compositional Model, and by exchanging the Material Balance Model for a more elaborate material balance program.

Sammendrag

Denne masteroppgave-rapporten beskriver en videreutvikling av en Network Solver som sjekker om det er mulig å produsere en gitt oljerate for et gitt reservoartrykk. Reservoartrykk og overflate- formasjonsrater (q_o, q_w og q_g) er inndata til solveren. Inndata kan genereres fra programvare (Eclipse eller liknende) eller legges inn i tabeller. I "main.m"-scriptet til solveren kan alle inndata, fluid-, reservoar- og nettverksegenskaper spesifiseres av brukeren.

Dersom ønsket produksjonsrate ikke kan oppnås med gitt input, prøver Solveren en gassløft-rate som vil gjøre produksjonen mulig. Dersom maksimal gassløft-rate overstiges, vil formasjonsraten senkes helt til en gyldig løsning finnes. Økonomi er enda ikke inkludert i Solveren, så i stedet for å benytte olje- og gasspriser til å bestemme optimal løsning, antar Solveren at "olje er mer verdifullt enn gass". Derfor, så snart maksimal gassløft-rate overstiges, vil gassløft-raten holdes på et maksimum mens Solveren forsøker å finne høyest gyldig formasjonsrate.

Network Solveren består av to hoveddeler: En Simulator som, basert på matematiske korrelasjoner, beregner trykkverdier i hele nettverket, og en Optimerer som forsøker å finne de beste, gyldige formasjons - og gassløft-ratene. Kun Simulatoren er videreutviklet i dette masterprosjektet, Optimereren er uendret.

Fire nye funksjoner er lagt til i Network Solveren: En mekanistisk metode for trykktapberegninger som et alternativ til Beggs og Brill, beregning av varmetap og fluidtemperatur i rørledningene, en komposisjonsmodell som et alternativ til Black Oil-modellen, og et enkelt materialbalanse-program.

Den mekanistiske metoden gir mer nøyaktige trykktapsberegninger enn Beggs og Brill-metoden. De beregnede trykk- og temperaturprofilene samsvarer godt med kommersiell programvare brukt i industrien. Komposisjonsmodellen beregner nøyaktige verdier for lokale fluidegenskaper, men kjøretiden er relativt høy sammenliknet med kjøretiden til Black Oil-modellen. Materialbalanse-programmet er et enkelt, men nyttig, tillegg til Network Solveren.

Network Solveren kan ytterligere forbedres ved å inkludere økonomiske beregninger, komposisjonsmodellen bør videreutvikles for å bedre kjøretiden, og materialbalanse-programmet kan erstattes med et mer avansert program.

Acknowledgements

The master thesis presented in this report was carried out from January to June 2017 at the Norwegian University of Science and Technology (NTNU). The thesis is a part of the course TPG4920 "Petroleum Engineering, Master's Thesis" at the Department of Geoscience and Petroleum.

I would like to thank my supervisor Milan Stanko, Associate Professor at NTNU, for his support, guidance and feedback during the project.

Contents

1. Introduction and project goals

This report is a documentation of a further development of a standalone Network Solver, consisting of a Simulator and an Optimizer, created for the purpose of investigating the effect of gas lift on oil production.

The input data to the Solver is the user specified oil production rates for a given network, reservoir pressure and the separator pressure. The Solver will try to find the optimal gas lift rate to produce the desired oil production rates. If the gas lift rates exceed a given (user specified) maximum – representing the platform/FPSO gas handling capacity at surface – the formation rates are reduced to yield a feasible solution.

Gas lift is an artificial lift method that lowers the mixture density of the producing formation fluids by injecting pressurized gas (from surface) into the tubing at the bottom of the well. The reduced mixture density will decrease the gravitational pressure drop of the fluid in the network, thus enabling increased formation flowrates for a given reservoir pressure.

Gas lift is advantageous in reservoirs with sand or solid material production, and deviated wells can easily be implemented with gas lift. In saturated oil reservoirs, or in reservoirs with pressure close to the bubble point, gas may flow through the bottom of the well, making for instance an ESP (Electrical Submersible Pump) an inferior alternative compared to gas lift. Gas lift has its shortcomings as well: Adequate gas supply needs to be provided throughout the life of the field, and gas lift may in many cases be inefficient [19]. The Network Solver may be used as a tool to indicate whether gas lift should be implemented or not, and compared to other artificial lift methods such as EMPs.

The Network Optimizer finds consistent optimal solutions, and does not need to be changed. The previous version of the Network Simulator, however, was only intended to return an approximate pressure profile in the network. The calculations were not validated, and the code was not compared to industry standard commercial software. Specific concerns were that the fluid temperature in the network was assumed constant, and that the Beggs and Brill pressure drop method was not precise.

Thus, the main goals of the master thesis project are:

1. To include a mechanistic pressure drop method as an alternative to Beggs and Brill.

2. To include calculation of fluid temperature in the network.

3. To measure the accuracy and performance of the Beggs and Brill method with and without temperature calculations, and of the mechanistic approach with and without temperature calculations, and to compare this with industry standard commercial software.

Additional tasks performed in this thesis are:

3. To include a Compositional Model to the Network Solver. This feature is added as an alternative to the Black Oil model that already exists in the Network Solver. The user is offered the flexibility of choosing between specifying the production stream by composition or by black oil properties.

4. To include a Material Balance Model to the Network Solver. This feature is added to enable the user to perform long term production studies. The model is very simplistic, and mostly offers an example of how more elaborate material balance simulators may be incorporated with the Network Simulator.

The report is structured in the following way:

- Chapter 2: Presents the background and a description of the previous Network Solver.

- Chapter 3: Presents the four additions to the Network Solver, and the underlying theory.

- Chapter 4: Presents the evaluations of the four additions.

- Chapter 5: Presents the recommendations for further work.

- Chapter 6: Presents the conclusions.

2. Background: Description of previous Network Solver

The current project is based on an already existing Network Solver, and this chapter gives a basic understanding of how it works. For more details about the software, discussions on optimality and instabilities, the original report should be viewed [27].

The Network Solver checks if a certain oil production rate is feasible for a given reservoir pressure. Reservoir pressure and surface formation rates (q_o, q_w and q_g) are the inputs to the Solver. These inputs may be generated from software (Eclipse or similar) or tables. In the "main.m" script of the Solver all inputs and properties of the fluids (at surface), the reservoir and the network may be specified by the user.

If the production rate cannot be attained with the given input data, the Solver tries to find a gas lift rate that will make the production feasible. If the maximum gas lift rate is exceeded, the formation rate will be lowered until a feasible solution is found. Economics is not part of this solver yet, thus instead of comparing oil- and gas prices to find the optimal solution, the Solver assumes that "oil is more valuable than gas". Therefore, once the maximum gas lift rate is exceeded, the gas lift rate will be kept at maximum while the Solver tries to find the highest formation rate possible.

The Network Solver consists of two main parts: A Simulator that, based on mathematical correlations, calculates pressure values in the entire network for the given inputs, and an Optimizer that tries to find the best formation- and lift rates that yields a feasible solution by the Simulator. In this project, only the Simulator has been changed, the Optimizer is unchanged.

The remainder of this chapter is structured in the following way:

- 2.1: Description of the Network Simulator.

- 2.2: Description of the Network Optimizer.

2.1. Network Simulator

2.1.1. Initialization

The pressure calculations start with two known pressures: The downstream separator pressure is constant and specified by the user, and the upstream flowing bottomhole pressure is calculated using the composite Vogel Equation for multiphase flow (Neely, A.B. 1967 [3]):

$$q_{o,\,max} = J \cdot \left(\bar{p}_R - p_b + \frac{p_b}{1.8} \right) \tag{2.1}$$

$$q_o = J \cdot \left(\bar{p}_R - p_{wf} \right) \qquad\qquad\qquad ,p_{wf} \geq p_b \tag{2.2}$$

$$q_o = \left(q_{o,\,max} - q_b \right) \left[1 - 0.2 \frac{p_{wf}}{p_b} - 0.8 \left(\frac{p_{wf}}{p_b} \right)^2 \right] \qquad ,p_{wf} \leq p_b \tag{2.3}$$

Where:

- q_o is the oil production rate (input) [Sm^3/D].

- $\bar{p}_R$ is the (average) reservoir pressure (input) [Bar].

- J is the productivity index (constant and specified by the user) [$Sm^3/D/Bar$].

- $q_{o,\,max}$ is the maximum oil production rate for the given reservoir conditions.

- p_b is the bubble pressure (Correlation in Appendix A) [Bar].

- q_b is the oil production rate from Eq. (2.2) with $p_{wf} = p_b$ [Sm^3/D].

- p_{wf} is the resulting flowing bottomhole pressure [Bar].

Pressures in the pipes are calculated sequentially, with a fixed interval separating the pressure nodes, using the Euler method:

$$p(L + \Delta L) = p(L) + \frac{\delta}{\delta L} p(L) \cdot \Delta L \tag{2.4}$$

Where:

- ΔL is the fixed step length [m].

- p(L) is the pressure at node L in the pipe [Bar].

- The pressure gradient $\frac{\delta}{\delta L} p(L)$ is, in the original version of the software, calculated using the Beggs & Brill method (Appendix B).

The pressure values in the tubing are calculated co-current from the flowing bottomhole pressure to the (upstream) wellhead pressure, and the pressure values in the riser and pipeline are calculated counter-current from the separator pressure to the PLEM (Pipeline End

Manifold) and further, in the flowline, to the manifold/(downstream) wellhead pressure. At the wellhead the choke pressure is measured:

$$\Delta p_{choke} = p_{wh, \, upstream} - p_{wh, \, downstream} \qquad (2.5)$$

This is the resulting output sent to the Optimizer. If the choking pressure is initially positive, the suggested production rate is feasible and the program may be terminated. If the choking pressure is negative, the solver needs to find gas lift rates or reduced production rates that drive the choking pressure to zero.

2.1.2. Fluid property - and pressure drop calculations

At each pressure point/node in the pipes, local (in situ) fluid rates, densities and viscosities are calculated. This is performed with the function "local_properties.m" in the solver. The inputs to the function are surface formation rates (q_o, q_w and q_g), surface gas lift rate (q_{gl}), local pressure and local temperature. For simplicity, the temperature was kept constant and equal to the reservoir temperature in the initial software. This is not always a very good assumption when gas flows in the pipes, and is a topic addressed in this project.

A number of different correlations are used in calculating the local properties. Because these calculations are more a "means to reach an end" and not the main focus of this project, the correlations are described in Appendix A, and not in this subsection.

The pressure values in the pipe are calculated from the known p_{sep} and p_{wf} using the Euler method (2.4). The pressure gradient is calculated using the Beggs & Brill correlation with inputs given by the outputs of "local_properties.m". The pressure gradient calculation is implemented by the "dpBeggs_Brill.m" function. For the same reasons as for the local property calculations, this correlation is described in Appendix B. In this master project, a mechanistic approach has been implemented as an alternative to the Beggs & Brill method.
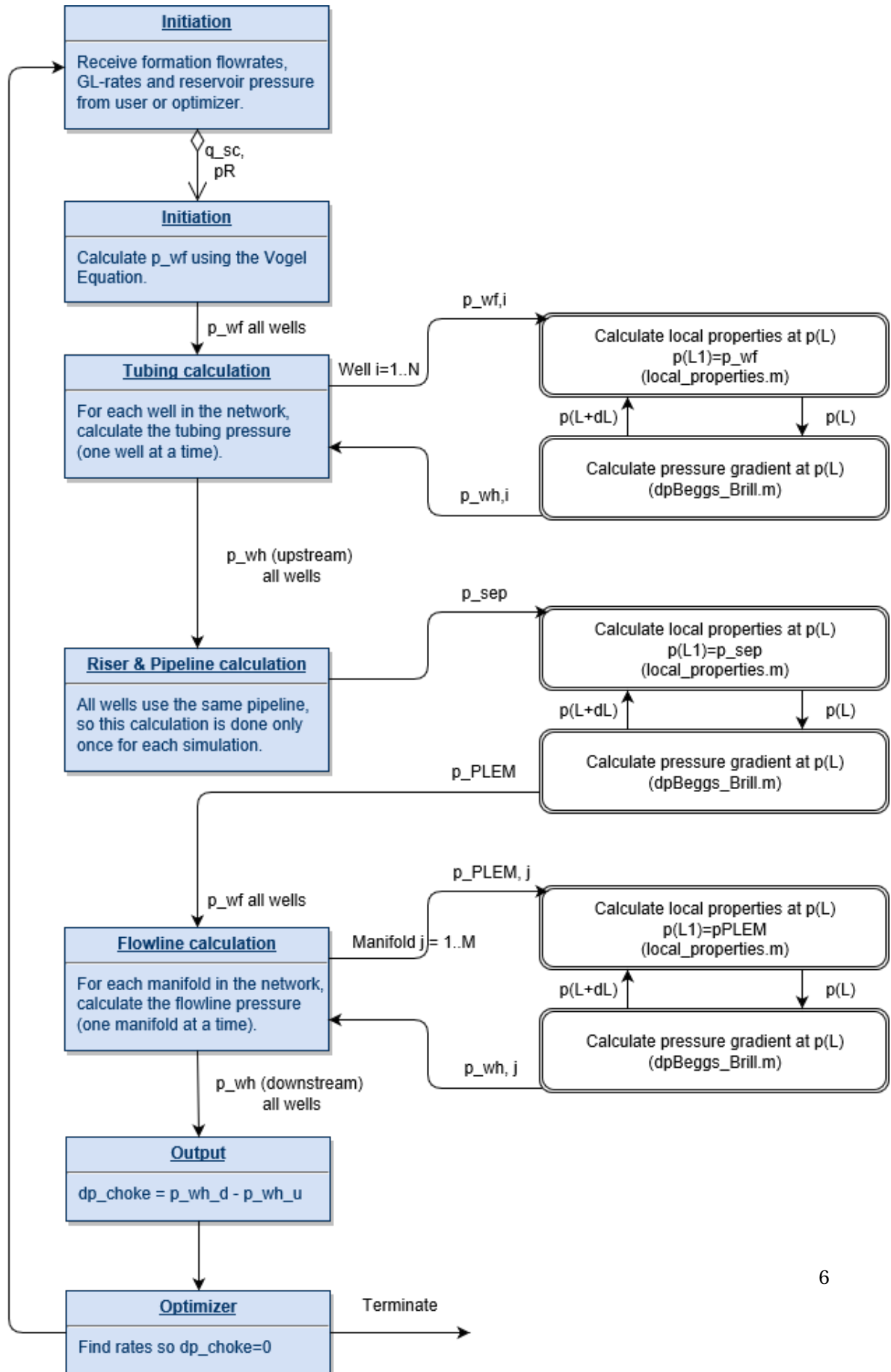
Initiation

Receive formation flowrates, GL-rates and reservoir pressure from user or optimizer.

q_sc, pR

Initiation

Calculate p_wf using the Vogel Equation.

p_wf all wells

Tubing calculation

For each well in the network, calculate the tubing pressure (one well at a time).

p_wf,i

Well $i=1..N$

Calculate local properties at $p(L)$
$p(L1)=p\_wf$
(local_properties.m)

$p(L+dL)$ $p(L)$

Calculate pressure gradient at $p(L)$
(dpBeggs_Brill.m)

p_wh,i

p_wh (upstream) all wells

Riser & Pipeline calculation

All wells use the same pipeline, so this calculation is done only once for each simulation.

p_sep

Calculate local properties at $p(L)$
$p(L1)=p\_sep$
(local_properties.m)

$p(L+dL)$ $p(L)$

Calculate pressure gradient at $p(L)$
(dpBeggs_Brill.m)

p_PLEM

p_wf all wells

Flowline calculation

For each manifold in the network, calculate the flowline pressure (one manifold at a time).

p_PLEM, j

Manifold $j = 1..M$

Calculate local properties at $p(L)$
$p(L1)=pPLEM$
(local_properties.m)

$p(L+dL)$ $p(L)$

Calculate pressure gradient at $p(L)$
(dpBeggs_Brill.m)

p_wh, j

p_wh (downstream) all wells

Output

$dp\_choke = p\_wh\_d - p\_wh\_u$

Optimizer

Find rates so $dp\_choke=0$

Terminate

6

Figure 2.1: Simulator Flow Chart

2.2. Network Optimizer

If the reservoir pressure is too low to provide the desired formation rates, gas has to be injected or the rates have to be lowered. Figure 2.2 and 2.3 illustrate the concept for one well (first well in "Network-model 1", section 4.2.1) under "Standard Testing Conditions" (STC, see Appendix F) using the Simulator. The objective is to find gas lift rates or formation (oil) rates that result in $\Delta p_{\text{choke}} = 0$.[1] One evident challenge is to search for gas lift rates that are not too high, and oil rates that are not too low. If these rates are suggested by the Optimizer it may either diverge or it may find a sub-optimal solution.
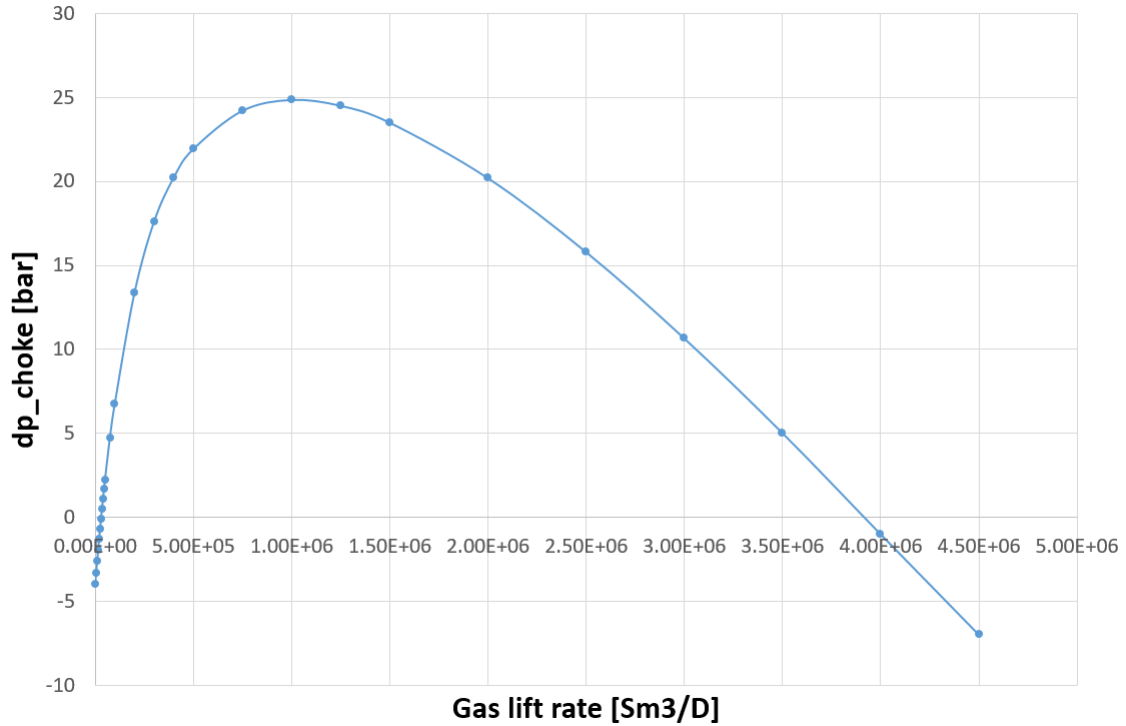
Figure 2.2: One well (STC) with $q_o = 2300$ Sm^3/D

---

[1]Throughout this report the ending criteria is written as "=0". In the actual code the error margin is 0.1 bar.
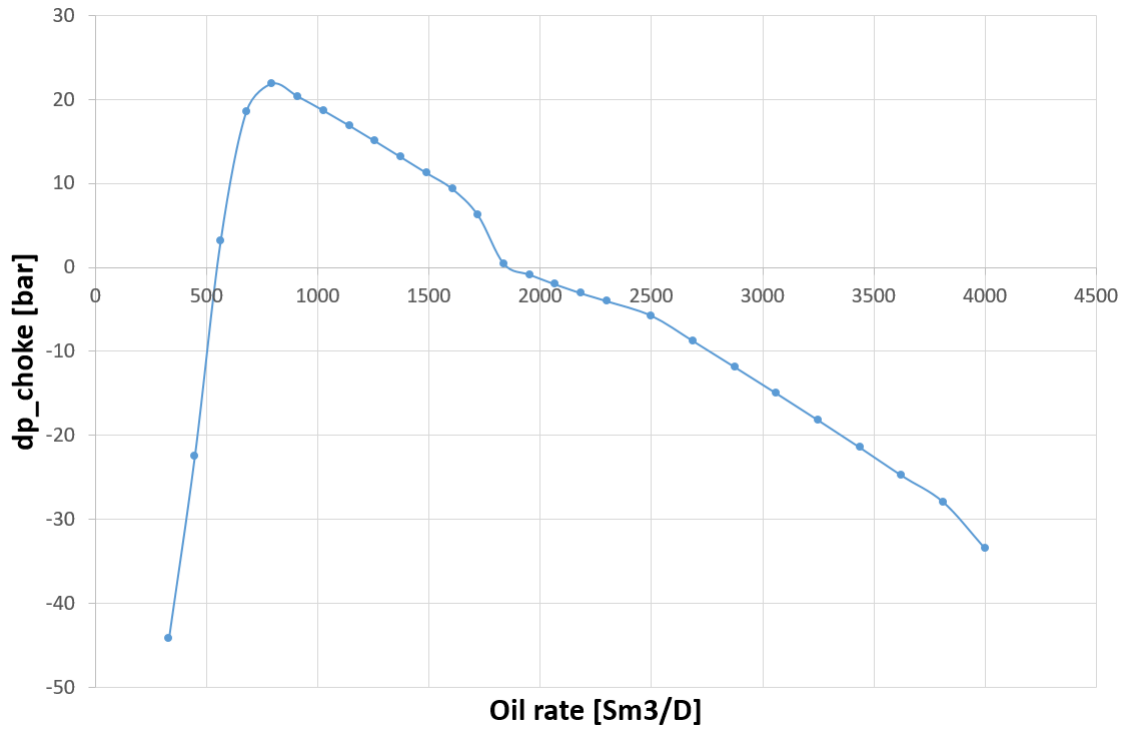
Figure 2.3: One well (STC) with $q_{gl} = 0$ Sm^3/D

Two different approaches have been taken to create a numeric scheme that generates feasible flowrates in the network: A sequential approach (Appendix D, "GL_sequential_NR.m") that changes the rates, one well at a time, keeping the rest of the network unchanged, and a parallel approach (Appendix E "GL_parallel_NR.m") that changes the rates in all wells simultaneously. Both approaches use the Newton-Raphson method to solve the system (Appendix C). The desired approach to be used is selectable in the "main.m"-file.

3. Methodology

This chapter describes the details and the underlying theory of the four additions made to the Network Solver in the current project. The chapter is structured in the following way:

- 3.1: The Mechanistic pressure drop method.

- 3.2: The Temperature calculations.

- 3.3: The Compositional Model.

- 3.4: The Material Balance Model.

3.1. Mechanistic approach: Pressure drop calculations

An alternative to the Beggs and Brill pressure drop calculation has been implemented. The mechanistic approach works in the same way as the Beggs and Brill method, using the Euler method to calculate pressure in the nodes along the pipeline co-current from the bottom of the well to the wellhead, and counter-current from the separator to the wellhead, as described in section 2.1. However, different formulas to determine the flow pattern and to calculate the liquid holdup and pressure drop are used. The mechanistic approach has already been programmed in Excel VBA by Shmueli (2010, [22]), and the method will not be discussed in this report. A major part of this thesis project involves converting formulas into the correct Matlab format.

3.2. Temperature calculations

In the Network Simulator the fluid temperature was previously kept constant and equal to the reservoir temperature. Local densities, flowrates and viscosities of both oil and, especially gas, depend upon the temperature. Thus, for the Simulator to accurately calculate pressure decline in the pipeline, a good temperature model is needed.

As with the pressures, the temperatures in the pipes are calculated sequentially, with a fixed length separating the nodes. The pressure calculations are temperature dependent, and the temperature calculations are pressure dependent.

In the tubing, pressure in a node is calculated using the temperature of the previous node. For small steps along the pipeline, this is a valid approach. The temperature of the node is then obtained using the calculated pressure of the same node.

Above the sea bed, however, pressure in the nodes are calculated counter-current, while temperature in the nodes must be calculated co-current. This is solved by first calculating pressure in the pipeline assuming a constant temperature, equal to the reservoir temperature. The temperature along the pipeline is then calculated co-current with the calculated pressure values, and finally the pressure values are re-calculated using the updated temperature profile.

Ideally this procedure should be repeated at least once more to check for convergence. This is computational expensive, however, and even though the pressure calculations depend on the temperature, and vice versa, the dependency is not very significant. This topic is further discussed in sec. 4.3. Thus, the temperature is not re-calculated after the pressure profile is updated.

Shoham (2006, [23]) has the following approach for calculating fluid temperature at node "i+1", given information at node "i":

$$
\begin{aligned}
T_{\mathrm{f,\,i+1}} = {} & T_{\mathrm{amb,\,i}} - g_e \cdot \Delta L \cdot \sin\theta + \left(T_{\mathrm{f,\,i}} - T_{\mathrm{amb,\,i}}\right) \cdot e^{-\frac{\Delta L}{A_i}} \\
& + \left[g_e \cdot A_i \cdot \sin\theta + \left(\frac{\Delta p}{\Delta L}\right)_i \cdot \left(\frac{\phi \cdot A}{C_p \cdot \rho_m}\right)_i \right] \cdot \left(1 - e^{-\frac{\Delta L}{A_i}}\right)
\end{aligned}
\tag{3.1}
$$

Where:

- T_{amb} is the ambient/surrounding temperature. In the tubing this is the rock formation temperature. T_{amb} equals T_R at the bottom of the well and T_{sea} at wellhead, both temperatures are specified by the user. In the riser and pipeline T_{amb} equals the sea temperature.

- g_e is the geothermal gradient at the given depth. In this model it's assumed constant. The thermal gradient in the sea is very small. As a standard it is set equal to zero, but this may be specified by the user.

- ΔL is the step length between nodes [m].

- θ is the pipe inclination.

- ϕ is a dimensionless parameter.

- "A" is the relaxation distance [m].

- ρ_m is the fluid mixture (slip) density generated from the pressure drop calculations.

- C_p is the fluid mixture specific heat capacity, calculated in "localproperties.m" $[\frac{J}{Kg\,K}]$.

The dimensionless parameter is calculated using:

$$\phi = \frac{\rho_m \cdot \eta \cdot C_p \cdot \left(\frac{\Delta P}{\Delta L}\right) - \rho_m \cdot g \cdot \sin\theta - \rho_m \cdot v \cdot \left(\frac{\Delta v}{\Delta L}\right)}{\left(\frac{\Delta P}{\Delta L}\right)} \qquad (3.2)$$

Where:

- "v" is the fluid velocity [m/s].

- η is the Joule Thomson coefficient $[\frac{m^3\,K}{J}]$

The Joule Thomson coefficient is calculated using:

$$\eta = -\frac{1}{C_p \cdot \rho_{ns}} \cdot \left\{ (1 - \lambda_l) \cdot \left[-\frac{T}{z} \cdot \left(\frac{\delta z}{\delta T}\right)_p \right] + \lambda_l \right\} \qquad (3.3)$$

Where:

- λ_l is the liquid holdup.

- ρ_{ns} is the no-slip fluid density.

- Z is the gas z-factor (See Appendix A).

Depending on the location in the pipeline, the relaxation distance and the overall heat transfer coefficient (HTC) may be calculated differently. The pipeline, from wellhead to surface, is surrounded by water, and is usually insulated. The tubing however, is surrounded by rock formations, casing and cement, and is usually not insulated.

3.2.1. Tubing in the formation

The relaxation distance is calculated using (in field units):

$$A = \frac{C_p \cdot W}{2 \cdot \pi} \cdot \left[\frac{k_e + (r_{ti} \cdot U_{ti} \cdot T_D)}{r_{ti} \cdot U_{ti} \; k_e} \right] \tag{3.4}$$

Where:

- W is the fluid mass flow [lbs/s].

- k_e is the earth formation conductivity $\left[\frac{\text{Btu}}{\text{hr ft °F}} \right]$

- r_{ti} is the tubing inner radius [ft].

- U_{ti} is the overall heat transfer coefficient with respect to r_{ti} $\left[\frac{\text{Btu}}{\text{hr ft}^2 \text{ °F}} \right]$.

- "A" is here given in [ft], C_p in $\left[\frac{\text{Btu}}{\text{lbm °F}} \right]$

The dimensionless temperature is calculated using:

$$
\begin{aligned}
T_D &= 1.1281 \cdot \sqrt{t_D} \cdot \left(1 - 0.3 \cdot \sqrt{t_D} \right) && , 10^{-10} \leq t_D \leq 1.5 \\
T_D &= (0.4063 + 0.5 \cdot \ln t_D) \cdot \left(1 + \frac{0.6}{t_D} \right) && , t_D > 1.5
\end{aligned}
\tag{3.5}
$$

The dimensionless time is calculated using:

$$t_D = \frac{\alpha \cdot t_{\text{prod}}}{r_{\text{wb}}^2} \tag{3.6}$$

Where:

- α is the Thermal diffusivity of earth [ft^2/hr].

- t_{prod} Is the production time [hr].

- r_{wb} is the wellbore radius [ft].

The overall HTC may be calculated using a simplified formula proposed by Sagar, Doty and Schmidt (1991, [24]):

$$\frac{1}{U_{ti}} = r_{ti} \cdot \left[\frac{\ln \left(r_{ci}/r_{to} \right)}{k_{\text{ann}}} + \frac{\ln \left(r_{\text{wb}}/r_{co} \right)}{k_{\text{cem}}} \right] \tag{3.7}$$

Where:

- r_{ci} is the inner casing radius [ft].

- r_{co} is the outer casing radius [ft].

- r_{to} is the outer tubing radius [ft].

- k_{ann} is the equivalent annular conductivity $\left[\frac{Btu}{hr\,ft\,°F}\right]$.

- k_{cem} is the cement conductivity $\left[\frac{Btu}{hr\,ft\,°F}\right]$.

The model neglects convection inside the tubing and conduction in all metallic pipe layers. The natural convection in the annulus is assumed to behave like conduction in a solid.

An iterative procedure proposed by Hasan and Kabir (1994, [25]) may also be used to determine the HTC:

$$\frac{1}{U_{ti}} = r_{ti} \cdot \left[\frac{1}{r_{ti} \cdot h_f} + \frac{\ln(r_{to}/r_{ti})}{k_t} + \frac{1}{r_{to} \cdot h_c} + \frac{\ln(r_{co}/r_{ci})}{k_{cas}} + \frac{\ln(r_{wb}/r_{co})}{k_{cem}} \right] \tag{3.8}$$

Where:

- h_f is the tubing fluid convective heat transfer coefficient $\left[\frac{Btu}{hr\,ft^2\,°F}\right]$.

- k_t is the tubing conductivity $\left[\frac{Btu}{hr\,ft\,°F}\right]$.

- h_c is the annulus fluid convective heat transfer coefficient $\left[\frac{Btu}{hr\,ft^2\,°F}\right]$.

$$h_c = \frac{0.049 \cdot (N_{pr} \cdot N_{gr})^{1/3} \cdot N_{pr}^{0.074} \cdot k_{ann}}{r_{to} \cdot \ln(r_{ci}/r_{to})} \tag{3.9}$$

Where the Prandtl Number for annulus is calculated by:

$$N_{pr} = \frac{C_{p,\,ann} \cdot \mu_{ann}}{k_{ann}} \tag{3.10}$$

And the Grashof number for free convection heat transfer in the annulus is calculated by:

$$N_{gr} = \frac{(r_{ci} - r_{to})^3 \cdot g \cdot \rho_{ann}^2 \cdot \beta \cdot (T_{to} - T_{ci})}{\mu_{ann}^2} \tag{3.11}$$

Where:

- ρ_{ann} is the density of the annular fluid $\left[\frac{lbm}{ft^3}\right]$.

- μ_{ann} is the viscosity of the annular fluid [cp].

- β is the inverse of the annulus temperature [°R^{-1}].

- T_{to} is assumed to equal the tubing fluid temperature T_f [°F].

- T_{ci} is the casing inner temperature [°F].

T_{ci} is calculated using:

$$T_{wb} = \frac{T_f \cdot T_D + \frac{k_e \cdot T_{amb}}{r_{ti} \cdot U_{ti}}}{T_D + \frac{k_e}{r_{ti} \cdot U_{ti}}} \tag{3.12}$$

$$T_{ci} = T_{wb} + \frac{(T_{to} - T_{wb}) \cdot r_{ti} \cdot U_{ti} \cdot \ln(r_{wb}/r_{co})}{k_{cem}} \tag{3.13}$$

As stated, $T_{to} = T_f$ is assumed. The iterative process is initiated using T_f from the previous node and an assumed U_{ti}. Eq. 3.12 and 3.13 is first calculated to generate U_{ti} from eq. 3.8 and T_f from eq. 3.11. The new T_f and U_{ti} is then input into Eq. 3.12 and 3.13. The system runs until convergence.

The two different approaches for determining the HTC are discussed in section 4.4.

3.2.2. Pipeline in water

The relaxation distance is calculated using a simplified model, with respect to outer radius:

$$A = \frac{C_p \cdot W}{2 \cdot \pi \cdot r_{ins} \cdot U_{ins}} \tag{3.14}$$

Where the overall HTC is calculated using:

$$\frac{1}{U_{ins}} = r_{ins} \left[\frac{1}{r_i \cdot h_f} + \frac{\cdot \ln(r_o/r_i)}{k_{pipe}} + \frac{\ln(r_{ins}/r_o)}{k_{ins}} + \frac{1}{h_{sea}} \right] \tag{3.15}$$

Where:

- r_{ins} is the pipeline outer radius including insulation [m].

- r_o is the pipeline outer radius excluding insulation [m].

- r_i is the pipeline inner radius [m].

- k_{pipe} equals the steel conductivity, k_{steel} $\left[\frac{W}{m\,K}\right]$.

- k_{ins} is the insulating material conductivity $\left[\frac{W}{m\,K}\right]$.

- h_{sea} is the sea convective heat transfer coefficient $\left[\frac{W}{m^2\,K}\right]$.

3.3. Compositional Model

A Compositional Model has been added to the Network Solver. The original basic compositional calculator, programmed by Nilsen, M.(2015, [26]) using theory from Whitson, Brulé (2000, [28]), inputs pressure, temperature and hydrocarbon fluid composition, together with component specific properties, and returns molar vapor fraction, gas density and oil density of the mixture at the given pressure and temperature. This code is already developed, and will not be further discussed in this report.

Some additions has been made to the model for it to work with the Network Simulator. The code is supposed to replace 'local_properties.m', thus phase viscosities, flowrate, heat capacity and surface tension must also be calculated. Further changes must be made to include gas lift.

When initiating the Network Solver, the user specifies the desired surface oil rate and the maximum surface gas lift rate. Because the molar amount of oil in the pipeline is a function of temperature and pressure, it is necessary to specify the target rate as a total molar rate, including the gas phase, as this will be constant. The Compositional Model is then initially run at surface conditions to calculate the total molar rate:

$$\dot{m}_{o, sc} = q_{o, sc} \cdot \rho_{o, sc} \tag{3.16}$$

$$\dot{n}_{o, sc} = \frac{\dot{m}_{o, sc}}{M_{o, sc}} \tag{3.17}$$

$$\dot{n}_{tot} = \frac{\dot{n}_{o, sc}}{1 - F_v} \tag{3.18}$$

Where:

- $\rho_{o, sc}$ is the oil density at surface [kg/m3].

- $\dot{m}_{o, sc}$ is the mass oil flow at surface [kg/s].

- $\dot{n}_{o, sc}$ is the molar oil flow at surface [kmol/s].

- M_o is the molar weight of the liquid at surface.

- F_v is the Vapor Fraction at surface.

- $\dot{n}_{tot}$ is the total molar flow rate [kmol/s].

The vapor fraction, molar oil weight and oil density is already generated by the Compositional Model. The liquid and gas compositions (x and y) are also determined. Component specific data such as critical properties, boiling points and composition are read from a data sheet. Pseudo-properties are all determined using Kay's mixing rule, here given with the example of boiling temperatures used to calculate the specific heat capacities (See Eq. A.40 and A.41 in Appendix A):

$$T_{\text{b, o}} = \sum_{i=1}^{N} x_i \cdot T_{\text{b, i}} \tag{3.19}$$

$$T_{\text{b, g}} = \sum_{i=1}^{N} y_i \cdot T_{\text{b, i}} \tag{3.20}$$

Where:

- x_i is the molar fraction of component "i" in liquid phase.

- y_i is the molar fraction of component "i" in vapor phase.

- $T_{\text{b, i}}$ is the boiling temperature of component "i".

- $T_{\text{b, o}}$ is the equivalent, or "pseudo", boiling point of the liquid composition.

- $T_{\text{g, o}}$ is the equivalent, or "pseudo", boiling point of the vapor composition.

The Network Solver assumes the surface gas is used for gas lift. Thus the gas molar composition at surface (y_{sc}) is stored as a value. In the same way as for the oil, the molar rate of the maximum surface gas lift may be calculated using:

$$\dot{m}_{\text{gl max, sc}} = q_{\text{gl max, sc}} \cdot \rho_{\text{gl max, sc}} \tag{3.21}$$

$$\dot{n}_{\text{gl max}} = \frac{\dot{m}_{\text{gl max, sc}}}{M_{\text{g, sc}}} \tag{3.22}$$

$$\tag{3.23}$$

At each node in the pipeline temperature, pressure, water cut, total molar flow of reservoir fluid (oil and gas), molar flow of gas lift and surface gas composition are input to the compositional calculator. If the well is gas lifted, the composition needs to be updated:

$$z_{\text{new}} = \frac{z_{\text{old}} \cdot \dot{n}_{\text{tot}} + y_{\text{sc}} \cdot \dot{n}_{\text{gl}}}{\dot{n}_{\text{gl}} + \dot{n}_{\text{tot}}} \tag{3.24}$$

Hydrocarbon densities are then calculated with the original code, using pressure, temperature and the new specified composition.

3.3.1. Local rates

The local liquid and gas rate is calculated using:

$$\dot{m}_{\text{o, g}} = \dot{n}_{\text{tot}} \cdot M_{o,g} \tag{3.25}$$

$$q_{\text{o, g}} = \frac{\dot{m}_{\text{o, g}}}{\rho_{\text{o, g}}} \tag{3.26}$$

$$q_w = \left(\frac{\text{WC} \cdot q_o}{1 - \text{WC}}\right)_{\text{sc}} \cdot \frac{\rho_{\text{w, sc}}}{\rho_{\text{w, local}}} \tag{3.27}$$

$$q_l = q_o + q_w \tag{3.28}$$

3.3.2. Local viscosities

The local liquid and gas viscosity is calculated using the LBC procedure (Lohrenz et Al. 1964, [31]):

$$\left[\left(\mu_{\text{o, g}} - \mu_{\text{o, g}}^0\right) \cdot \xi_{\text{T o, g}} + 10^{-4}\right]^{\frac{1}{4}} = a_0 + a_1 \cdot \rho_{\text{pr o, g}} + a_2 \cdot \rho_{\text{pr o, g}}^2 + a_3 \cdot \rho_{\text{pr o, g}}^3 + a_4 \cdot \rho_{\text{pr o, g}}^4 \tag{3.29}$$

Where:

- $\mu_{\text{o, g}}$ is the effective oil/gas viscosity [cp]

- $\rho_{\text{pr o, g}}$ is the pseudoreduced density of oil/gas.

- $a_0 = 0.1023$

- $a_1 = 0.023364$

- $a_2 = 0.058533$

- $a_3 = -0.040758$

- $a_4 = 0.0093324$

$$\rho_{\text{pr o, g}} = \frac{\rho_{\text{o, g}}}{M_{\text{o, g}}} \cdot v_{\text{pc o, g}} \tag{3.30}$$

$$\xi_{\text{T o, g}} = \left(\frac{T_{\text{pc o, g}}}{M_{\text{o, g}}^3 \cdot p_{\text{pc o, g}}^4}\right)^{\frac{1}{6}} \tag{3.31}$$

$$\mu_{\text{o, g}}^0 = \frac{\sum_{i=1}^{n} z_{\text{i o, g}} \cdot \mu_i \cdot \sqrt{M_i}}{\sum_{i=1}^{n} z_{\text{i o, g}} \cdot \sqrt{M_i}} \tag{3.32}$$

$$\begin{aligned} \mu_i \cdot \xi_{\text{Ti}} &= 34 \cdot 10^{-5} \cdot T_{\text{ri}}^{0.94} && , T_{\text{ri}} > 1.5 \\ \mu_i \cdot \xi_{\text{Ti}} &= 17.78 \cdot 10^{-5} \cdot (4.58 \cdot T_{\text{ri}} - 1.67)^{\frac{5}{8}} && , T_{\text{ri}} \le 1.5 \end{aligned} \tag{3.33}$$

Since the LBC method is developed with focus on oil, the accuracy for gas viscosity is not perfect. A second method, correlated by Lee et al. (1964, [32]), is used as an alternative for gases:

$$
\begin{aligned}
A_1 &= \frac{\left(9.379 + 0.01607 \cdot M_g\right) \cdot T^{1.5}}{209.2 + 19.26 \cdot M_g + T} \\
A_2 &= 3.448 + \frac{986.4}{T} + 0.01009 \cdot M_g \\
A_3 &= 2.447 - 0.2224 \cdot A_2 \\
\mu_g &= A_1 \cdot e^{A_2 \cdot \left(\rho_g^{A_3}\right)} \cdot 10^{-4}
\end{aligned}
\tag{3.34}
$$

Where:

- Temperature is given in [Rankine].

- ρ_g is the local vapor density in [g/cm^3].

- M$_g$ is the molar weight of the vapor phase [kg/kmole].

3.3.3. Interfacial tension

The Interfacial tension (in [Dyne/cm]) is calculated using a correlation from Weinaug and Katz (1943, [20]):

$$
\sigma^{\frac{1}{4}} = \sum_{i=1}^{N} P_i \cdot \left(x_i \cdot \frac{\rho_o}{M_o} - y_i \cdot \frac{\rho_g}{M_g} \right)
\tag{3.35}
$$

Where the Parachor is determined using:

$$
P_i = 25.2 + 2.86 \cdot M_i
\tag{3.36}
$$

For heavy compounds, c7+, Saltman and Katz (1939, [21]) gives the following correlation:

$$
P_i = 35 + 2.4 \cdot M_i
\tag{3.37}
$$

3.3.4. Specific heat capacities

The oil and gas specific heat capacity is calculated using the same procedure as in "local_properties.m" (Eq. A.40 and A.41 in Appendix A), using liquid and gas boiling points:

$$
T_{\text{b, o}} = \sum_{i=1}^{N} x_i \cdot T_{\text{b, i}}
\tag{3.38}
$$

$$
T_{\text{b, g}} = \sum_{i=1}^{N} y_i \cdot T_{\text{b, i}}
\tag{3.39}
$$

3.4. Material Balance Model

The development of a full material balance simulator is outside the scope of this project, but a simple Material Balance Model has been implemented to show the potential. A more thorough material balance simulator may be included at a later stage.

The program receives production rates from the Network Simulator and reservoir pressure and reservoir temperature from the previous production period. The material balance equation may be described by net withdrawal (withdrawal - injection) = expansion of the hydrocarbon fluids in the system + cumulative water influx. The resulting equation is (Fekete.com, [16]):

$$
\begin{aligned}
&= N_p \cdot \left[B_{o2} + B_{g2} \cdot \left(R_p - R_{s2}\right)\right] + W_p \cdot B_{w2} - W_{\text{inj}} \cdot B_{\text{w, inj}} - G_{\text{inj}} \cdot B_{\text{g, inj}} \\
&= \text{IOIP} \cdot \left\{ \left[B_{o2} - B_{o1} + B_{g2}\left(R_{s1} - R_{s2}\right)\right] + \frac{\text{IGIP}}{\text{IOIP}} \cdot \left(B_{g2} - B_{g1}\right) + B_{o1} \cdot \left(1 + \frac{\text{IGIP} \cdot B_{g1}}{\text{IOIP} \cdot B_{o1}}\right) \cdot \left(\frac{c_f + c_w \cdot S_w}{1 - S_w}\right) \cdot \Delta P \right\} \\
&+ W_e \cdot B_{w2}
\end{aligned}
$$

(3.40)

All the reservoir fluid volumes (IGIP, IOIP, IWIP), the water and formation compressibility (c_w and c_f) and the production period are specified by the user. Production values are input from the Network Simulator. The unknown values are ΔP and all the formation volume factors (B_o, B_g and B_w) and the solution GOR (R_s) at times 1 and 2. The reservoir temperature, oil and gas gravities and reservoir composition are assumed constant over time (See Appendix A for the specific equations used to calculate the properties). All the unknown values are thus only pressure dependent. p_{R1}, the previous reservoir pressure, is known. If the LHS of Eq. 3.41 is transferred to the RHS, this expression should equal zero. It is also only dependent upon p_{R2}, so that:

$$
\begin{aligned}
f(p_{R2}) =& -\left\{ N_p \cdot \left[B_{o2} + B_{g2} \cdot \left(R_p - R_{s2}\right)\right] + W_p \cdot B_{w2} - W_{\text{inj}} \cdot B_{\text{w, inj}} - G_{\text{inj}} \cdot B_{\text{g, inj}} \right\} \\
&+ \text{IOIP} \cdot \left\{ \left[B_{o2} - B_{o1} + B_{g2}\left(R_{s1} - R_{s2}\right)\right] + \frac{\text{IGIP}}{\text{IOIP}} \cdot \left(B_{g2} - B_{g1}\right) + B_{o1} \cdot \left(1 + \frac{\text{IGIP} \cdot B_{g1}}{\text{IOIP} \cdot B_{o1}}\right) \cdot \left(\frac{c_f + c_w \cdot S_w}{1 - S_w}\right) \cdot \Delta P \right\} \\
&+ W_e \cdot B_{w2} = 0
\end{aligned}
$$

(3.41)

This expression may then be solved with a simple Newton Raphson scheeme, as shown in Appendix C. The resulting reservoir pressure is the output from the Material Balance Model, and the input for the next Network Solver iteration.

4. Results and Discussion: Network Solver evaluation

This chapter contains an evaluation of the Network Solver functionality and performance with special emphasis on the new features.

With the addition of the mechanistic approach and the temperature calculations, there exists four different configurations of the Network Simulator:

- Beggs and Brill, assuming constant $T = T_R$. Referred to as "BB-ConsT".

- Beggs and Brill, assuming T calculated as in sec. 3.2. Referred to as "BB-VarT".

- Mechanistic approach, assuming constant $T = T_R$. Referred to as "Me-ConsT".

- Mechanistic approach, assuming T calculated as in sec. 3.2. Referred to as "Me-VarT".

The structure of the evaluation is as follows:

- 4.1: Accuracy of the configurations.

- 4.2: Performance and runtime of the configurations.

- 4.3: The convergence of the pressure and temperature profiles.

- 4.4: The effect of difference in overall HTC.

- 4.5: The Compositional Model.

- 4.6: The Material Balance Model.

4.1. Accuracy of the configurations

To quantify the accuracy of the different pressure and temperature calculations, a comparison with Pipesim, a commercial network simulator from Schlumberger, has been made. Pipesim is considered as the reference simulator, using "OLGAS 200 version 7.3.1 flow correlations, Feb. 2014".

The configurations are compared to each other and to Pipesim by performing different simulation cases varying water cut, GOR and liquid surface rate. This section is structured accordingly:

- 4.1.1: Simulation cases varying the water cut and GOR.

- 4.1.2: Simulation cases varying the surface liquid rate.

sec. 4.1.1 and 4.1.2 will indicate that Me-VarT is the most precise Simulator configuration. Thus only Me-VarT is further evaluated:

- 4.1.3: Comparison between Me-VarT and Pipesim.

All the calculations are performed co-current, assuming initial pressure at 150 bar and initial temperature at 100°C. Only one well is used. Tubing length and height is 2000 m, pipeline hight is 300 m, total pipeline length is 2020 m, riser length and height is 500 m. The rest of the conditions are as given in STC (Appendix F).

Pipesim is run with properties as described in STC (Appendix F). The overall HTC in Pipesim is set to $0.8 \left[\frac{\text{Btu}}{\text{hr ft}^2 \, °\text{F}} \right]$ in the pipeline, so as to correspond with the values calculated in sec. 4.4 (See Fig. 4.47). In the tubing, Pipesim calculates the HTC using its own heat transfer correlations.

4.1.1. Varying GOR and WC

Setup:
In this subsection all simulation cases are performed with a liquid surface flowrate of 500 Sm3/D. Three WC values are given: 0, 0.25 and 0.5. Three GOR values are given: 100, 250 and 500 Sm3/Sm3. In total 9 combinations. Pressure profiles along with corresponding temperature profiles are graphed in the following pages.

Evaluation:
Observations from the graphs are as follows:

- All of the calculated pressure profiles are close in correspondence.

- Calculating (lowering) the temperature in the pipeline increases pressure loss. This is evident from the pressure profiles of BB-VarT and Me-VarT consistently being lower than the pressure profiles of BB-ConT and Me-ConT respectively. Changing temperature alters the local viscosities and gas properties. The combination of changes may for instance increase the fluid velocity, increasing the frictional pressure drop.

- The increased pressure drop from temperature calculations is not very high, and the choice of pressure drop method has a larger impact on the pressure profile. This is evident from the difference in pressure profile between Me-VarT/Me-ConsT and BB-VarT/BB-ConsT consistently being less than the difference between Me-VarT/BB-VarT and Me-ConsT/BB-ConsT.

- The calculated temperature profiles correspond well with Pipesim. The minor differences do not have a large effect on the pressure calculations (see the point above).

- The Beggs and Brill method tends to calculate a larger pressure drop than both Pipesim and the mechanistic approach. This may be due to the acceleration term in the calculation being assumed negligible, and thus not calculated in the program (See Appendix B). Also, programming errors in the previous version or the nature of the Beggs and Brill method may cause overestimation of the pressure drop.

- Me-VarT corresponds fairly well with Pipesim.
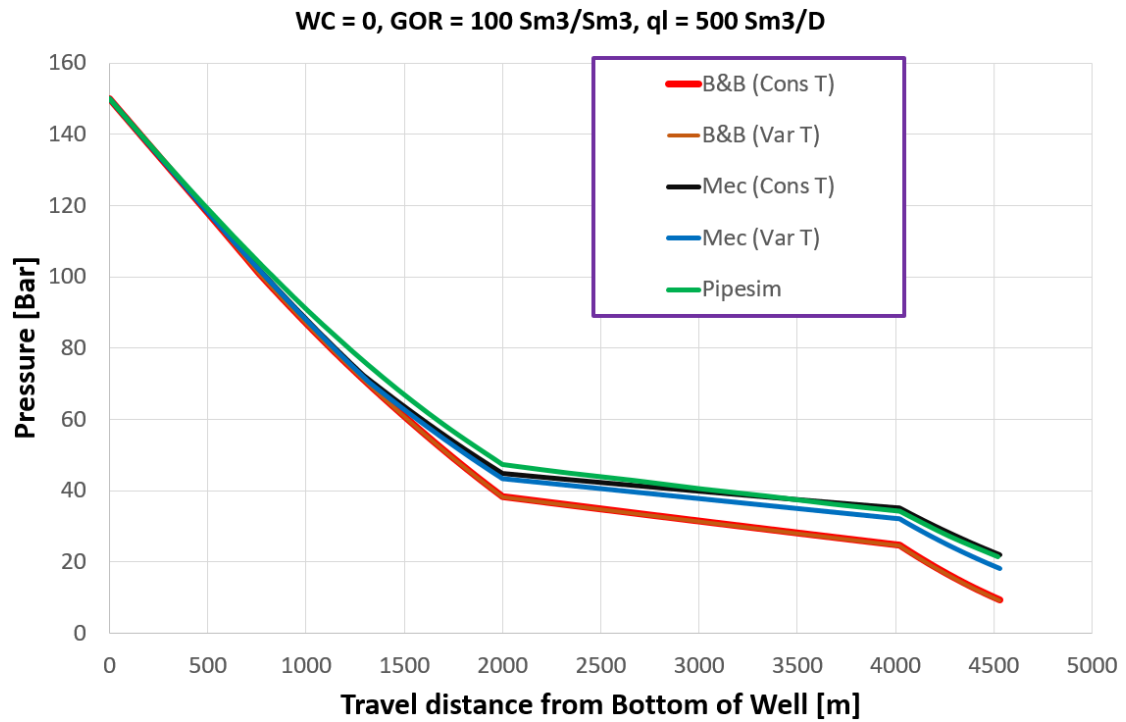
Figure 4.1: Pressure profile along the pipeline.
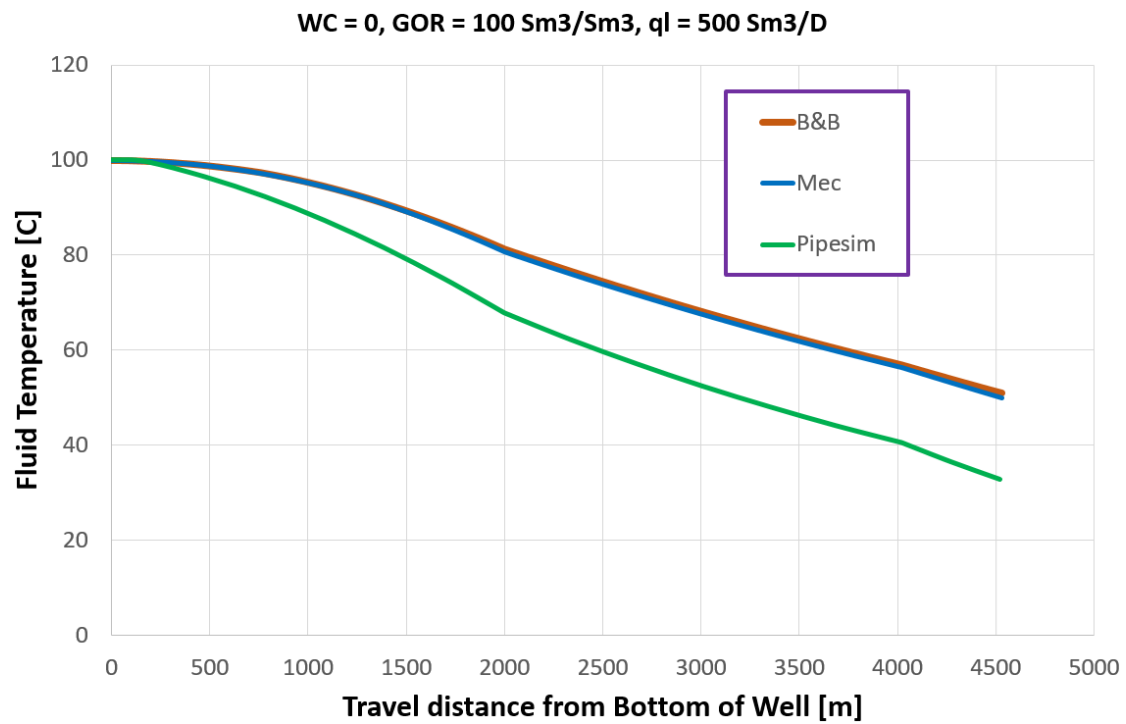
Figure 4.2: Temperature profile along the pipeline.
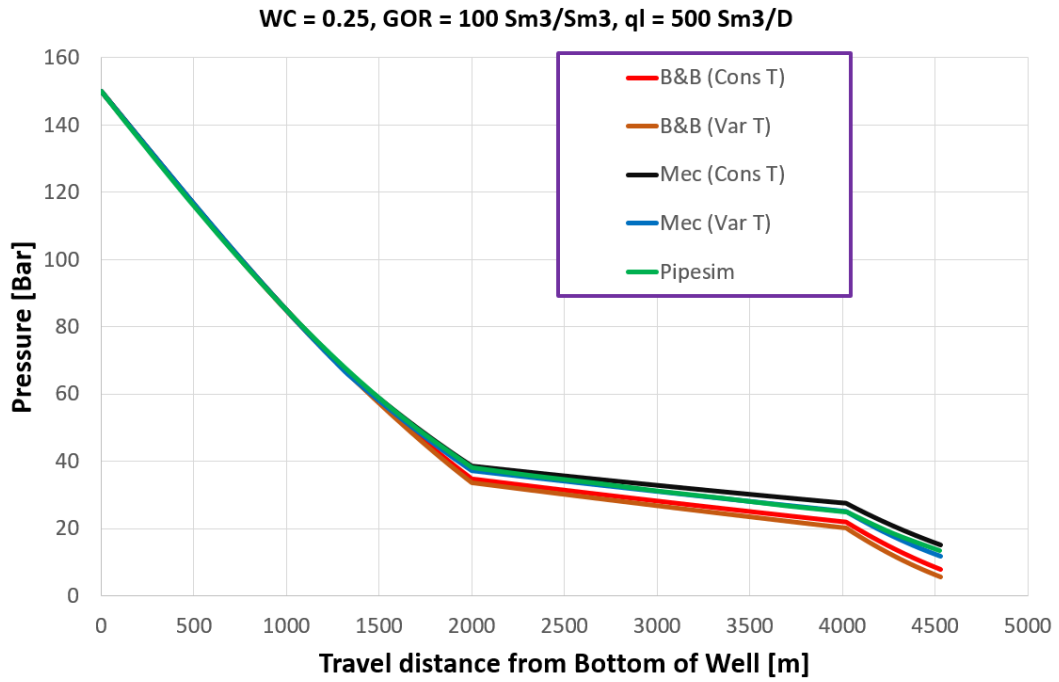
Figure 4.3: Pressure profile along the pipeline.
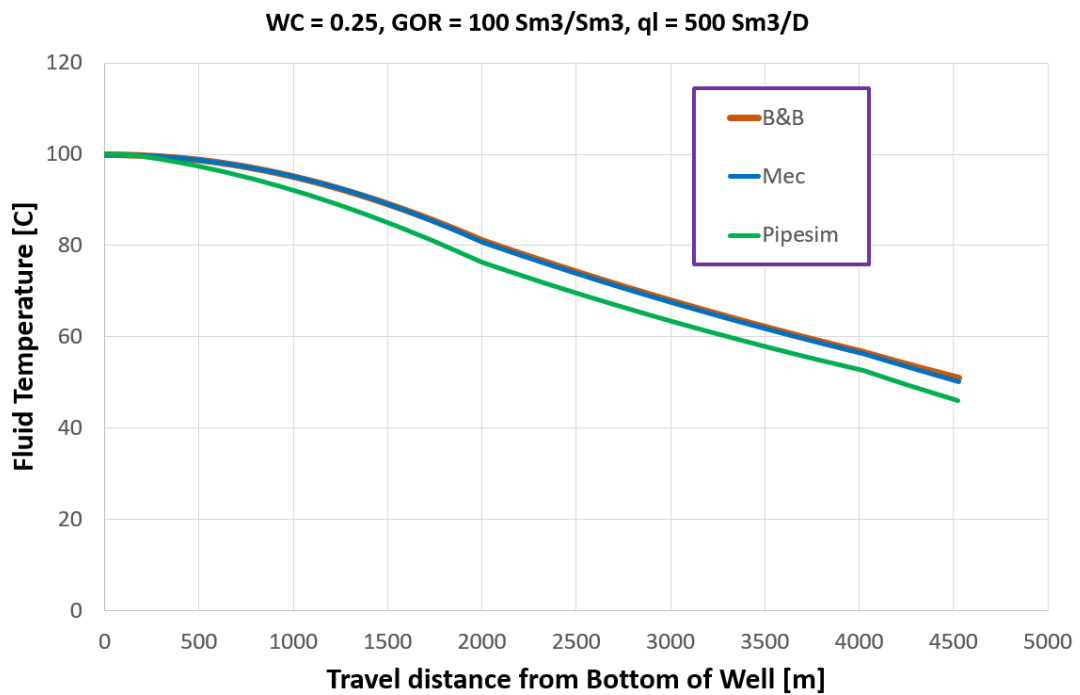
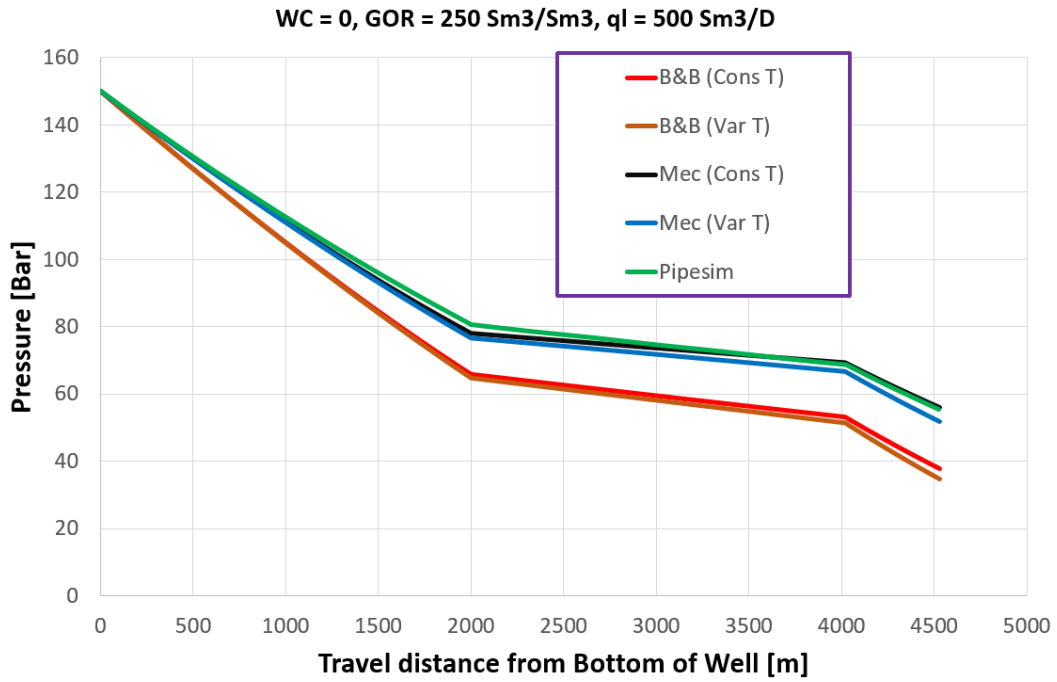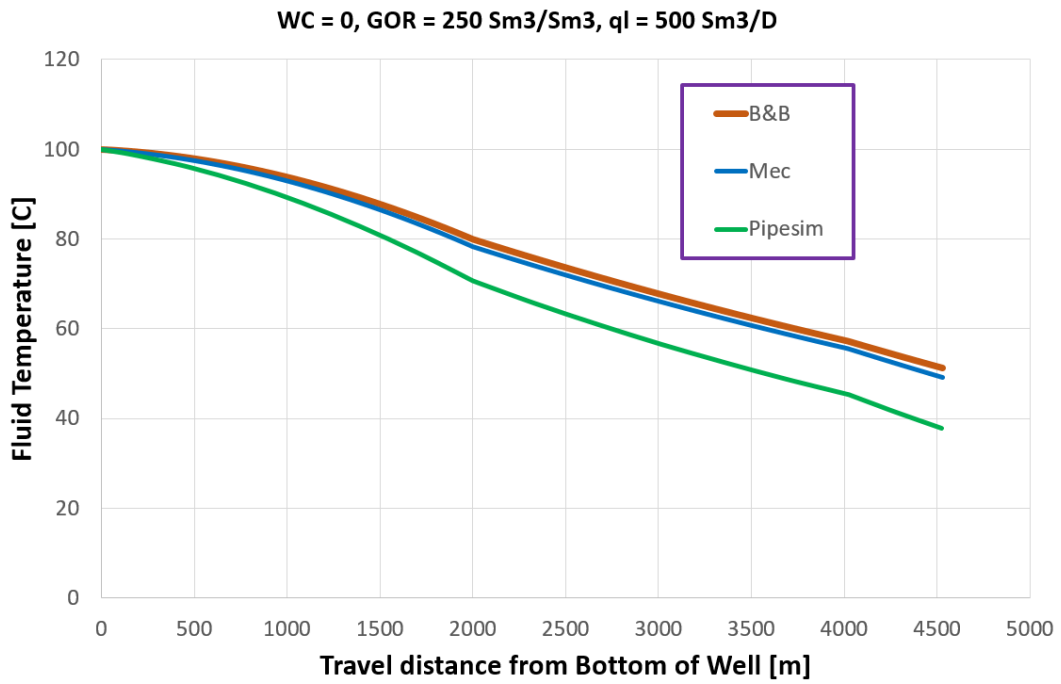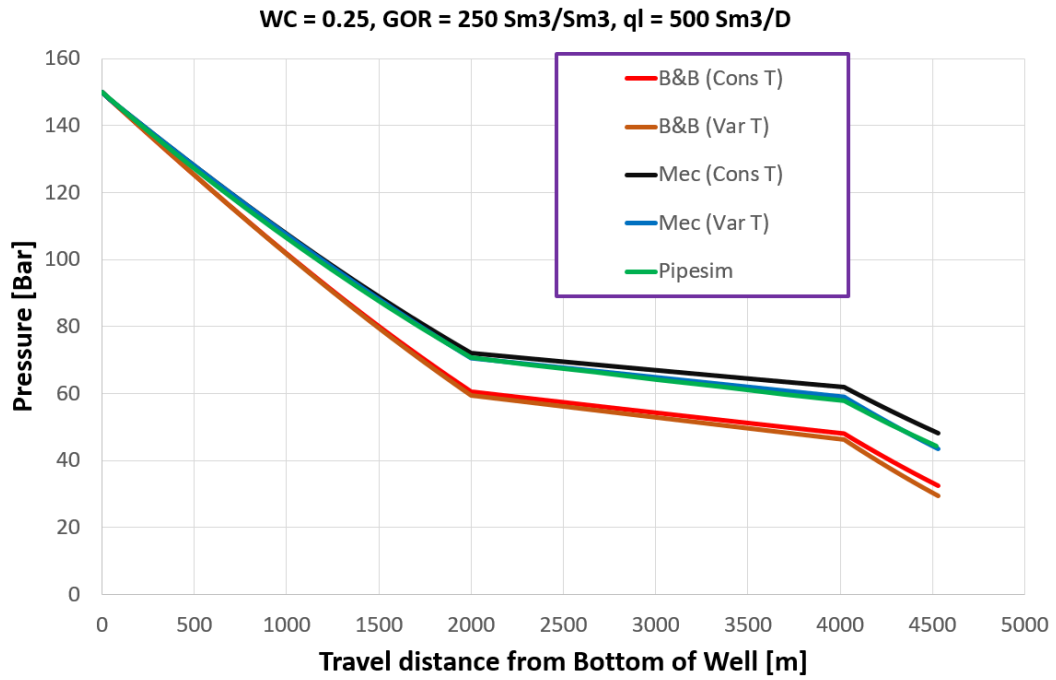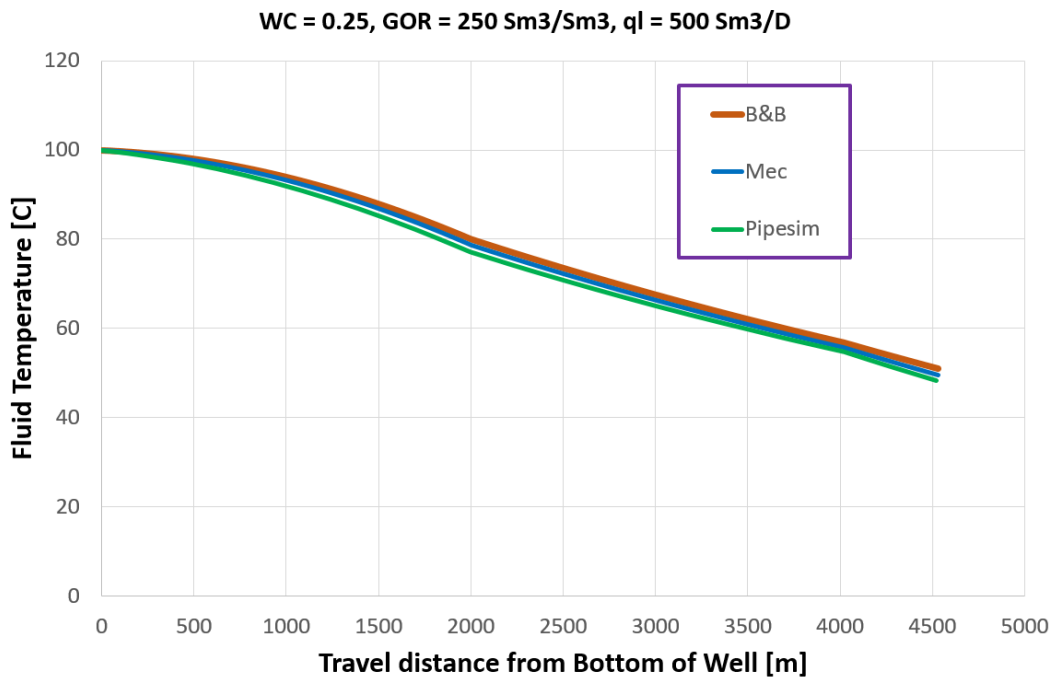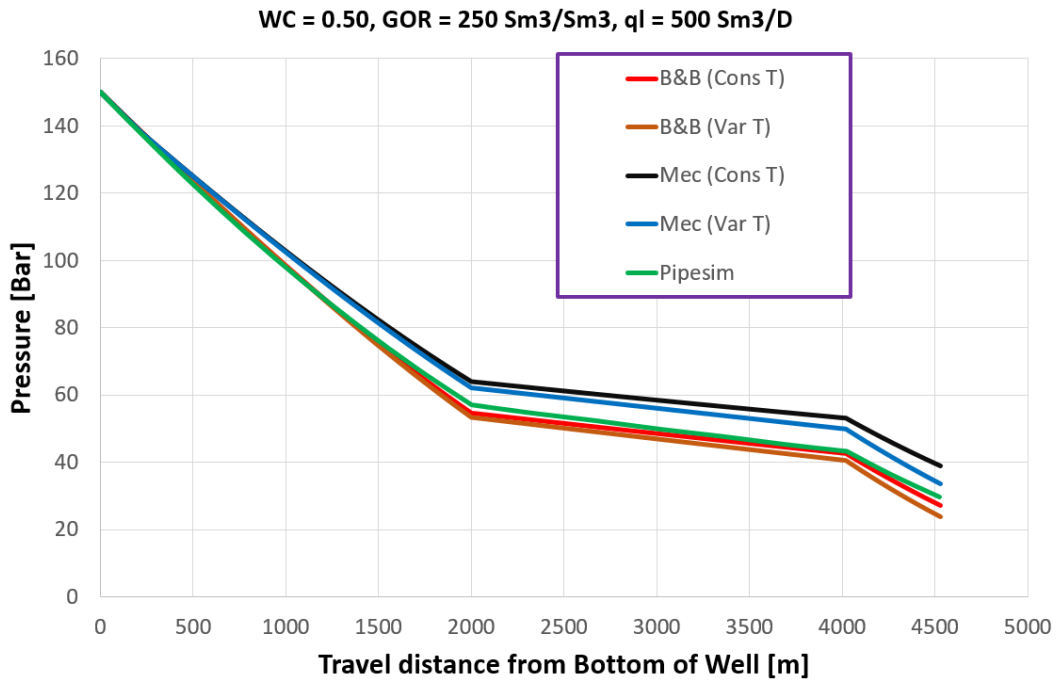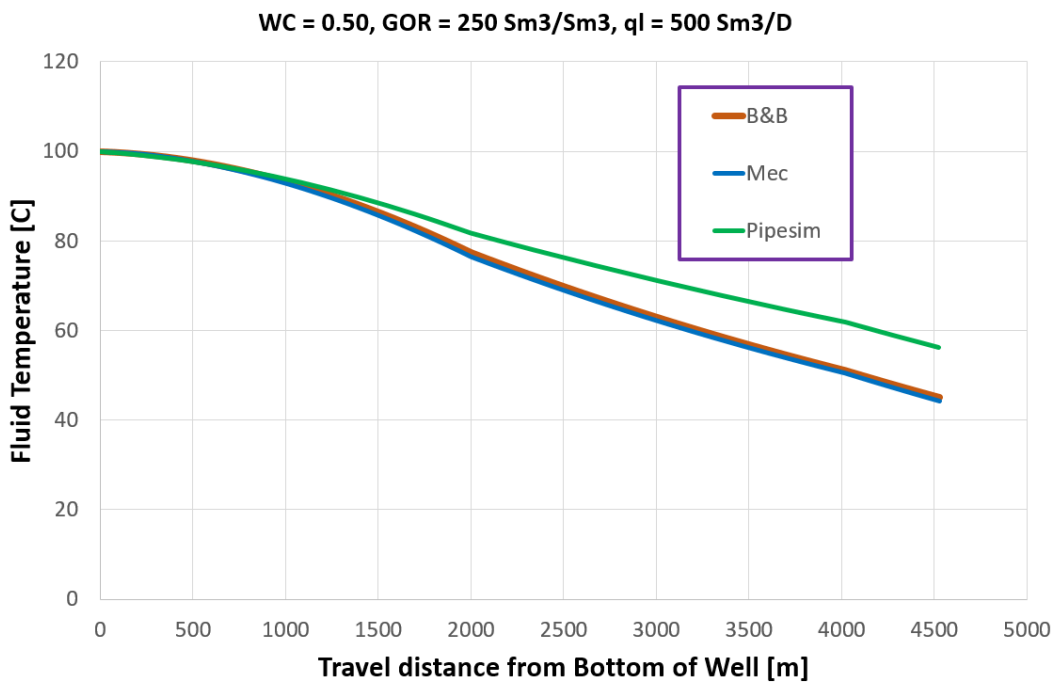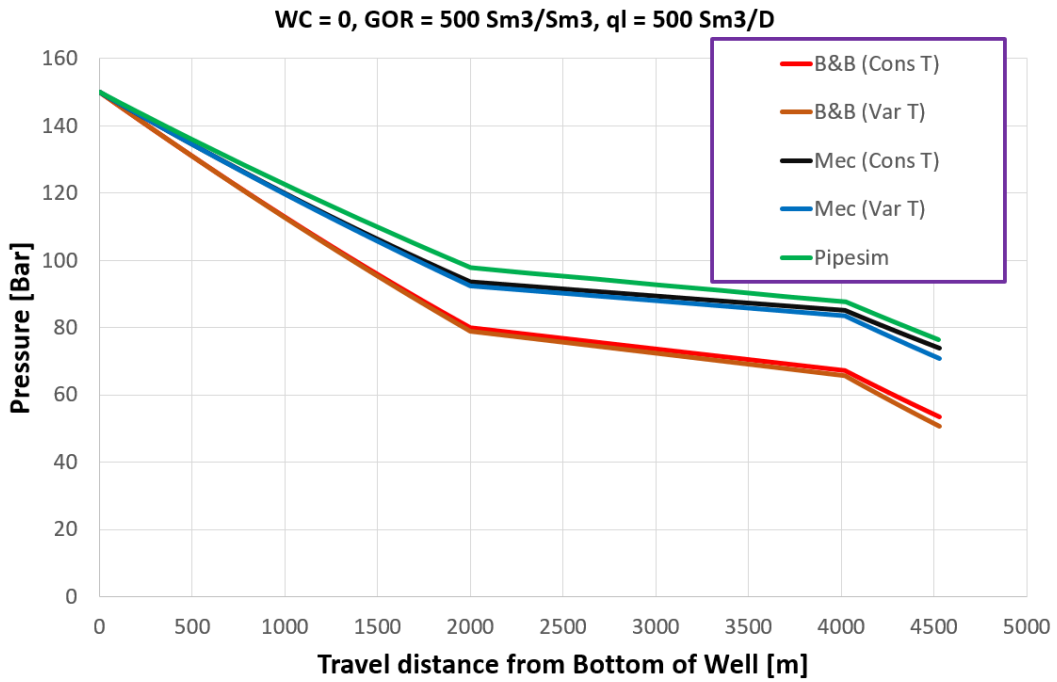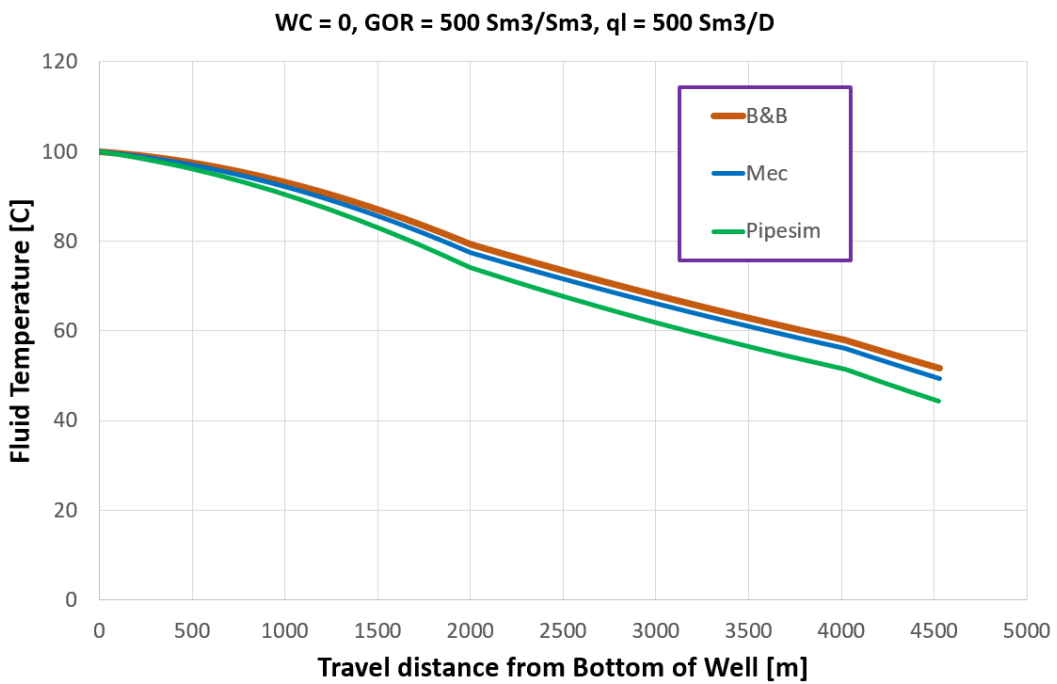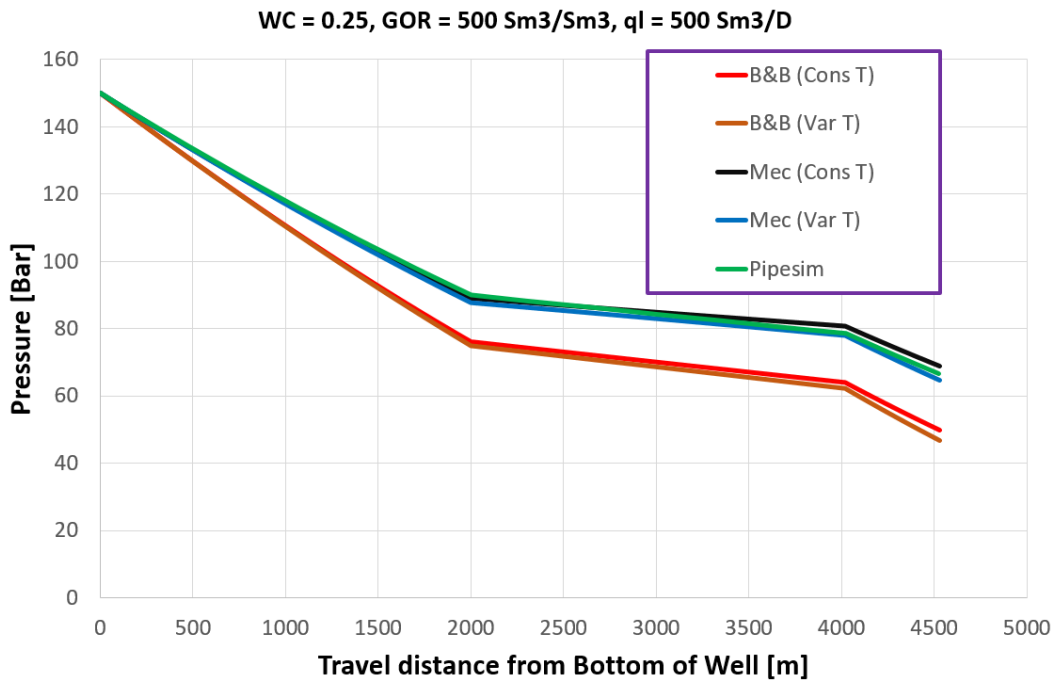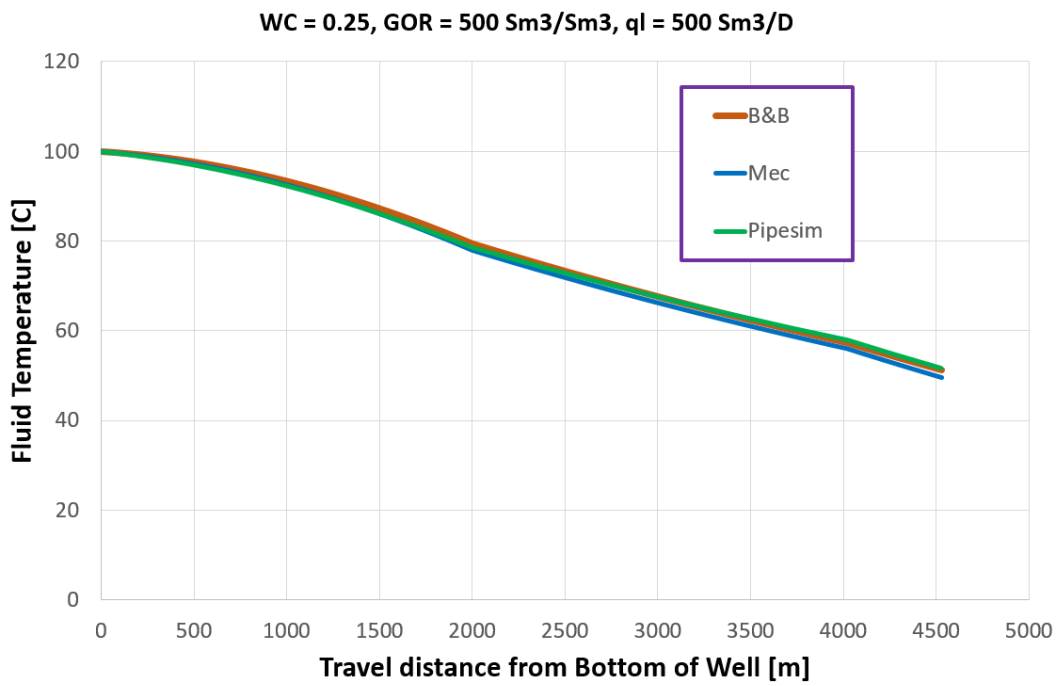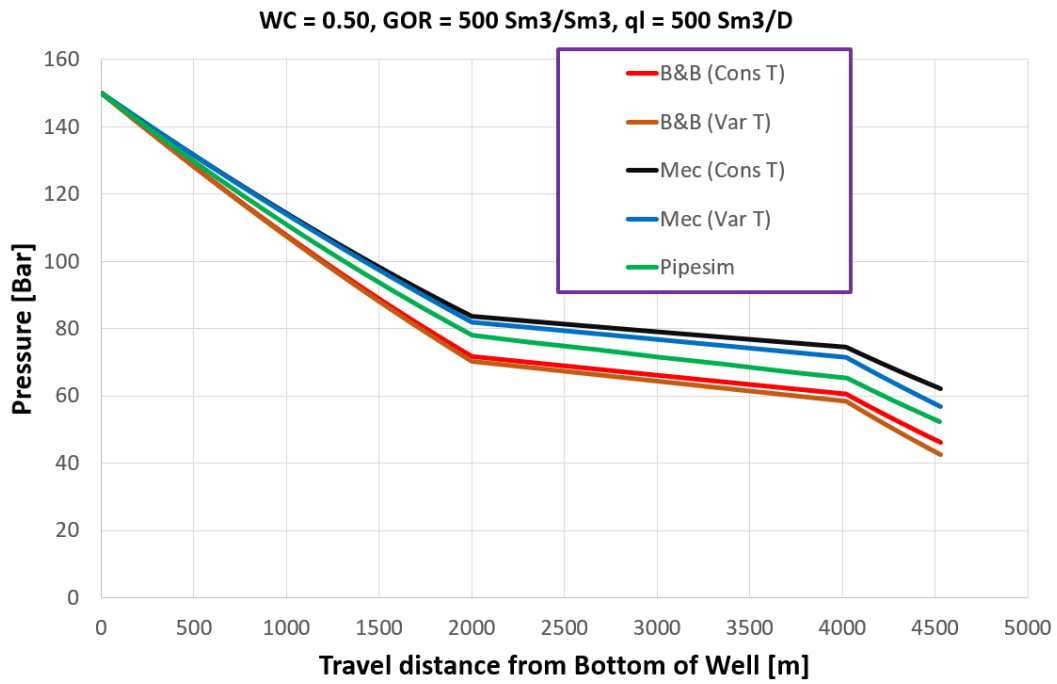Figure 4.4: Temperature profile along the pipeline.

WC = 50, GOR = 100 Sm3/Sm3, ql = 500 Sm3/D
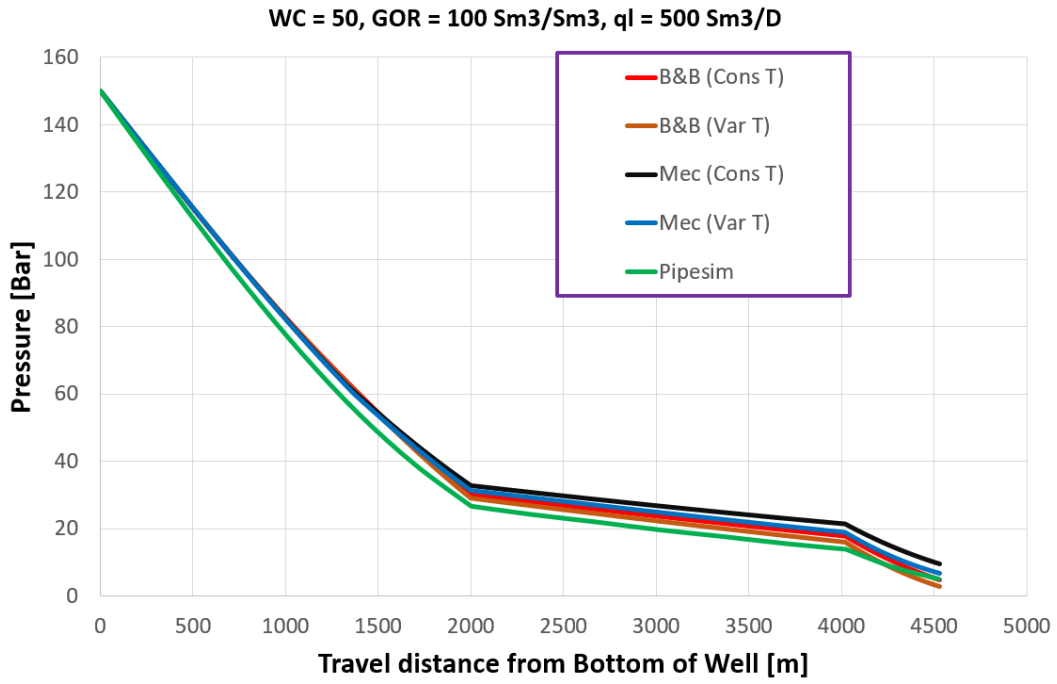
Figure 4.5: Pressure profile along the pipeline.

WC = 50, GOR = 100 Sm3/Sm3, ql = 500 Sm3/D
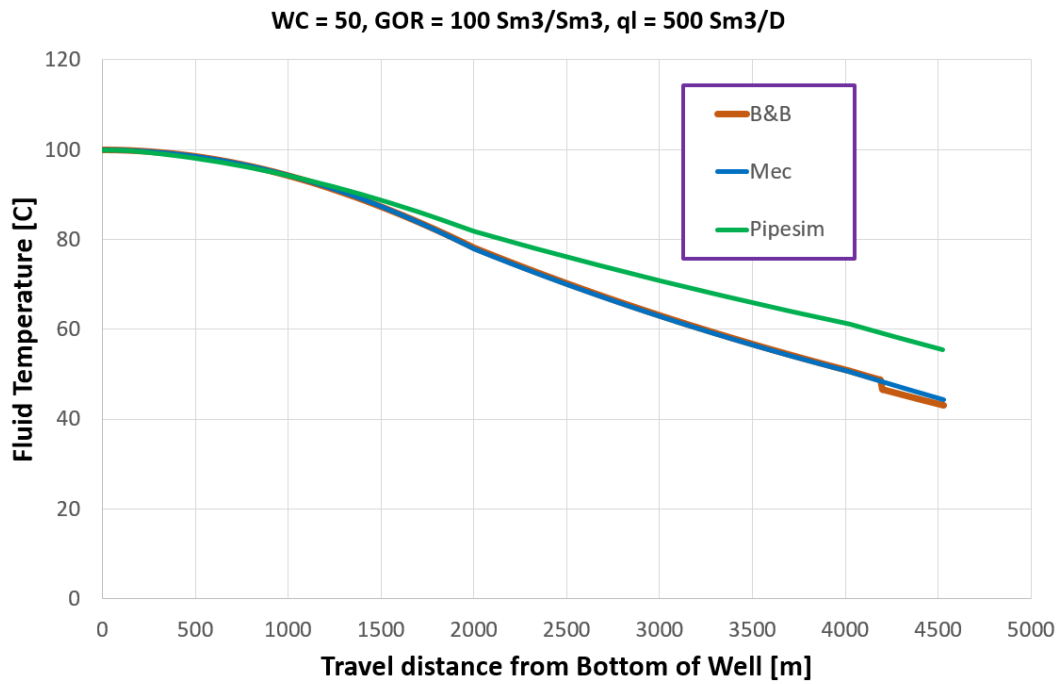
Figure 4.6: Temperature profile along the pipeline.

WC = 0, GOR = 250 Sm3/Sm3, ql = 500 Sm3/D

Figure 4.7: Pressure profile along the pipeline.

WC = 0, GOR = 250 Sm3/Sm3, ql = 500 Sm3/D

Figure 4.8: Temperature profile along the pipeline.

WC = 0.25, GOR = 250 Sm3/Sm3, ql = 500 Sm3/D

Figure 4.9: Pressure profile along the pipeline.

WC = 0.25, GOR = 250 Sm3/Sm3, ql = 500 Sm3/D

Figure 4.10: Temperature profile along the pipeline.

Figure 4.11: Pressure profile along the pipeline.

Figure 4.12: Temperature profile along the pipeline.

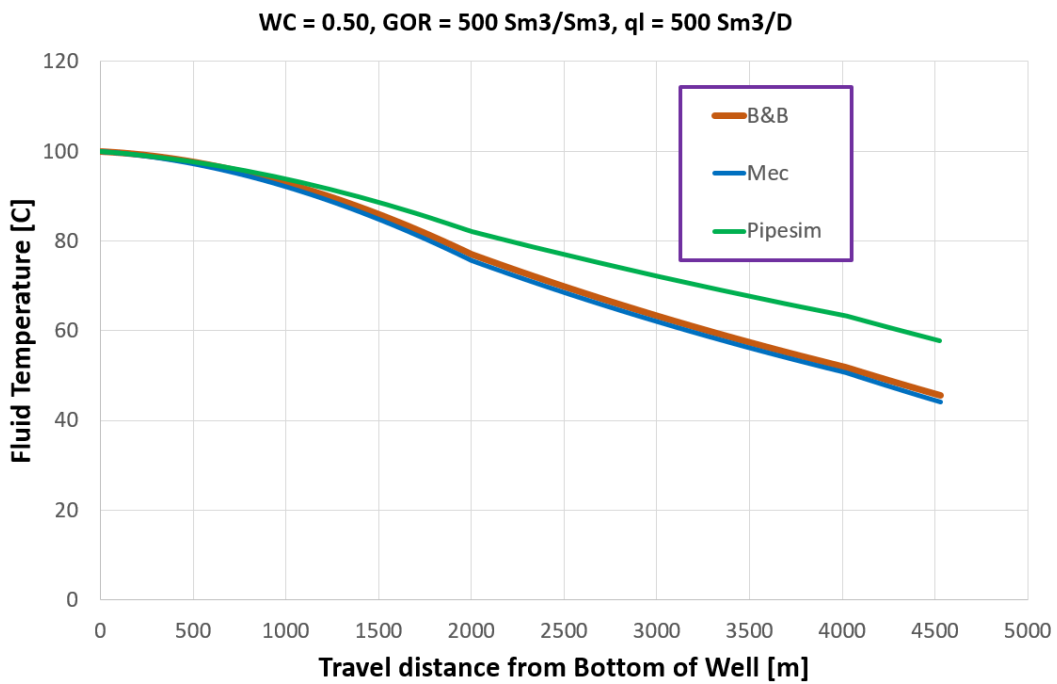Figure 4.13: Pressure profile along the pipeline.

Figure 4.14: Temperature profile along the pipeline.

Figure 4.15: Pressure profile along the pipeline.

Figure 4.16: Temperature profile along the pipeline.

Figure 4.17: Pressure profile along the pipeline.

Figure 4.18: Temperature profile along the pipeline.

4.1.2. Varying liquid surface rate

Setup:
In this subsection all simulation cases are performed with a WC of 0.25 and GOR of 250 Sm3/Sm3. Four liquid surface rates are given: 500, 1000, 1500 and 2000 Sm3/D. Pressure profiles along with corresponding temperature profiles are graphed in the following pages.

Evaluation:
Observations from the graphs are as follows:

- Increasing the liquid rate increases the overestimation of the pressure drop in the Beggs and Brill method. As suggested previously, this may be due to errors in the code, the accelleration term being ignored or the nature of the Beggs and Brill method.

- The calculated fluid temperature increases with flow rate. This is mostly caused by the surroundings having less time to reduce the fluid temperature of the production stream.

- In addition to the fluid temperature increasing, frictional pressure drop increases when increasing the liquid flow rate. Thus the pressure drop becomes less dependent on the fluid temperature, and the pressure profiles assuming constant temperature are close to those assuming varying temperature.

- The mechanistic approach underestimates the pressure drop for higher flow rates compared with Pipesim, but still it is in close correspondence.

- Me-VarT is concluded from this and the previous subsection (4.1.1) to be the most accurate Simulator configuration. Thus, this is the configuration used for further evaluation.
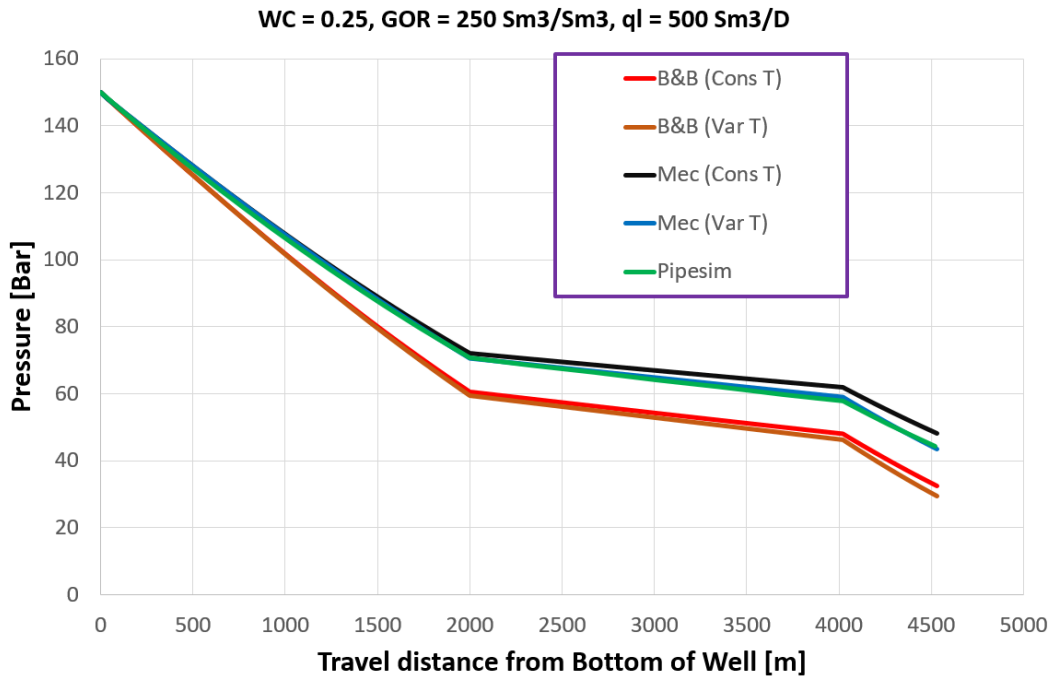
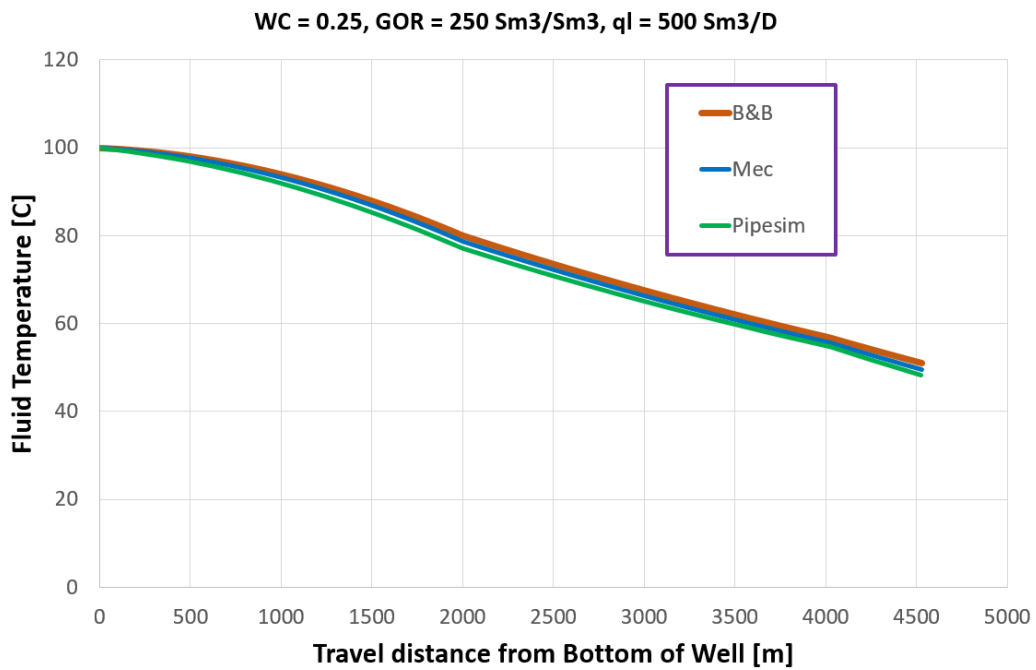Figure 4.19: Pressure profile along the pipeline.

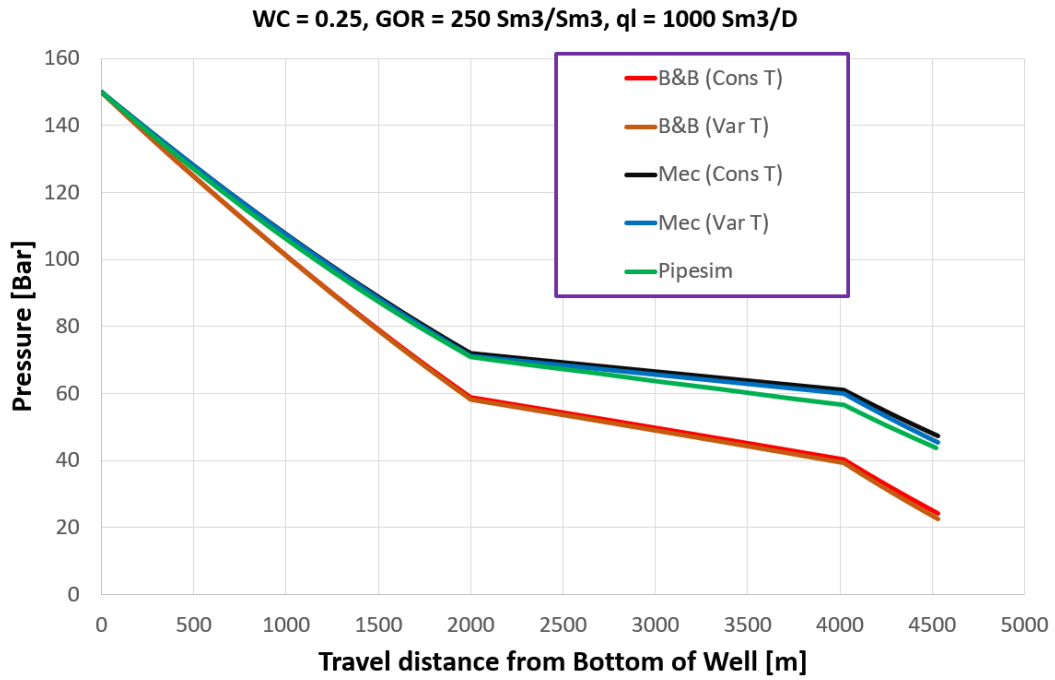Figure 4.20: Temperature profile along the pipeline.

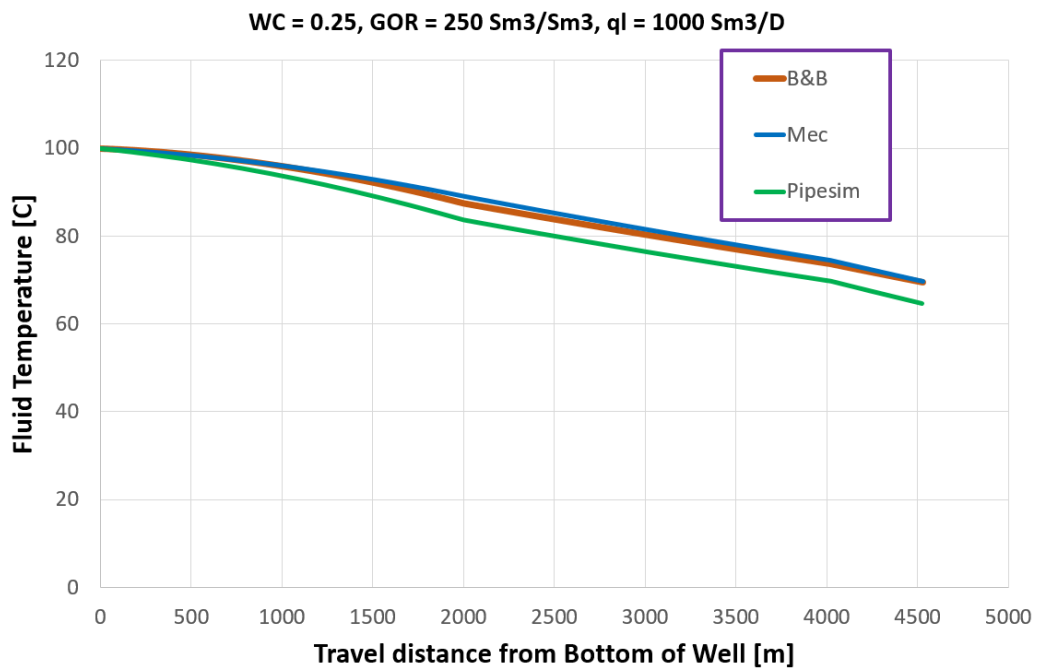Figure 4.21: Pressure profile along the pipeline.

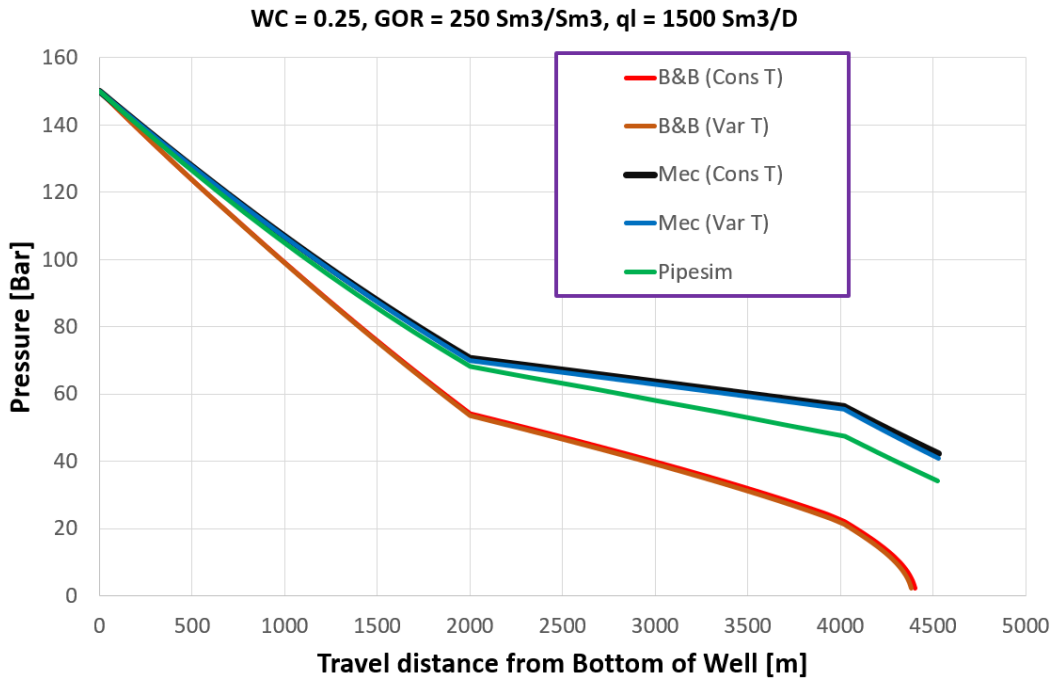Figure 4.22: Temperature profile along the pipeline.

Figure 4.23: Pressure profile along the pipeline.
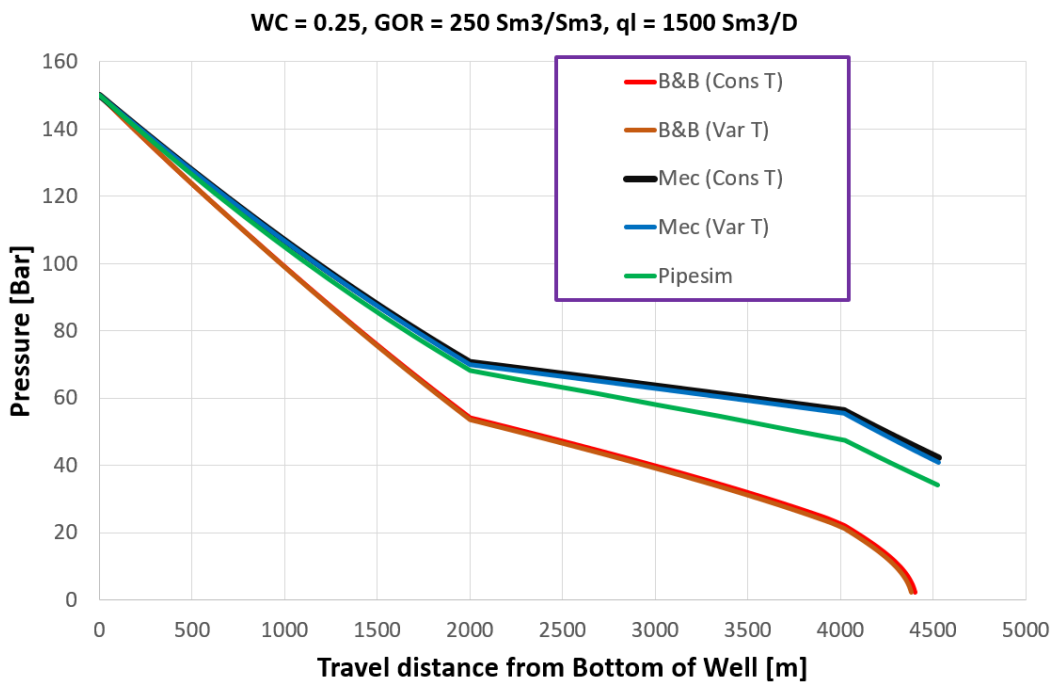

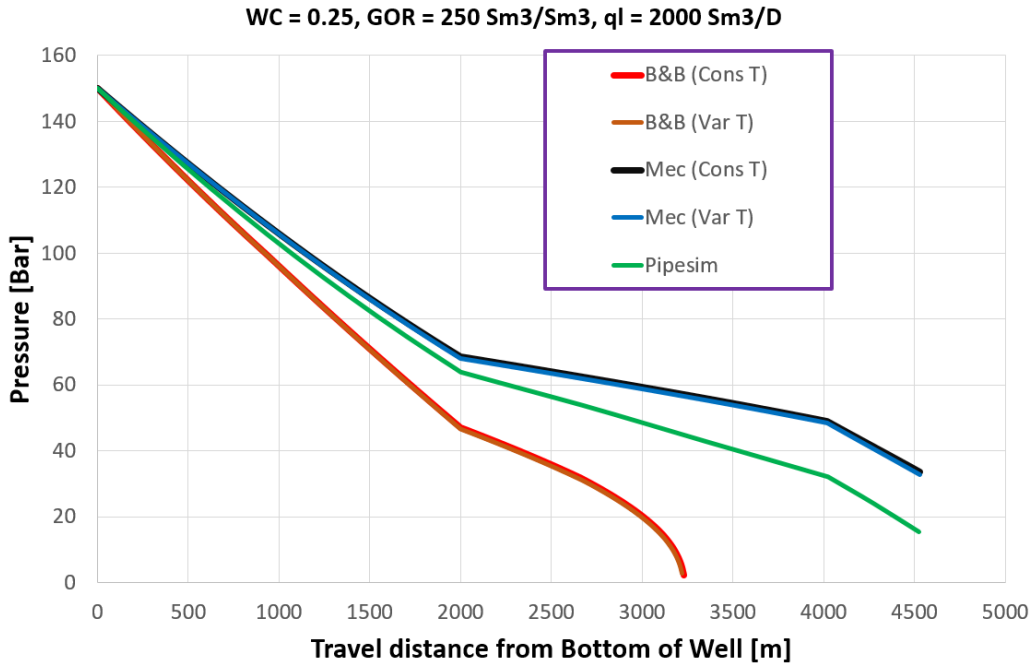Figure 4.24: Temperature profile along the pipeline.

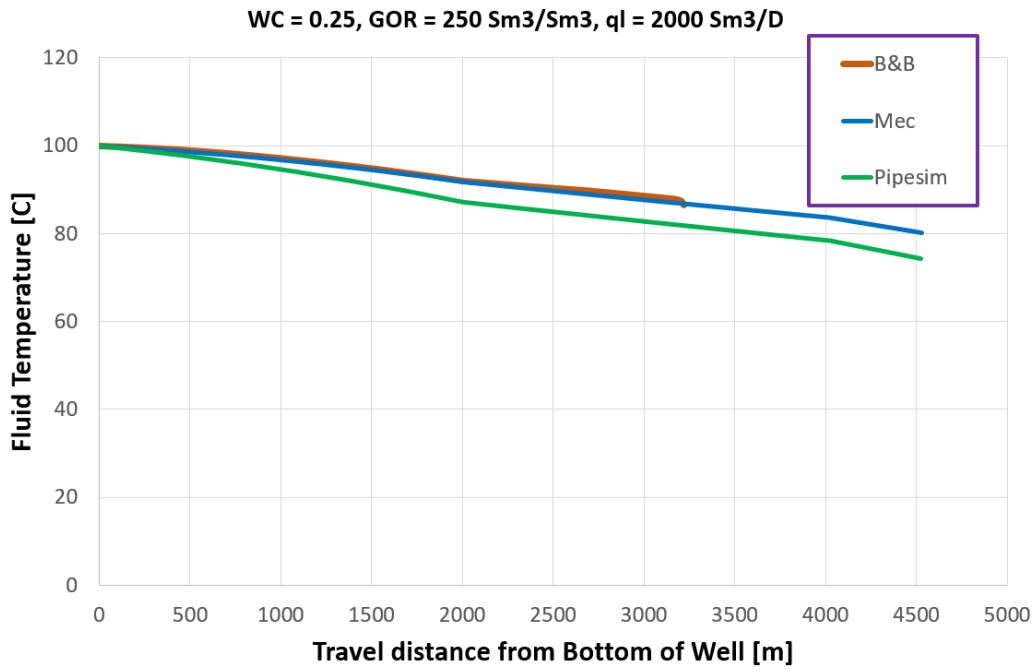Figure 4.25: Pressure profile along the pipeline.

Figure 4.26: Temperature profile along the pipeline.

4.1.3. Comparison between Me-VarT and Pipesim

In the previous subsections it has been shown that Me-VarT performs similar to Pipesim when they are compared one simulation case at a time. Pipesim may have a lower pressure profile than Me-VarT in one simulation case, a but higher pressure profile in another. In addition, it should be evaluated whether Me-VarT and Pipesim respond similarly and consistently from one simulator case to another.

Setup:
The same simulation cases as in sec. 4.1.1 and 4.1.2 are used in this subsection:

- Variation of WC: 0, 0.25 and 0.5. With constant GOR of 250 Sm3/Sm3 and liquid flow rate of 500 Sm3/D.

- Variation of GOR: 100, 250 and 500 Sm3/Sm3. With constant WC of 0.25 and liquid flow rate of 500 Sm3/D.

- Variation of Liquid flow rate: 500, 1000, 1500 and 2000 Sm3/D. With constant GOR of 250 Sm3/Sm3 and WC of 0.25 Sm3/D.

Pressure profiles along with corresponding temperature profiles are graphed in the following pages.

Evaluation:
Observations from the graphs are as follows:

- **Increased WC:** Pressure drop increases with water cut for both simulators. Water has a higher density than oil, thus increasing the water cut increases the gravitational pressure drop.

- **Increased GOR:** Pressure drop decreases with GOR for both simulators. Increasing the vapor fraction in the fluid stream reduces the fluid density, and therefore also the gravitational pressure drop. Increasing the GOR has the same effect as including gas lift.

- **Increased Liquid flowrate:** Pressure drop increases with liquid flowrate for both simulators. This is caused by the increased frictional pressure drop due to higher fluid velocities.

- Temperature and pressure profiles for both simulators are closely matched. Pipesim and Me-VarT respond in a similar way to changes in production. This further suggests that Me-VarT is a good Simulator configuration.

Figure 4.27: Pressure profile along the pipeline.

Figure 4.28: Temperature profile along the pipeline.

Mec, GOR = 250 Sm3/Sm3, ql = 500 Sm3/D

Figure 4.29: Pressure profile along the pipeline.

Mec, GOR = 250 Sm3/Sm3, ql = 500 Sm3/D

Figure 4.30: Temperature profile along the pipeline.

Figure 4.31: Pressure profile along the pipeline.

Figure 4.32: Temperature profile along the pipeline.

Figure 4.33: Pressure profile along the pipeline.

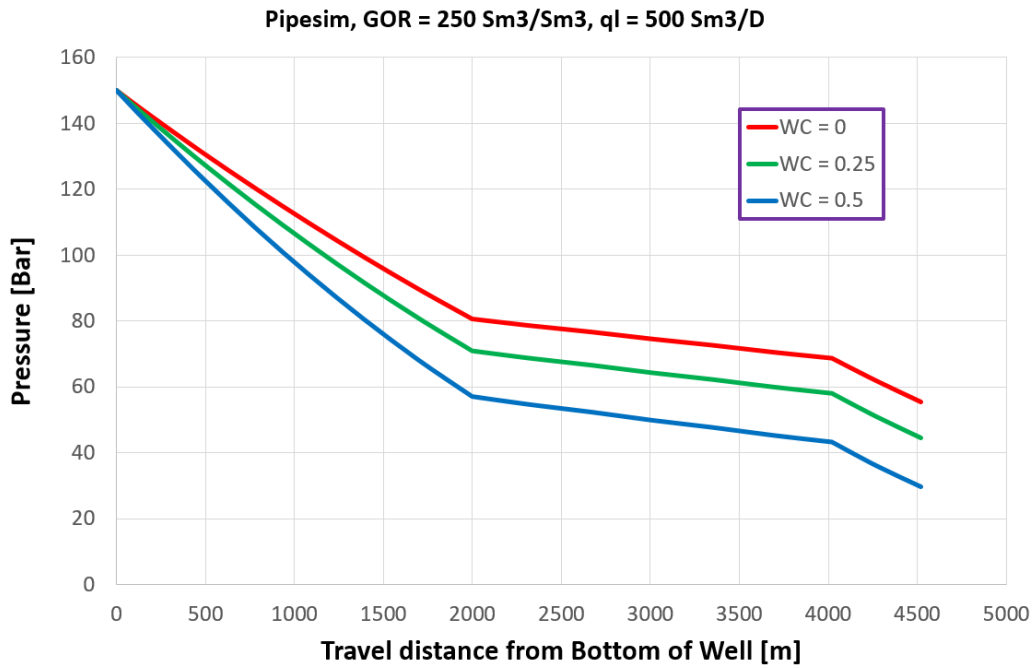Figure 4.34: Temperature profile along the pipeline.

Figure 4.35: Pressure profile along the pipeline.
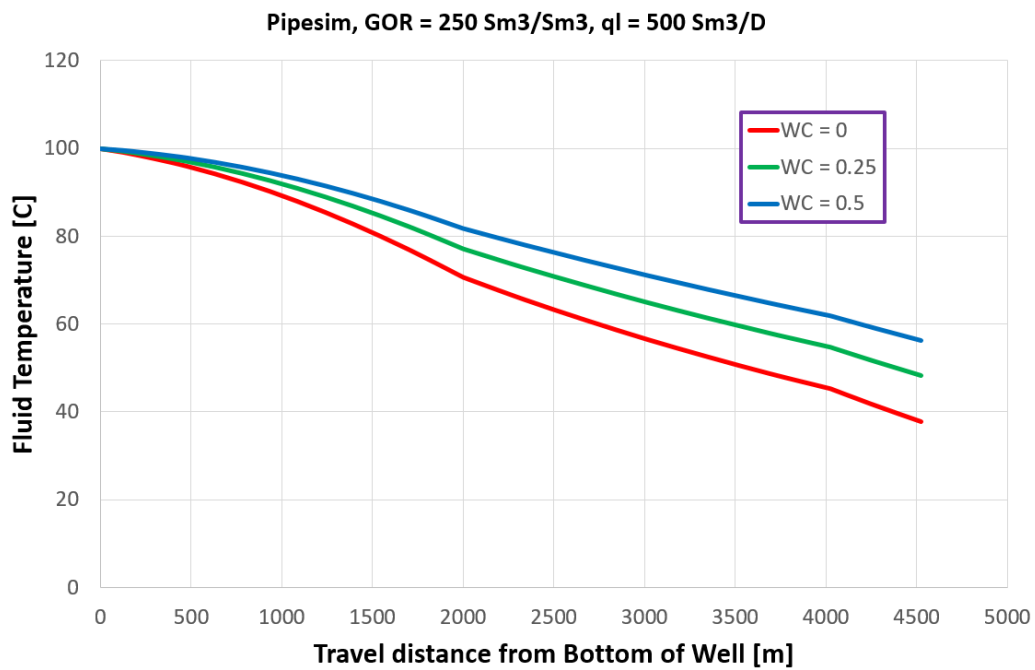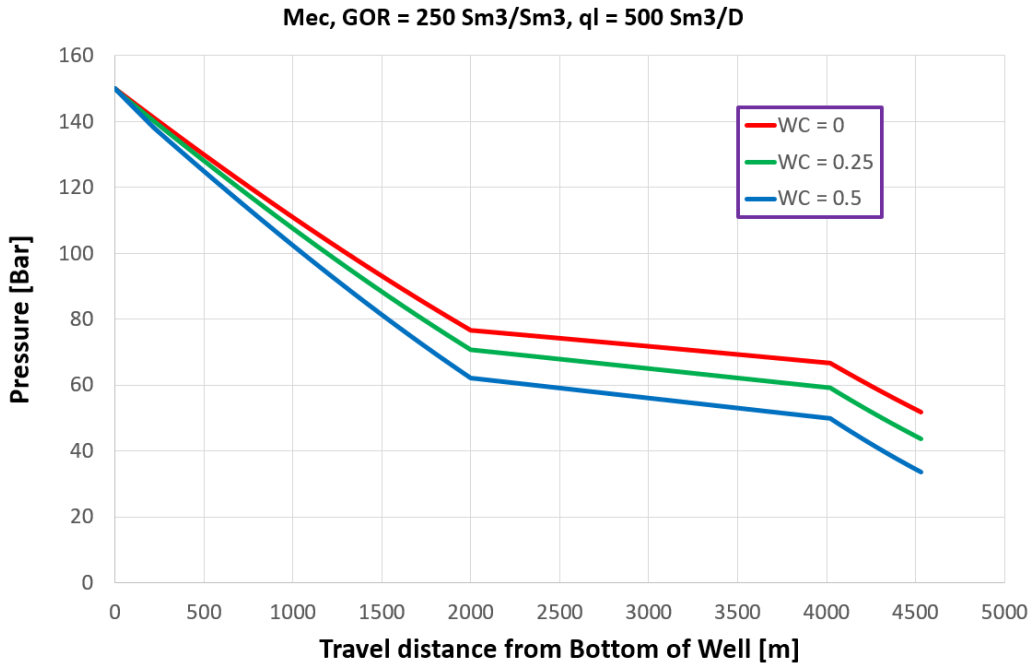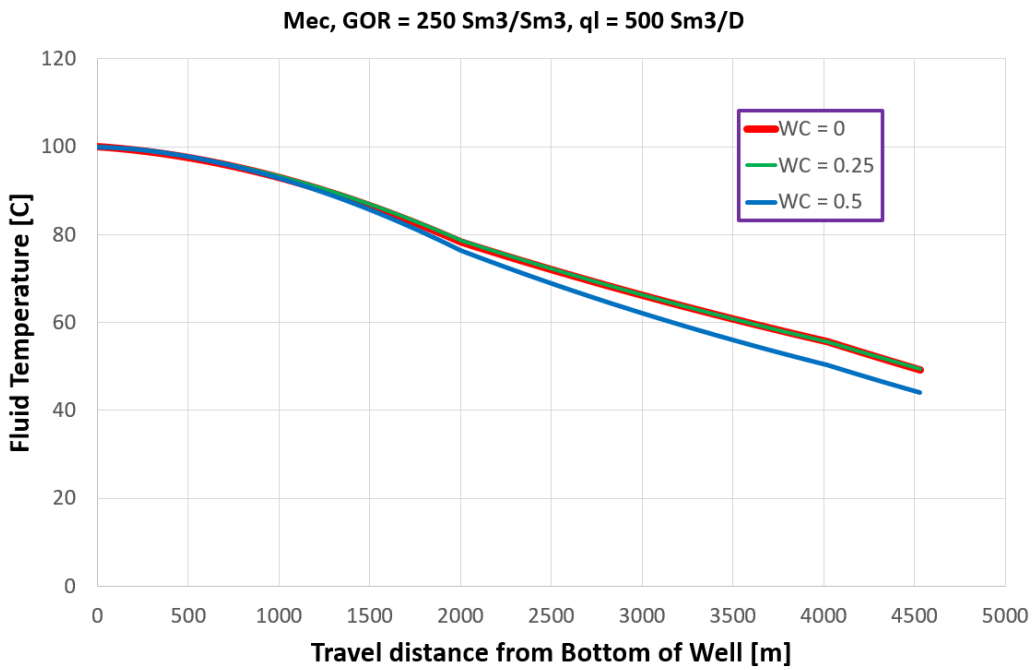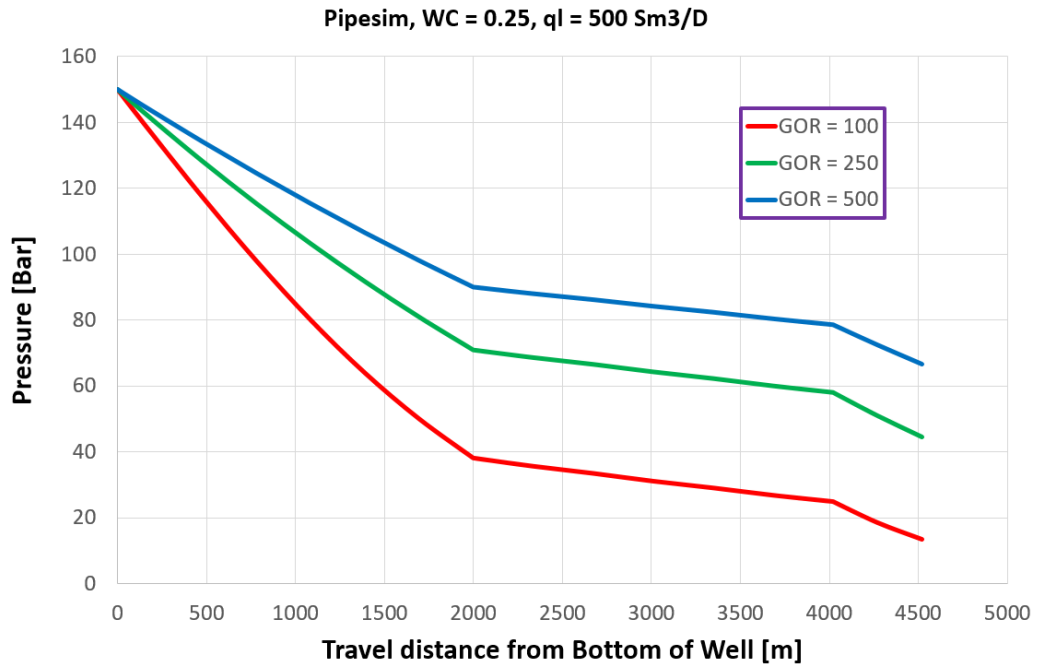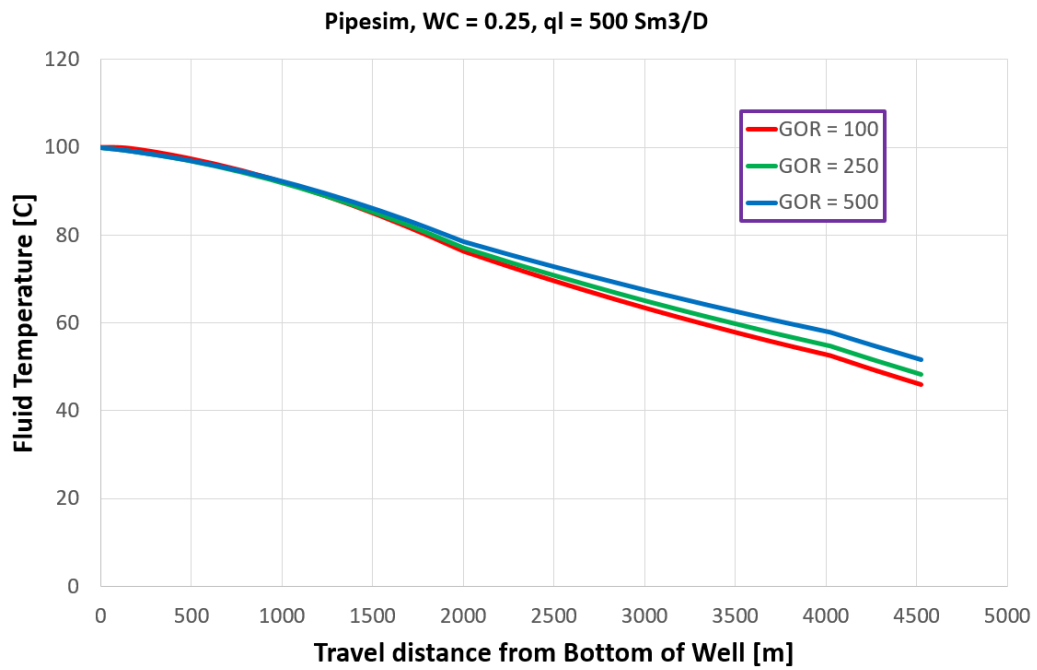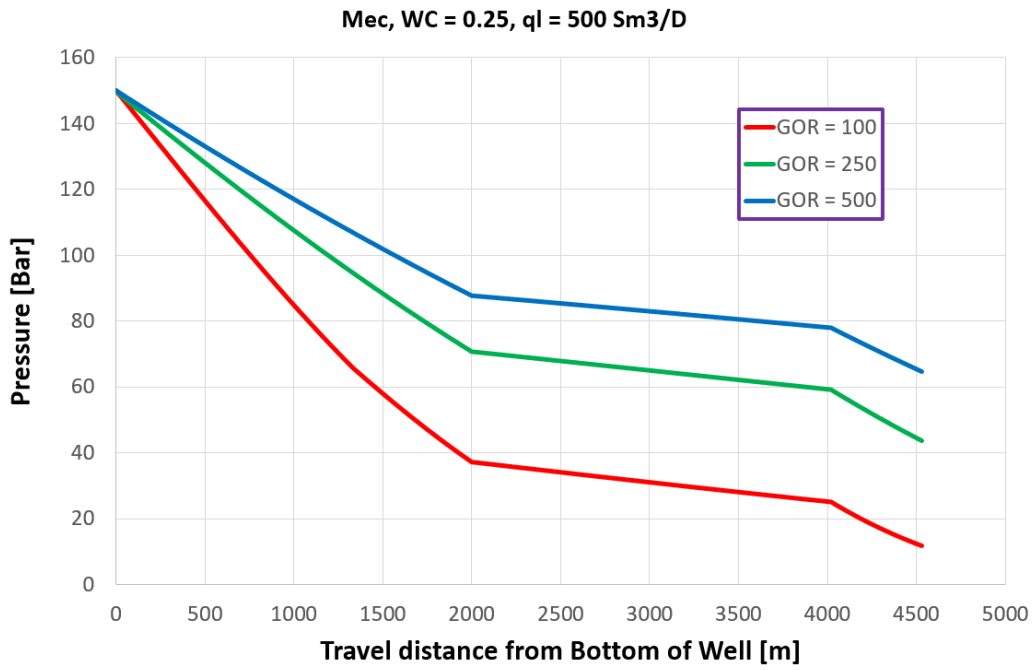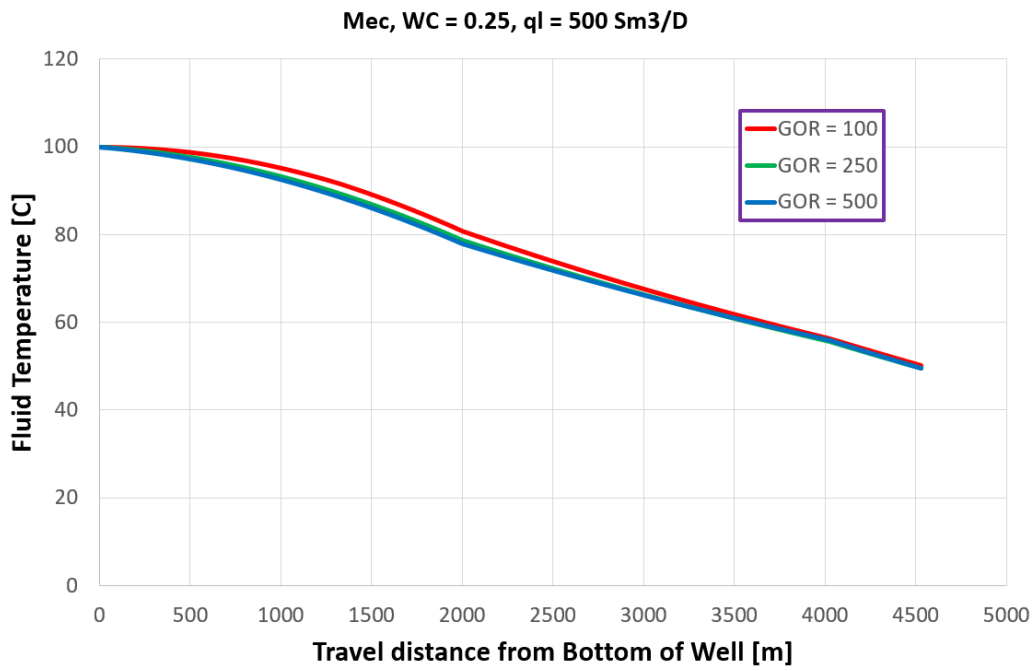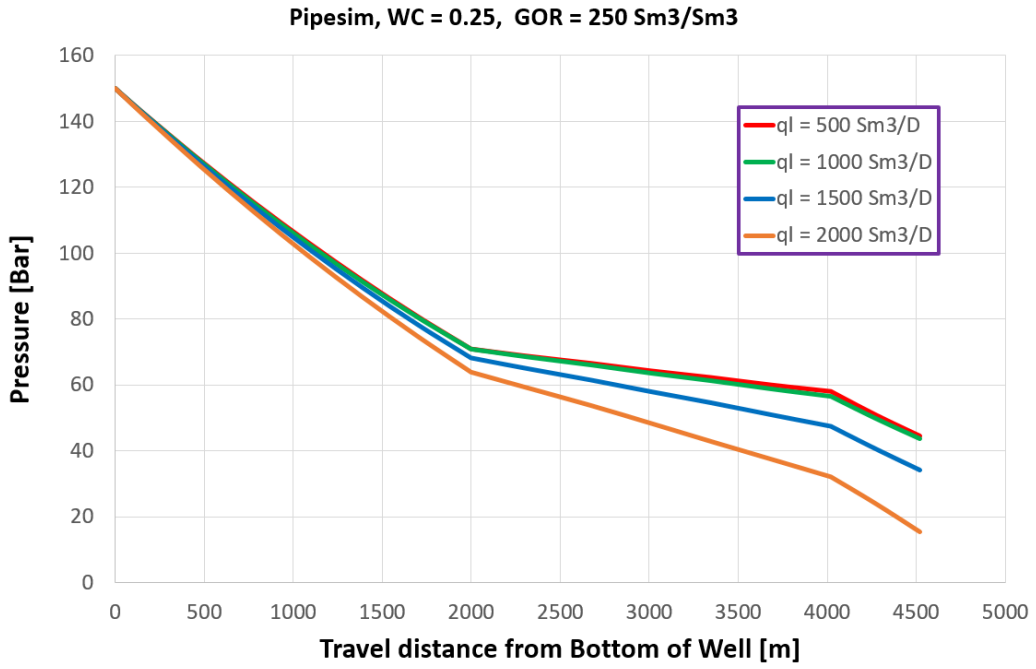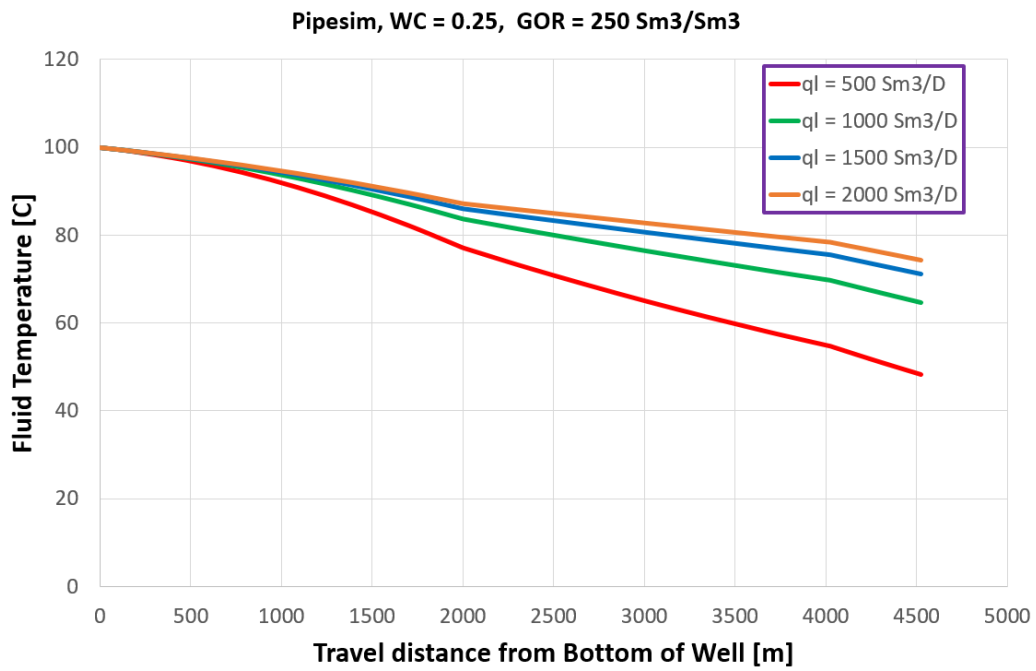

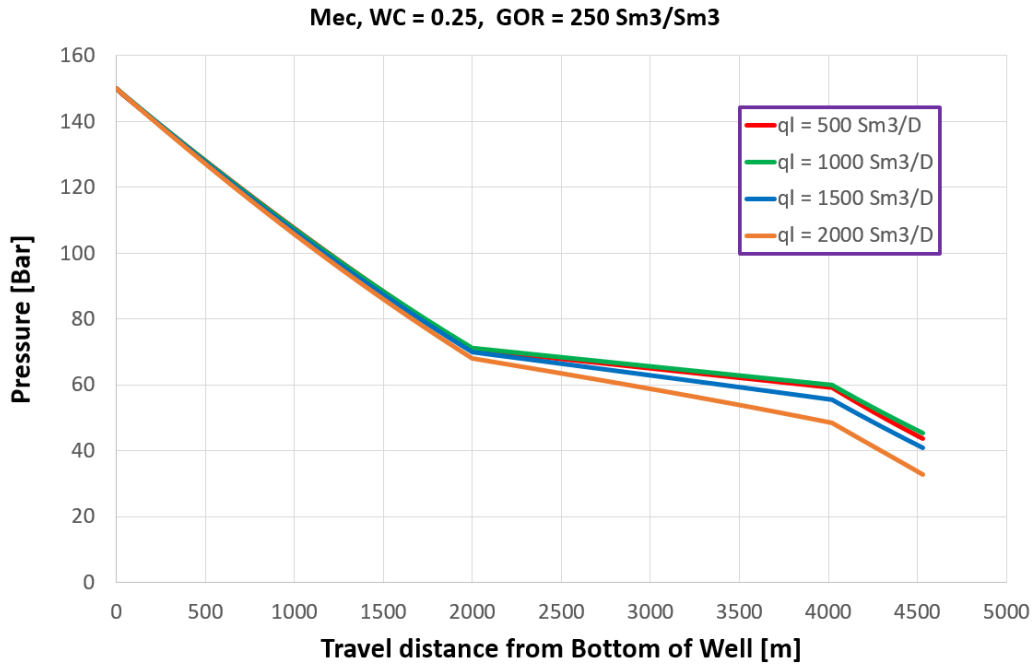Figure 4.36: Temperature profile along the pipeline.

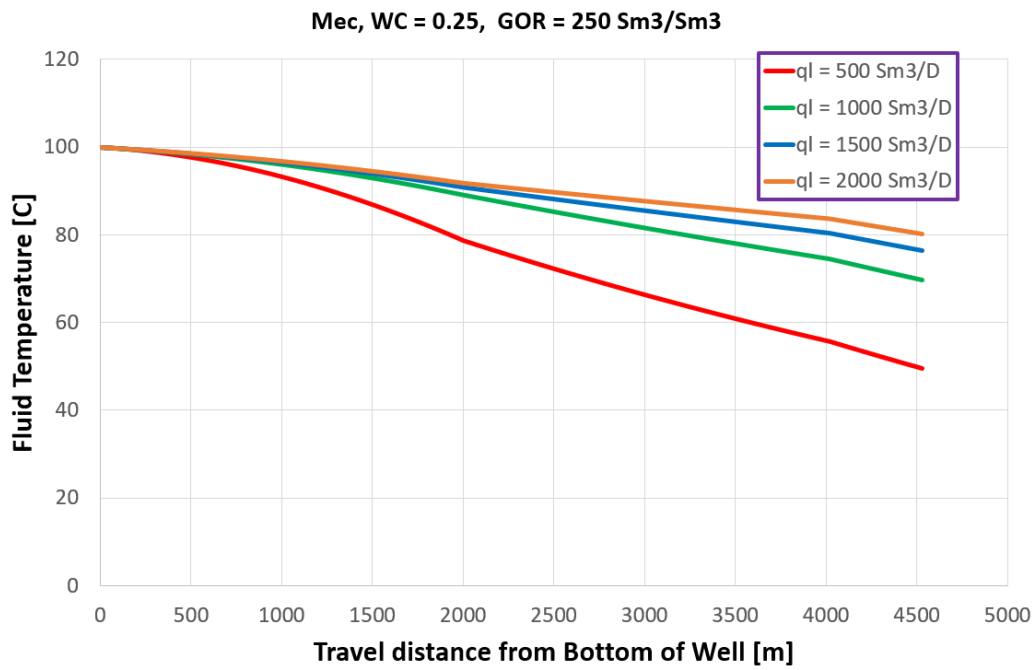Figure 4.37: Pressure profile along the pipeline.

Figure 4.38: Temperature profile along the pipeline.

4.2. Performance of the configurations

The performance of the Simulator configurations are tested for three different network-models[2]. The purpose is to check and compare the runtime and stability of the different configurations. The simulations are performed with the network optimization algorithm, described in sec. 2.1. The sequential approach (Appendix D) is used as optimization algorithm.

Setup:
The basis for each network-model is a 9-well network with a given set of basis-rates, water cuts and pipe-lengths. In order to test each model with multiple rates, the base-rates ($q_{o, target}$) of each network-model are multiplied by a factor α that goes from 0.1 to 3 with a step length of 0.1. For all the examples in this section, each manifold includes three wells, and the GOR equals 100 Sm3/Sm3. BB-ConsT are compared with Me-ConsT and Me-VarT to investigate the individual differences in performance - field production rates, solver runtime and solver stability - between the pressure drop methods, and between the constant or varying temperature methods. The network models and the corresponding graphed production data and runtimes are described in the following pages.

Evaluation:
Observations from the graphs are as follows:

- All the Simulator configurations are stable for all production values. This is indicated by the gas lift rate and field oil production rate consistently increasing with increased target rate. A small drop in these values may indicate the Network Solver having trouble finding the optimal solution, but no such drop occurs for any of the Simulator configurations.

- As expected, the production data for Me-VarT and Me-ConsT are quite similar.

- All the configurations reach a production maximum for high target rates. This indicates that the network is unable to produce more from the reservoir. This production plateau is lower for the Beggs and Brill method than for the mechanistic approach. As indicated in sec. 4.1.2 this might be because the Beggs and Brill method overestimates the pressure drop for high flow rates.

- Calculating temperature increases the runtime with about 100%, as can be seen by comparing the runtimes of Me-ConsT and Me-VarT.

- Both pressure drop approaches have a low runtime, but the mechanistic approach is in general quicker than the Beggs and Brill method. This can be seen by comparing the runtimes of Me-ConsT and BB-ConsT.

- For low target rates Me-VarT may even be quicker than the BB-ConsT.

---

[2]All simulations are run using the same computer setup. See Appendix H for further details.

4.2.1. Network-model 1

The first model is "well balanced", with rates, water cuts and pipe-lengths quite similar for all wells.

Property	Well 1	Well 2	Well 3	Well 4	Well 5	Well 6	Well 7	Well 8	Well 9	Unit
$q_{o, \text{target}}$	1000	1200	1300	900	1000	1000	1200	1300	900	Sm^3/D
WC	0.3	0.25	0.35	0.4	0.3	0.35	0.35	0.4	0.2	-
L_{tubing}	2000	2100	2100	2000	2000	2000	2000	2100	2100	m
h_{tubing}	2000	2100	2100	2000	2000	2000	2000	2100	2100	m
L_{flowline}			100			150			300	m
h_{flowline}			0			20			30	m
L_{pipeline}									2000	m
h_{pipeline}									500	m
L_{riser}									100	m
h_{riser}									100	m

Figure 4.39: Network-model 1, 9 wells: Field rates.
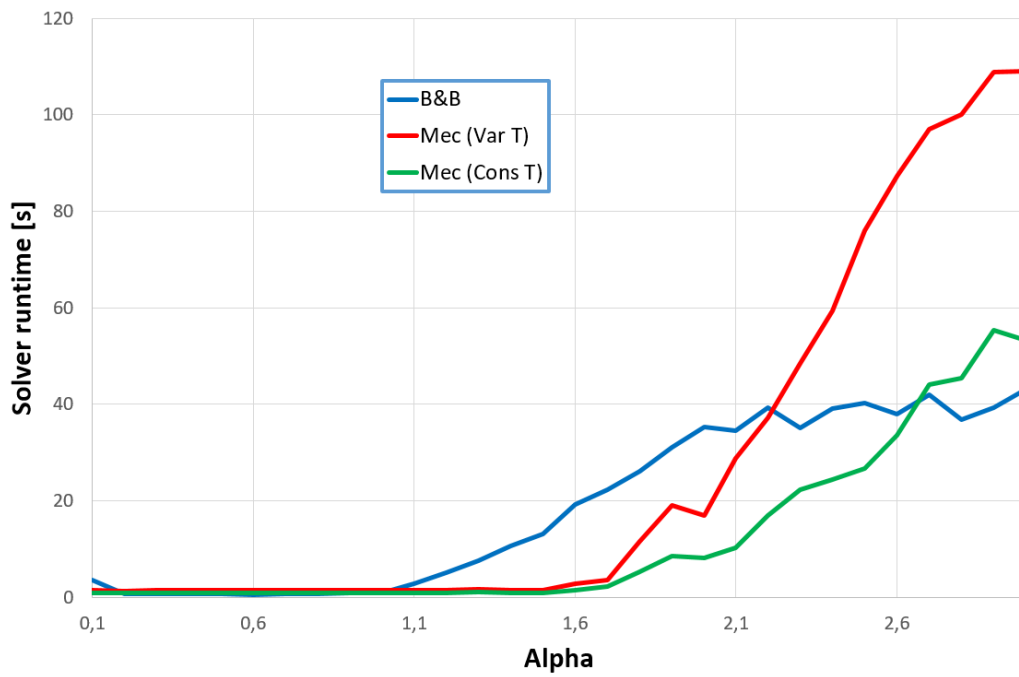
Figure 4.40: Network-model 1, 9 wells: Solver runtime.

4.2.2. Network-model 2

The second model is "well spread", with rates, water cuts and pipe-lengths varying significantly for all wells. The flowline length is increased while the height is reduced.

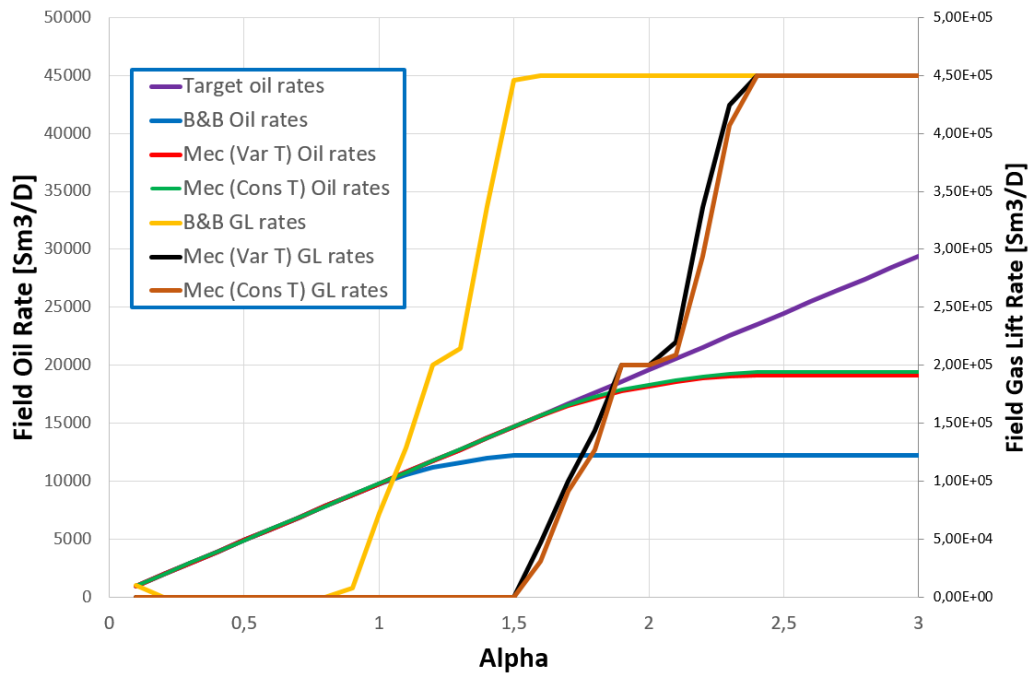| Property	Well 1	Well 2	Well 3	Well 4	Well 5	Well 6	Well 7	Well 8	Well 9	Unit
$q_{o,\,target}$	1600	900	850	1000	1300	800	2000	1000	700	Sm^3/D
WC	0.7	0.25	0.5	0.3	0.4	0.6	0.1	0.35	0.2	-
L_{tubing}	2000	2100	2100	2000	2000	2000	2000	2100	2100	m
h_{tubing}	2000	2100	2100	2000	2000	2000	2000	2100	2100	m
$L_{flowline}$			100			200			400	m
$h_{flowline}$			0			100			40	m
$L_{pipeline}$									5000	m
$h_{pipeline}$									0	m
L_{riser}									100	m
h_{riser}									100	m
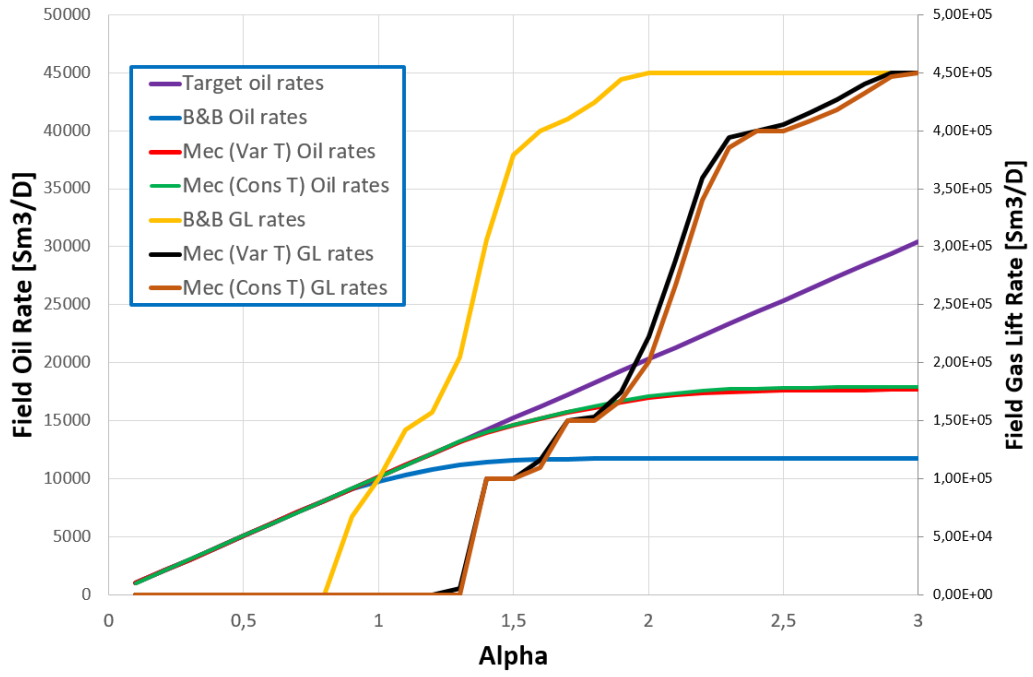
Figure 4.41: Network-model 2, 9 wells: Field rates.
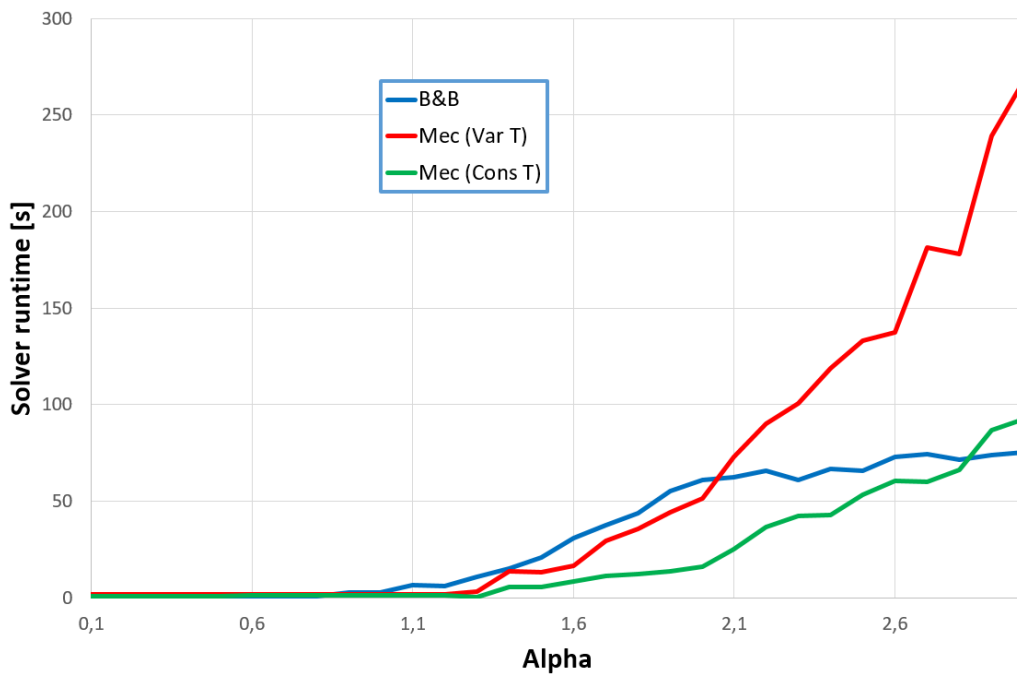
Figure 4.42: Network-model 2, 9 wells: Solver runtime.

4.2.3. Network-model 3

The third model is also "well spread", with rates, water cuts and pipe-lengths varying significantly for all wells. The tubing lengths and heights are also altered for some of the wells.

Property	Well 1	Well 2	Well 3	Well 4	Well 5	Well 6	Well 7	Well 8	Well 9	Unit
$q_{o, target}$	1200	900	850	1100	1000	950	1200	1500	600	Sm^3/D
WC	0.4	0.25	0.5	0.1	0.4	0.25	0.3	0.6	0.3	-
L_{tubing}	2000	2100	2100	1800	2200	2100	2000	1900	2000	m
h_{tubing}	1900	2100	1900	1800	2100	2100	1800	1900	2000	m
$L_{flowline}$			800			300			1000	m
$h_{flowline}$			30			40			20	m
$L_{pipeline}$									3000	m
$h_{pipeline}$									400	m
L_{riser}									100	m
h_{riser}									100	m
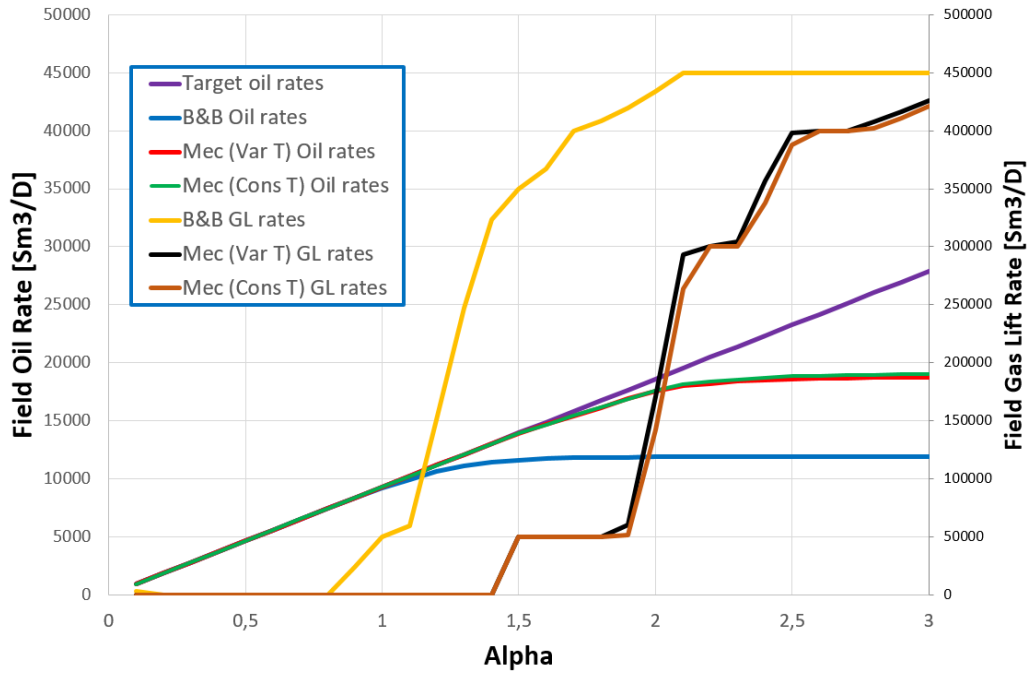
Figure 4.43: Network-model 3, 9 wells: Field rates.
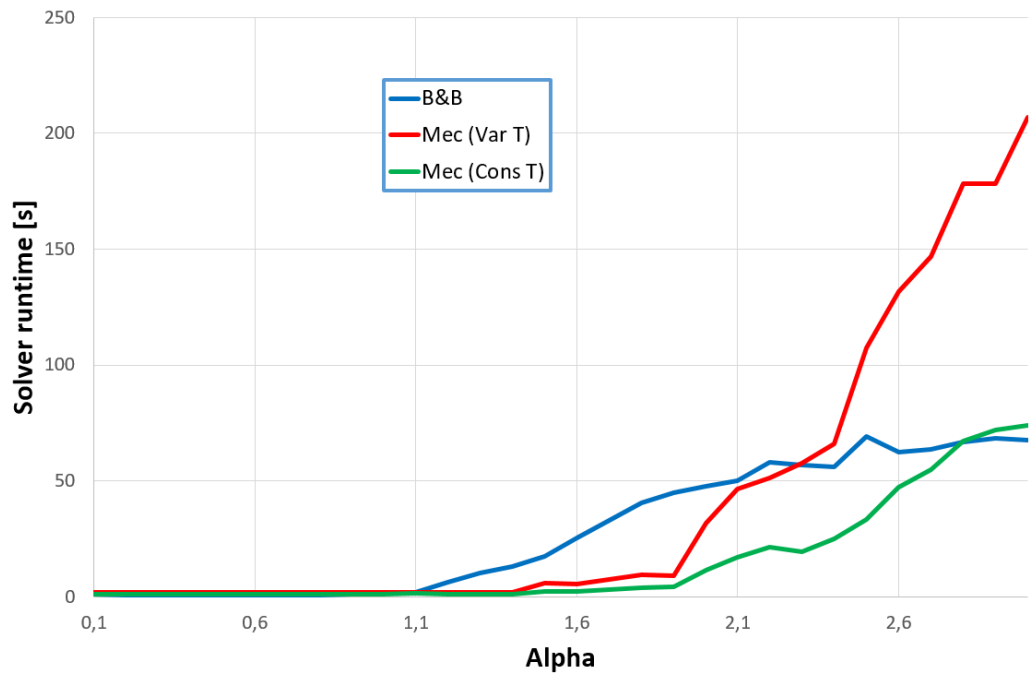
Figure 4.44: Network-model 3, 9 wells: Solver runtime.

4.3. Convergence of pressure and temperature profiles

As stated in sec. 3.2, the temperature is calculated co-current from the wellhead to the separator, while the pressure is calculated counter-current from the separator to the wellhead. The temperature calculations are directly dependent on the pressure, but the pressure calculations are only indirectly dependent on the temperature, through the local properties. Thus the pressure is calculated first, assuming a constant temperature equal to the reservoir temperature ("First p iteration"). This pressure profile is used to calculate the temperature profile ("First T iteration), and the pressure profile is then re-calculated using the updated temperatures ("Second p iteration"). It was hypothesized that this procedure was sufficient for convergence of the temperature and pressure profiles. This section seeks to strengthen this claim by considering the hypothesis is wrong: That an additional calculation of the temperatures, using the newly updated pressure profile ("Second T iteration"), and then re-calculating the pressure profile a second time ("Third p iteration"), will yield significantly different results.

Setup:
The Me-VarT is used to calculate the pressure and temperature profiles. The simulation is run with the exact same setup as in sec. 4.1, assuming a liquid surface flow rate of 500 Sm3/D, WC = 0.25 and GOR = 250 Sm3/Sm3. Only the pressure and temperature profiles in the riser and pipeline are considered, as temperatures and pressures both are calculated co-current in the tubing.

Evaluation:
Observations from the graphs are as follows:

- The first pressure iteration, with constant temperature, is significantly different from the second pressure iteration. This is as expected.

- The first temperature iteration is very similar to the second temperature iteration, resulting in the second and third pressure iterations being practically equal.

- The hypothesis is strengthened. Only one re-calculation of the pressure profile is needed for sufficient convergence.
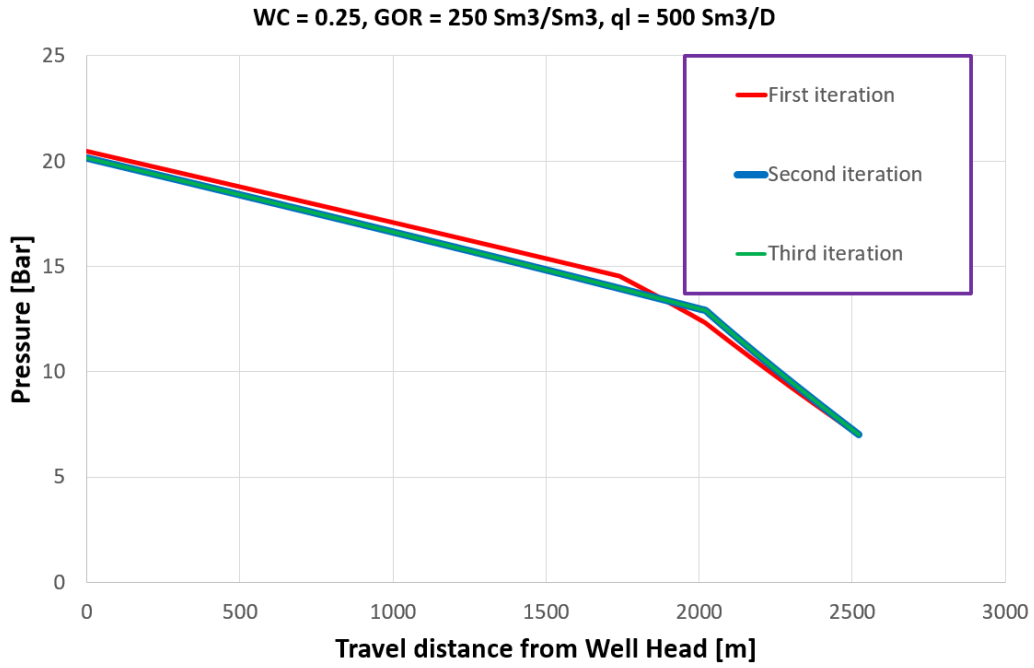
WC = 0.25, GOR = 250 Sm3/Sm3, ql = 500 Sm3/D

Figure 4.45: Pressure profile along the pipeline.

WC = 0.25, GOR = 250 Sm3/Sm3, ql = 500 Sm3/D
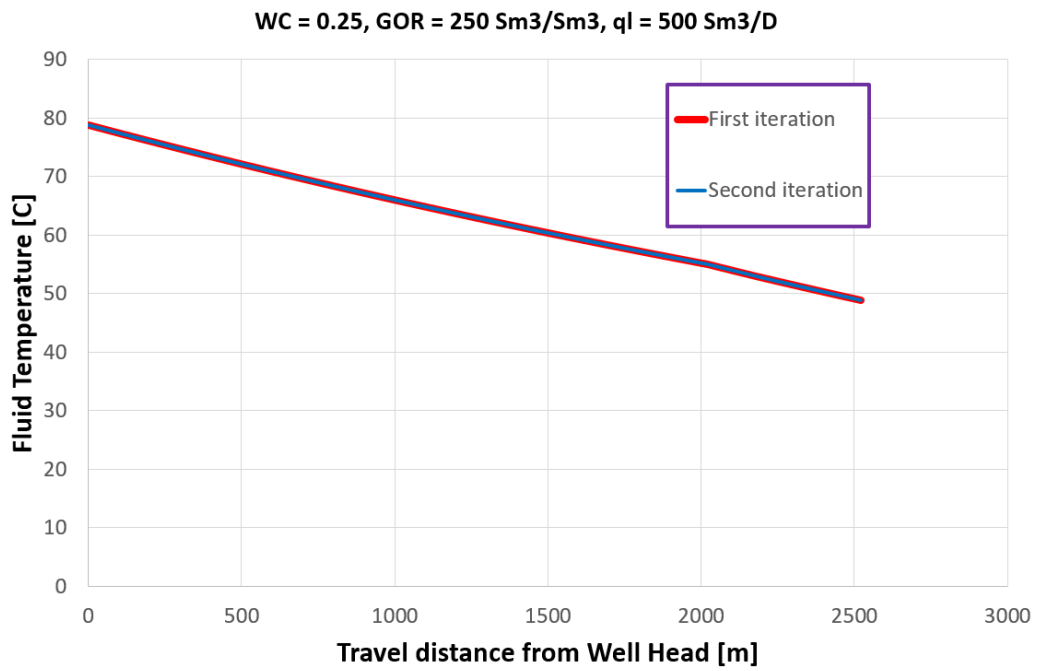
Figure 4.46: Temperature profile along the pipeline.

4.4. Differences in calculated overall HTC

As described in section 3.2, two different approaches may be taken to calculate the overall heat transfer coefficient in the tubing: A simplified equation (Eq. 3.7) and an iterative procedure (Eq. 3.8- 3.13). The two HTC-methods are compared using Me-VarT.

Setup:
Pressure and temperature profiles are calculated and compared with Pipesim as in sec. 4.1, assuming a liquid flowrate of 500 Sm3/D, WC = 0.25 and GOR = 250 Sm3/Sm3.

Performance plots are generated as in sec. 4.2, using the second network model. The results are graphed in the following pages.

Evaluation:
Observations from the graphs are as follows:

- The calculated HTC in the tubing is different for the two methods, as depicted in Fig. 4.47 . The simplified method generates an overall HTC of about $2.1 \left[\frac{\text{Btu}}{\text{hr ft}^2 \text{ °F}} \right]$, while the iterative procedure gives an overall HTC of about $7.2 \left[\frac{\text{Btu}}{\text{hr ft}^2 \text{ °F}} \right]$.

- The calculated HTC in the riser and pipeline is about $0.8 \left[\frac{\text{Btu}}{\text{hr ft}^2 \text{ °F}} \right]$. This is used as input HTC for Pipesim in the pipeline and riser.

- The difference in HTC alters the temperature profile somewhat, as seen in Fig. 4.51.

- The difference in temperature profile has a very small impact on the pressure profile, as seen in Fig. 4.50. This is as expected from the results in the previous sections.

- A lower HTC increases the temperature profile, because less heat is transferred from the fluids to the formation. This causes the pressure profile to increase as well, although the difference is very small. This is as expected from the results in sec. 4.1.

- The difference in performance between the two methods is negligible, as seen in Fig. 4.50 and 4.51. The user is thus able to choose either of the methods without effecting the pressure calculations much.

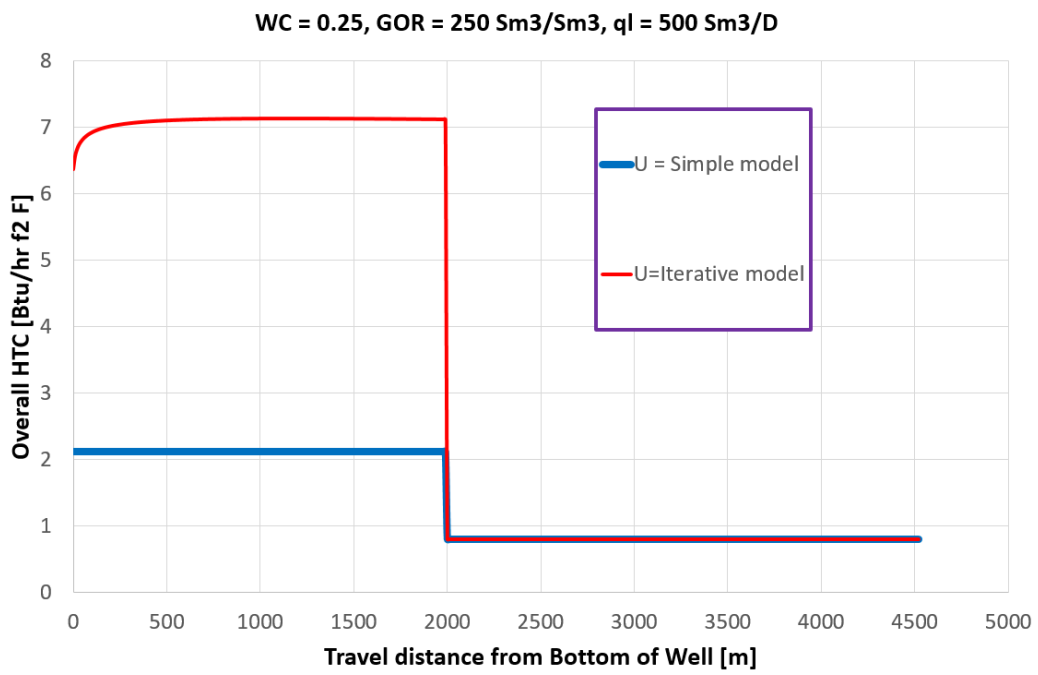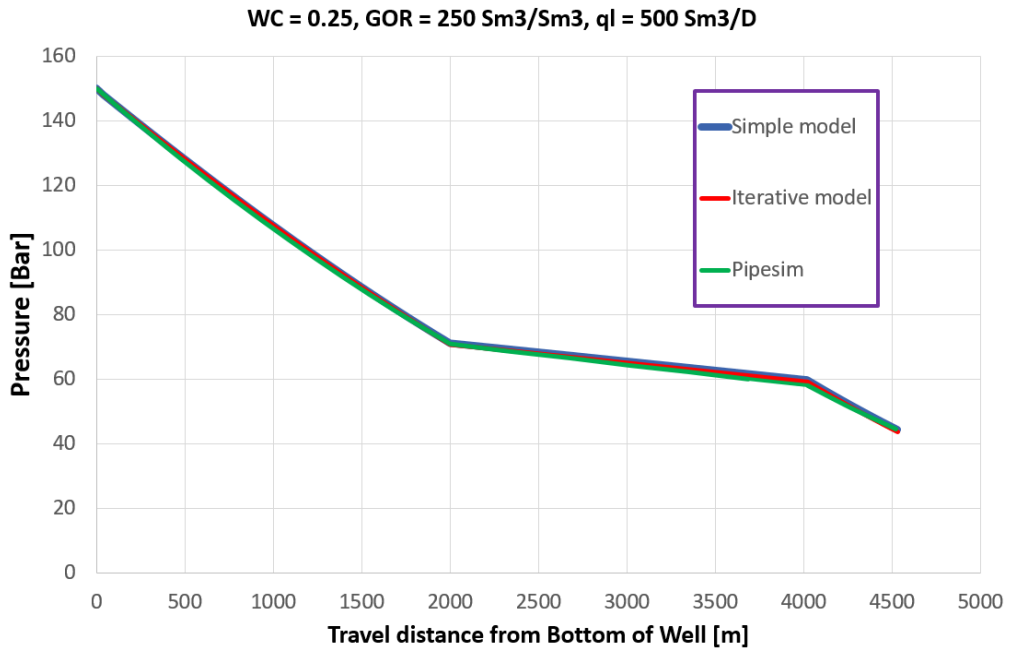Figure 4.47: Overall HTC profile along the pipeline.

Figure 4.48: Pressure profile along the pipeline.
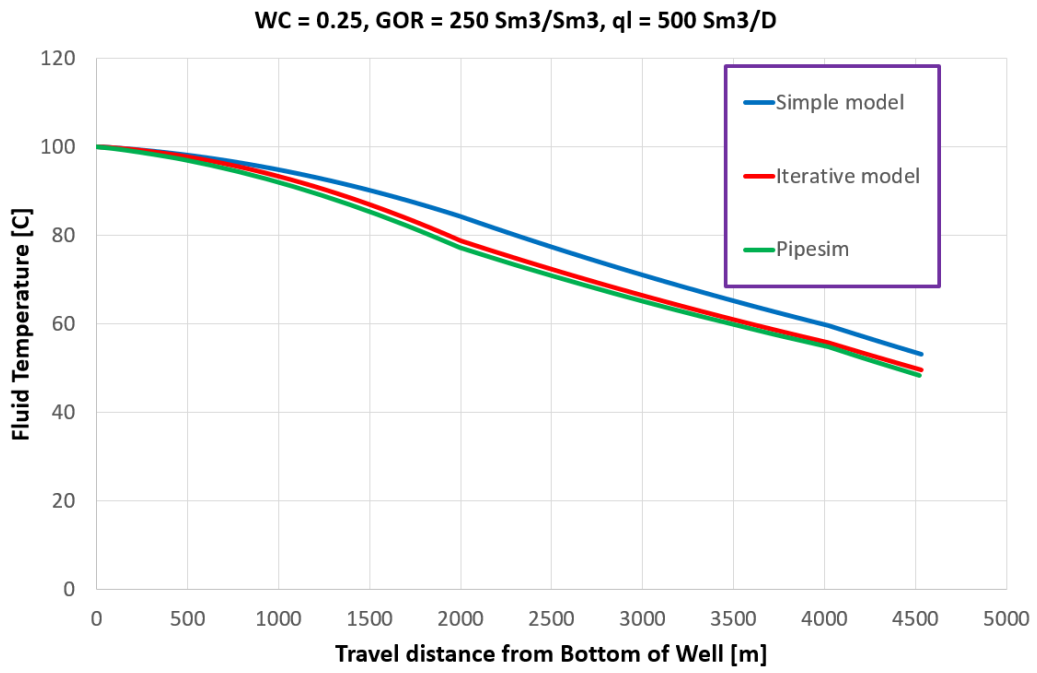
Figure 4.49: Temperature profile along the pipeline.
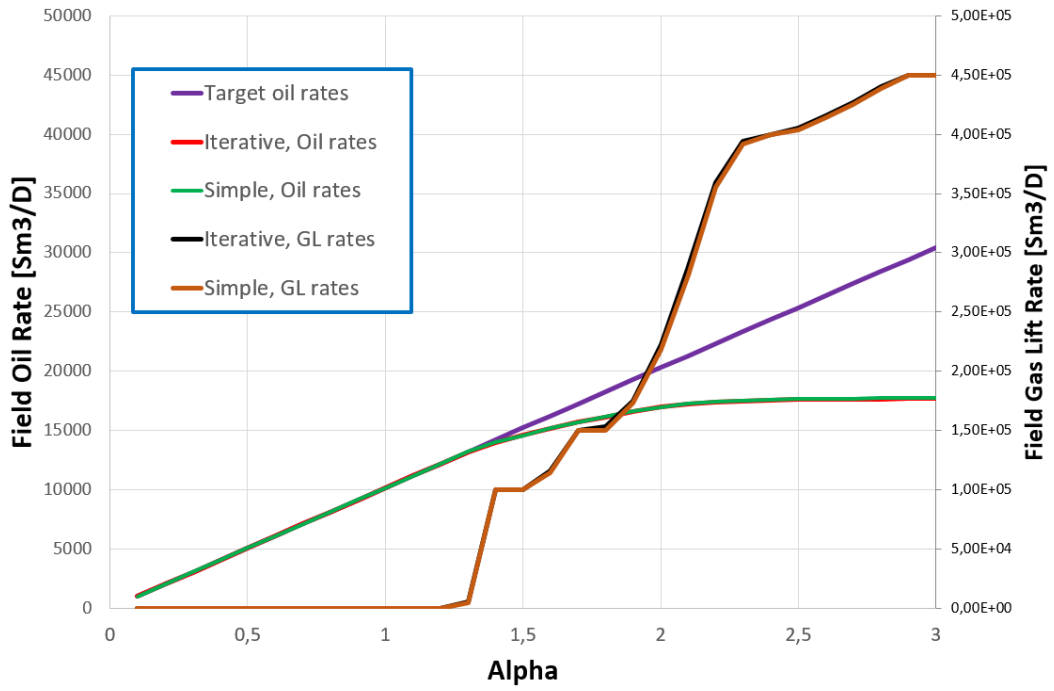
Figure 4.50: Network-model 2, 9 wells: Field rates.
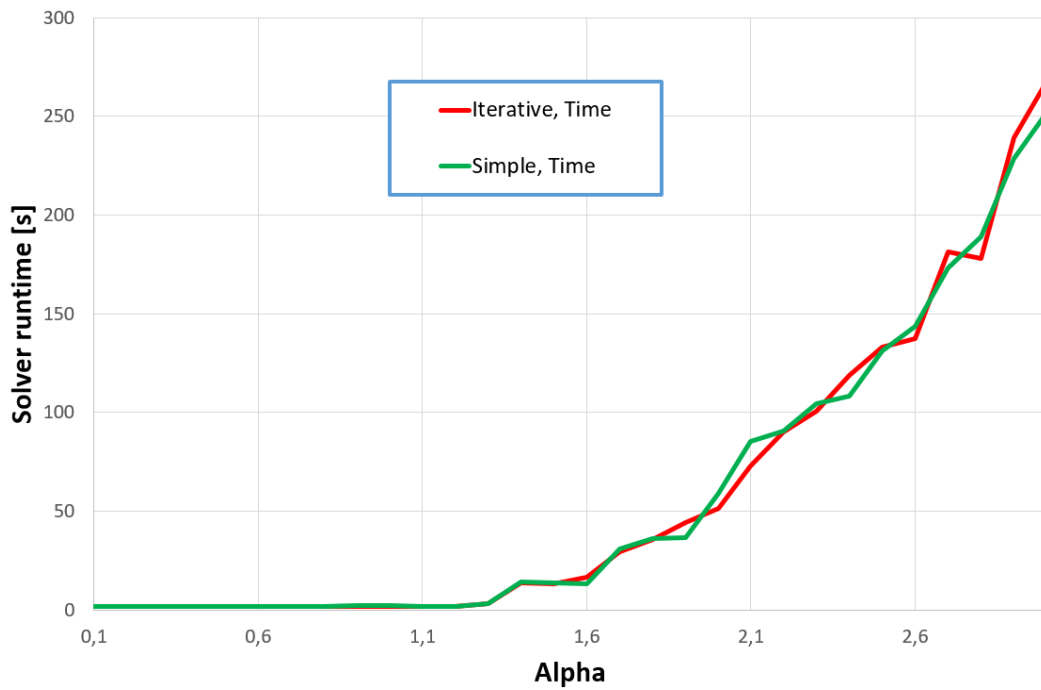
Figure 4.51: Network-model 2, 9 wells: Solver runtime.

4.5. Compositional Model

The Compositional Model is compared with HYSYS, a commercial software by AspenTech. Me-VarT is used for all pressure and temperature calculations in this section. The section is structured in the following way:

- 4.5.1: The fluid properties calculated by the Compositional Model are compared with the same properties calculated by HYSYS.

- 4.5.2: Pressure and temperature profiles are calculated for a given simulation case using the Compositional Model, and compared with the same simulation performed using HYSYS.

- 4.5.3: The performance of the Compositional Model is evaluated.

4.5.1. Comparison of fluid property calculations

Setup:
Fluid property comparison: Densities, viscosities, vapor fraction and Surface Tension are compared for pressure varying from 20 to 100 Bar and three temperatures: 50°C (continuous line), 100°C (long stapled line) and 150°C (short stapled line). The fluid composition is as given in Appendix G. The properties are graphed in the following pages.

Evaluation:
Observations from the graphs are as follows:

- Both liquid and vapor density of the Compositional Model correspond well with the HYSYS values, as seen in Fig. 4.52 and 4.53.

- The Vapor fraction of the Compositional Model is equal to the vapor fraction calculated by HYSYS.

- The LBC liquid viscosity is close, but not completely matching the HYSYS liquid viscosity. This should not affect the results too much, but since the LBC viscosities are a bit lower the frictional pressure drop may be lower as well.

- The gas viscosity calculated using the Lee, Gonzalez method (Eq. 3.34) is quite close to the HYSYS calculated values, while the LBC calculated gas viscosities are not. Thus, the Lee, Gonzalez method is use in all further calculations.

- The gas heat capacities are lower, and the liquid heat capacities are higher, for the Compositional Model compared to HYSYS, as seen in Fig. 4.58 and 4.59. This may somewhat affect the temperature calculations.

- The surface tension of the Compositional Model is a fairly close match to the HYSYS values. The difference should not make a substantial change to the pressure or temperature profiles.
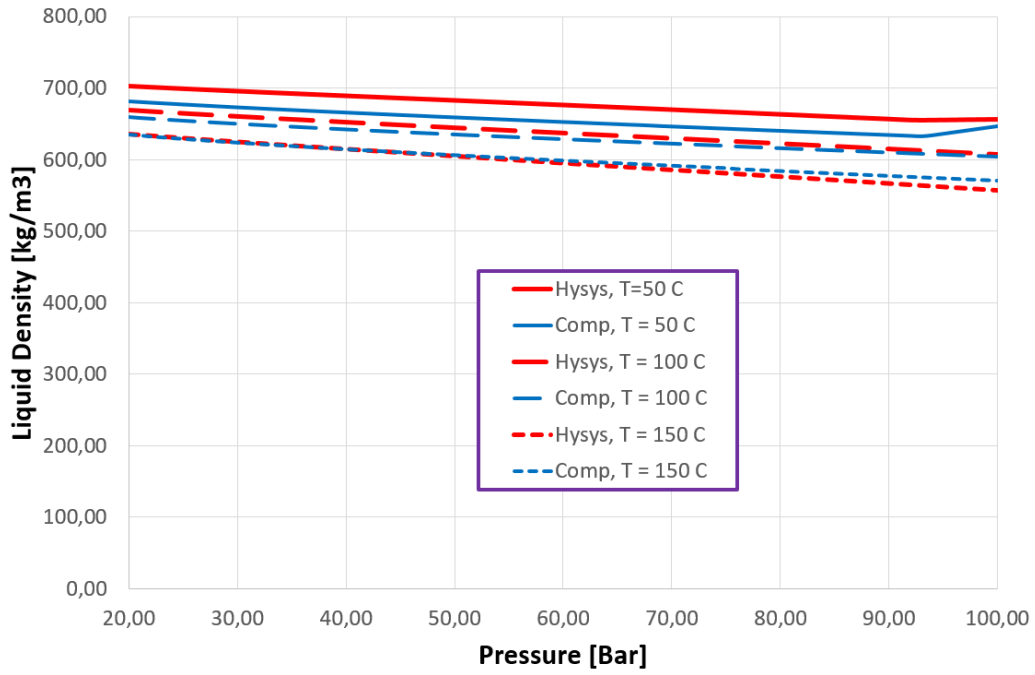
Figure 4.52: Plot of Liquid Density.
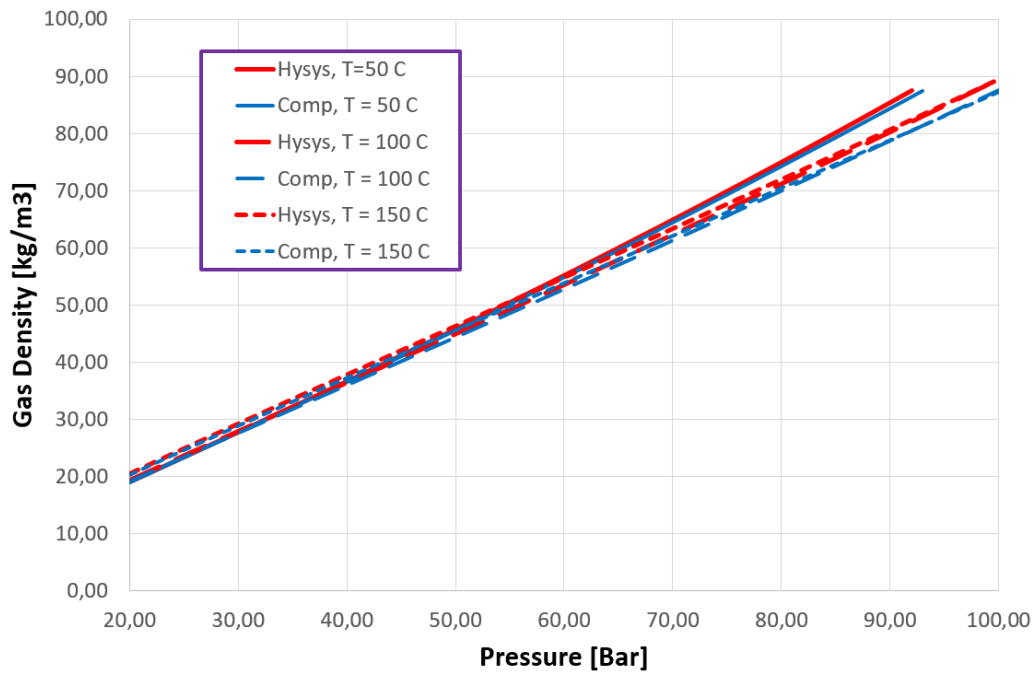
Figure 4.53: Plot of Gas Density.
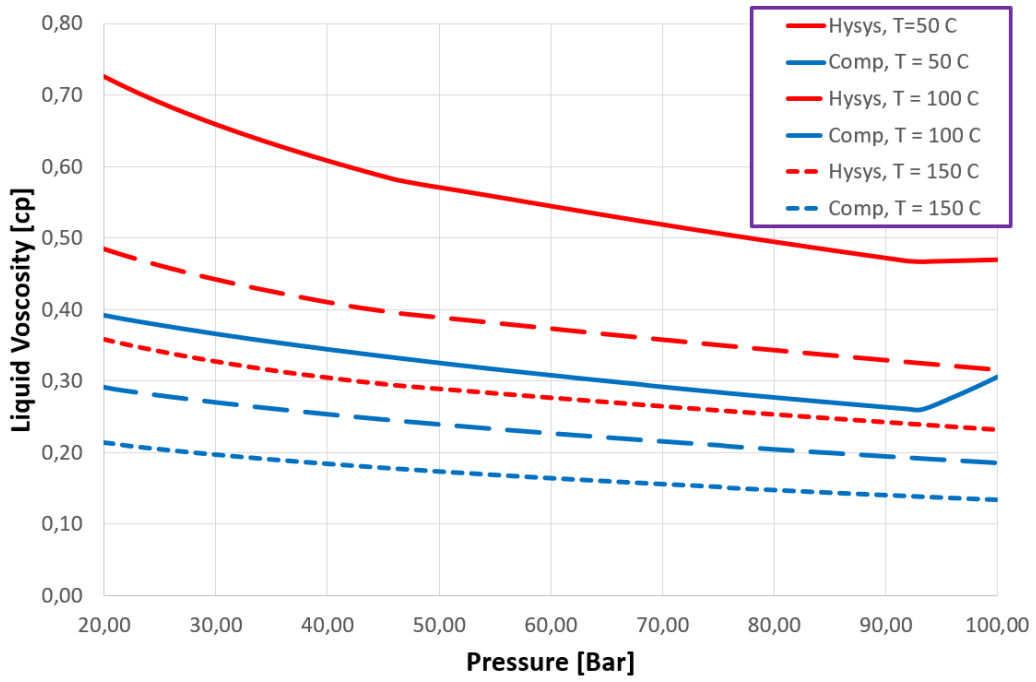
Figure 4.54: Plot of Liquid Viscosity (LBC).
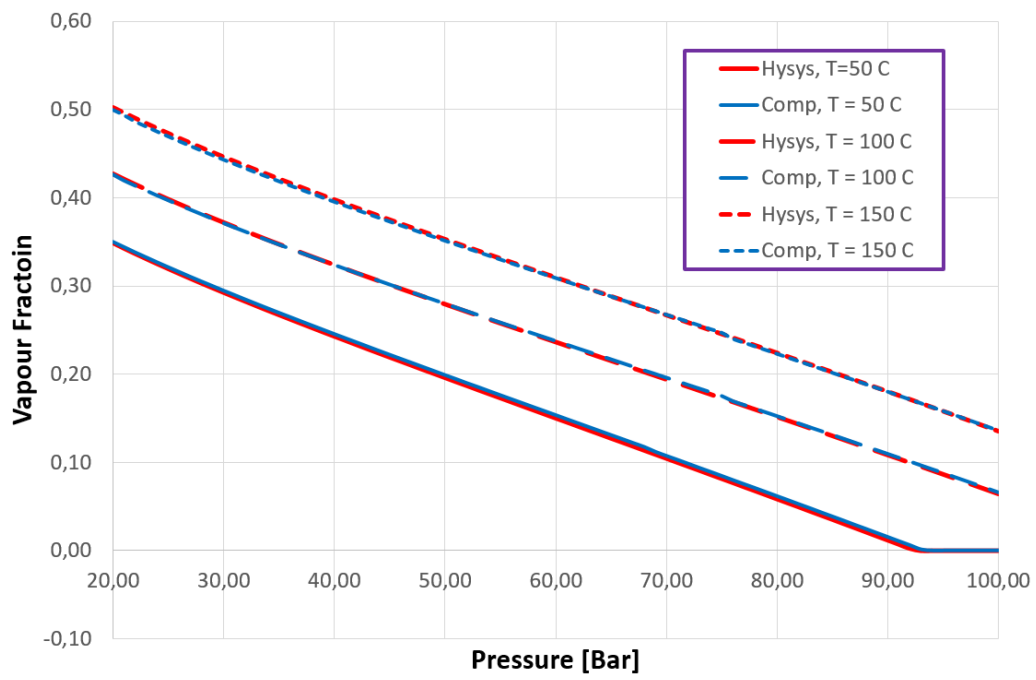
Figure 4.55: Plot of Vapor Fraction.
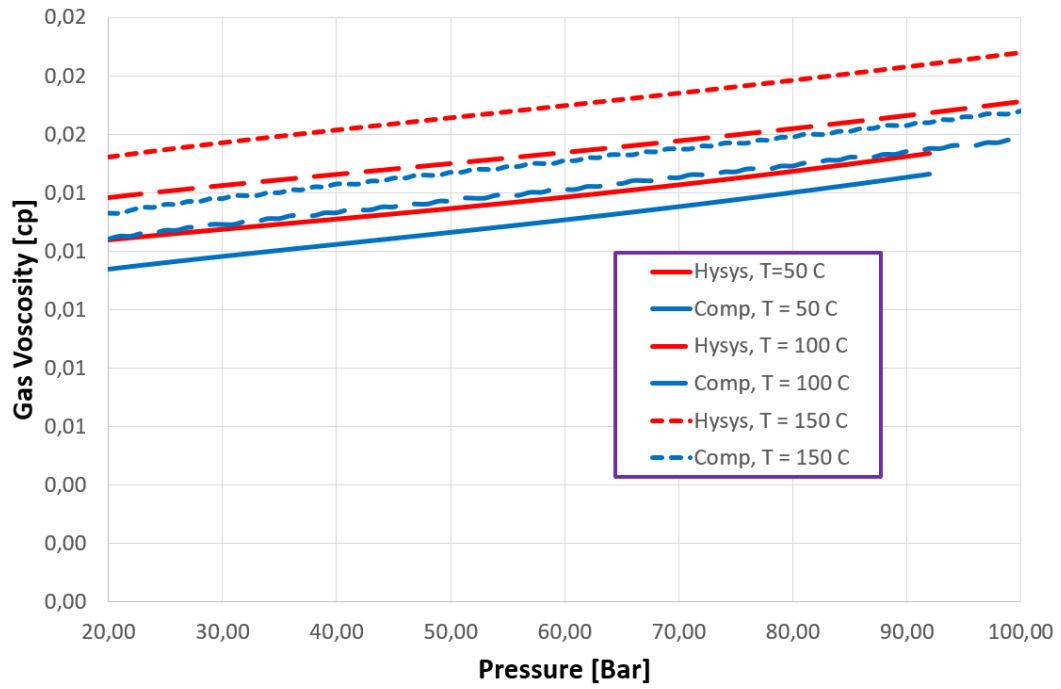
Figure 4.56: Plot of Gas Viscosity (Lee, Gonzalez [32]).
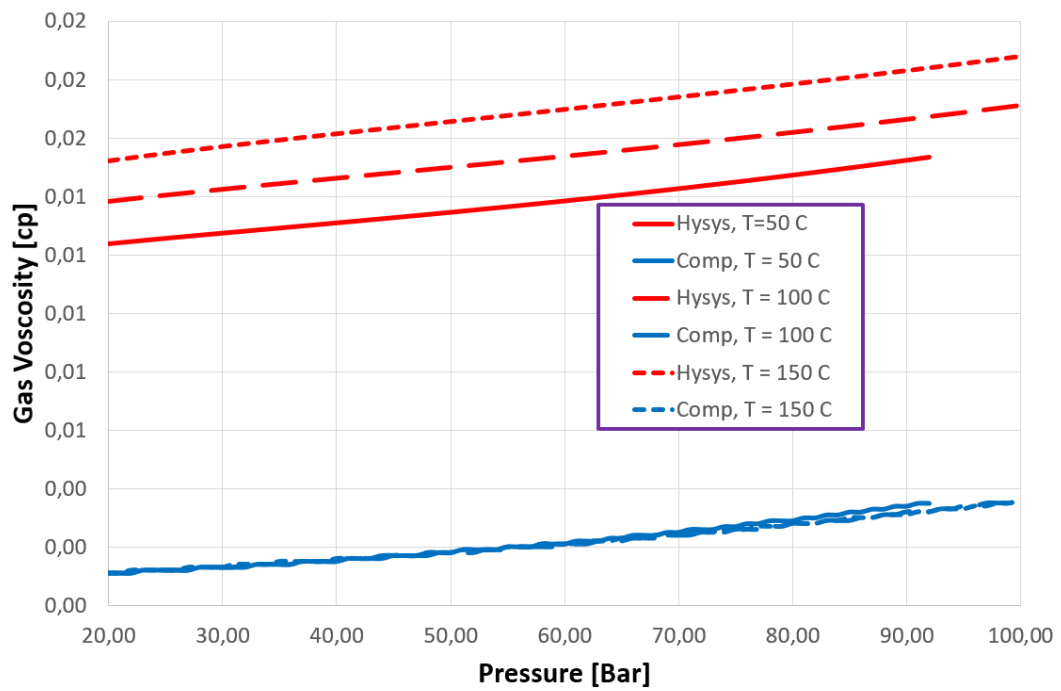
Figure 4.57: Plot of Gas Viscosity (LBC).
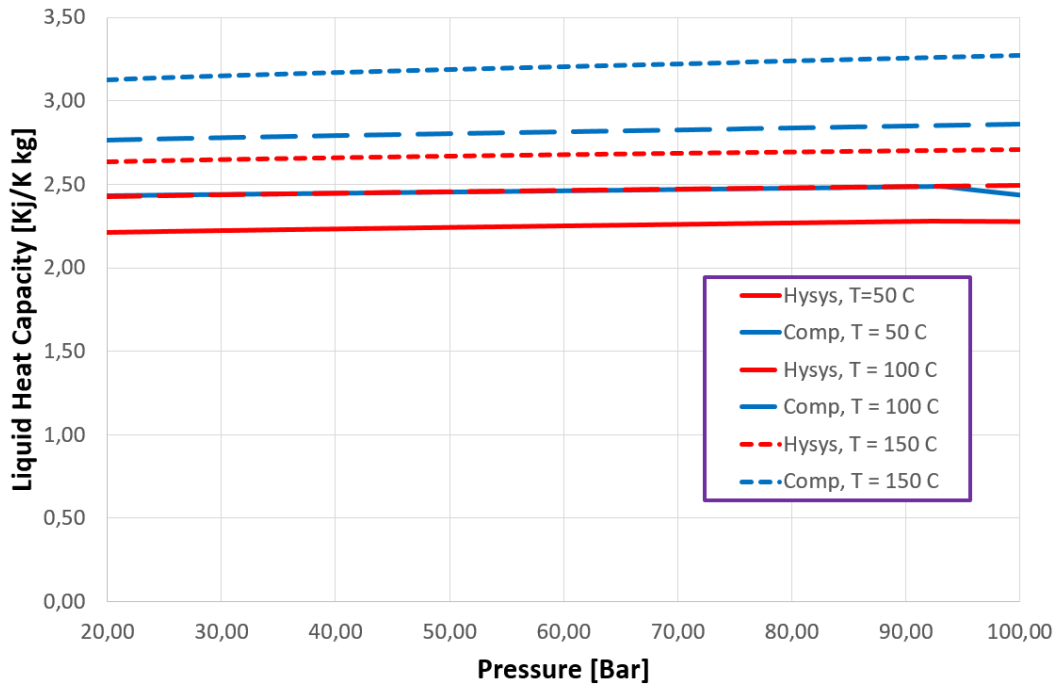
Figure 4.58: Plot of Liquid Heat Capacity.
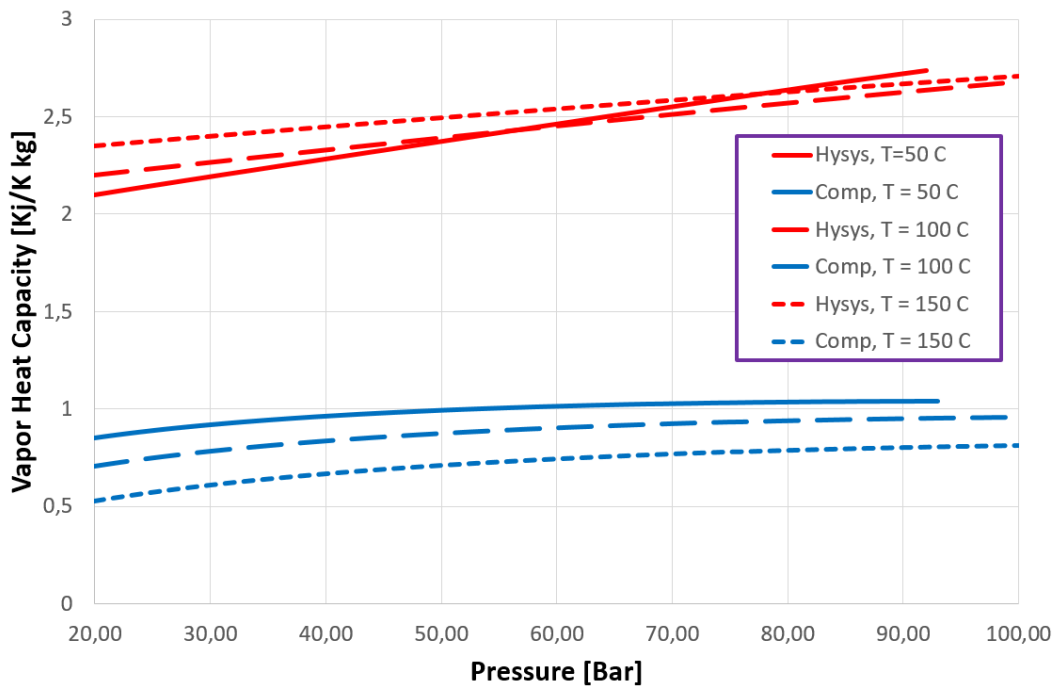
Figure 4.59: Plot of Gas Heat Capacity.
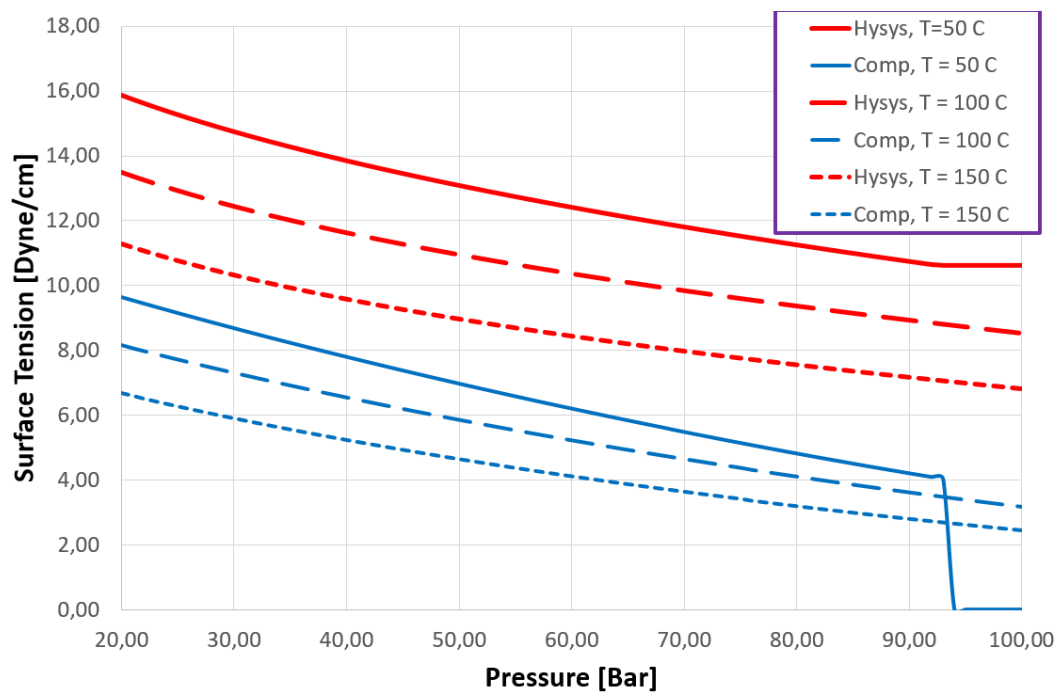
Figure 4.60: Plot of Surface Tension.

4.5.2. Comparison of pressure and temperature profiles

Me-VarT is used together with the Compositional Model and compared with HYSYS in the following simulation case.

Setup:
A surface oil of 1000 Sm3/D is used as a basis for the calculations. The water cut is assumed zero. GOR does not need to be specified, because the surface gas rate is calculated based on fluid composition and surface oil rate (See sec. 3.3).

A simple network structure with a 5000 m horizontal pipe section and 500 m vertical riser section is used. Initial temperature equals 150 °C, and initial pressure equals 100 Bar. The rest of the network properties are as described in Appendix F (STC). All fluid properties, both local and at surface, are calculated using the Compositional Model. In HYSYS, an overall HTC of 5.3 $\frac{W}{m^2 K}$ is assumed. This value is close to the calculated HTC in the simulations. Pressure profiles along with corresponding temperature profiles are graphed on the next page.

Evaluation:
Observations from the graphs are as follows:

- The pressure and temperature profiles correspond well with those of HYSYS.

- This further strengthens the claim that the fluid properties calculated by the Compositional Model are well estimated.

- Me-VarT, already shown to correspond well with Pipesim, also seems to correspond well with HYSYS. This further indicates that Me-VarT is a suitable Simulator configuration for determining pressures and temperatures in the network.
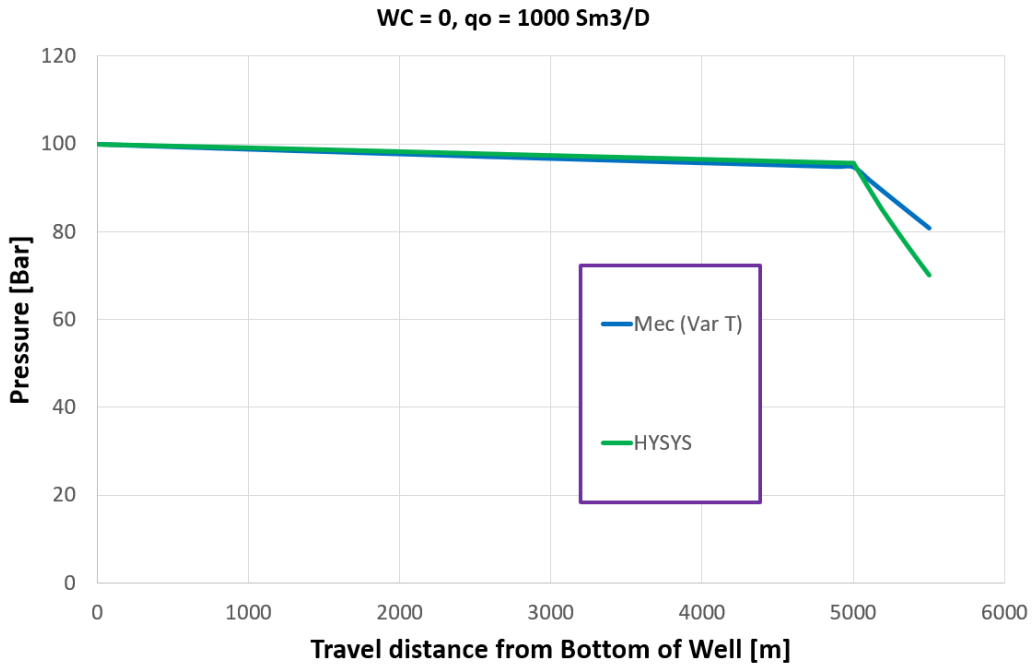
Figure 4.61: Pressure profile along the pipeline.
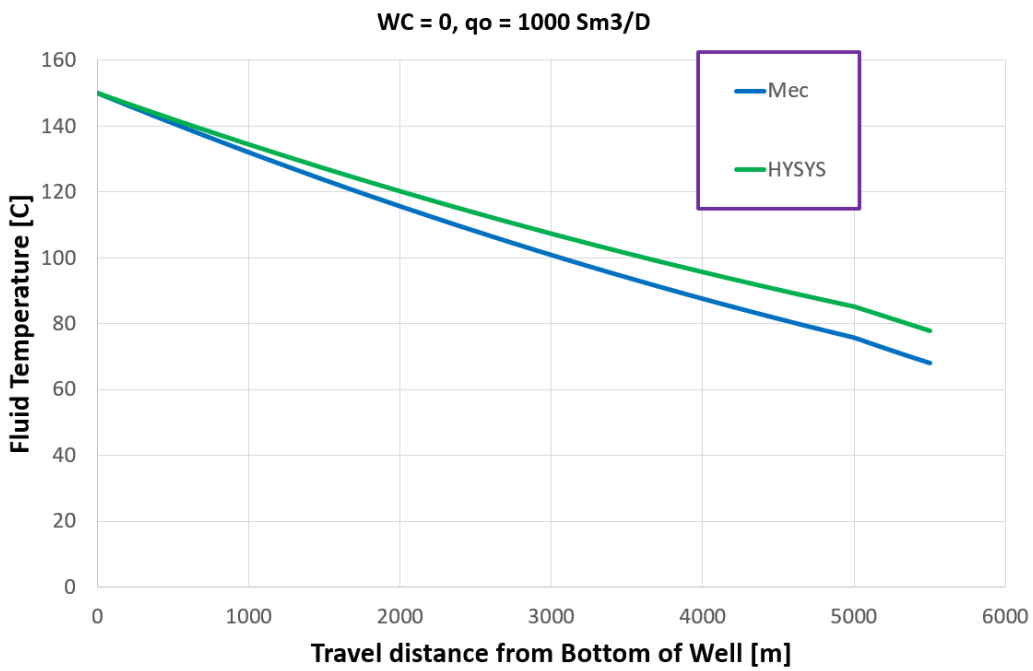
Figure 4.62: Temperature profile along the pipeline.

4.5.3. Performance of the Compositional Model

The runtime of the Compositional Model is quite long compared to the runtime of the black oil model. For a pipeline with only about 50 nodes, the equivalent of 2000 m tubing, 3000 m pipeline and 100 m step length, the runtime is about 2 to 3 minutes[3]. Including gas lift and reducing the initial oil rates requires several re-iterations. For a complicated multiple well-system one complete run of the Network Simulator may take hours. Thus, to evaluate the performance of the Compositional Model, none of the network models used in sec. 4.2 are suited.

Setup:
A single well network is used instead. The tubing length and height is 2000 m, the flowline length and height is 100 m and 30 m respectively, the pipeline length and height is 2000 m and 500 m respectively, and the riser length and height is 100 m. The rest of the network properties are as described in Appendix F (STC). All fluid properties are calculated using the Compositional Model. Me-VarT is used as Simulator configuration. The step length is 100 m.

The performance is evaluated in the same way as in sec. 4.2, using the sequential optimization algorithm (Appendix D)[4]. The base rate ($q_{o, \text{target}}$) is set equal to 1000 Sm3/D, and is multiplied by a factor α that goes from 0.1 to 2 with a step length of 0.1. Water cut equals 0.3, reservoir pressure equals 190 bar, and reservoir temperature equals 100 °C. Gas lift is performed with a 100% methane composition.

---

[3]All simulations are run using the same computer setup. See Appendix H for further details.
[4]See footnote 3.

Evaluation:
Observations from the graphs are as follows:

- For $\alpha \leq 1.6$: Re-calculation is not performed in any of the simulation cases, and the Simulator is only iterated once. The runtime varies from four to five minutes for each simulation.

- For $\alpha \geq 1.6$: The choking pressure becomes negative and the Solver requires re-iterations.

- For $\alpha = 1.7$ the runtime is 54.6 minutes, $q_{o,\,sc}$ = 1700 Sm3/D and $q_{gl,\,sc}$ = 3276.1 Sm3/D. The Optimizer only needs to find the correct gas lift rate.

- For $\alpha = 1.8$ the runtime is 128.5 minutes, $q_{o,\,sc}$ = 1754.5 Sm3/D and $q_{gl,\,sc} = q_{gl,\,sc,\,max}$ = 50,000 Sm3/D. The production from the network is maximized, and the Optimizer will search for a reduced oil rate. Higher α-values will only require the Simulator to run more times, as the initial Δp_{choke} becomes more negative with higher target rates, and the Optimizer needs more attempts at gradually reducing the oil rate. This is seen by an increase in Solver runtime for $\alpha = 1.9$ and $\alpha = 2$.

- The simulations are stable for all production values. As in sec. 4.2, this is indicated by the gas lift rate and the field oil production rate consistently increasing with increased target rate.

- Currently, the Compositional Model is too slow to be used in a practical way together with the Network Solver.

Remarks:
An attempt to improve the runtime was made by inputting the vapor fraction from the previous iteration into the solver as a starting point for the program to search for a new vapor fraction, as this is what determines convergence. This however, had no apparent impact on the runtime.

Improving the runtime of the Compositional Model is a possible topic for further work.
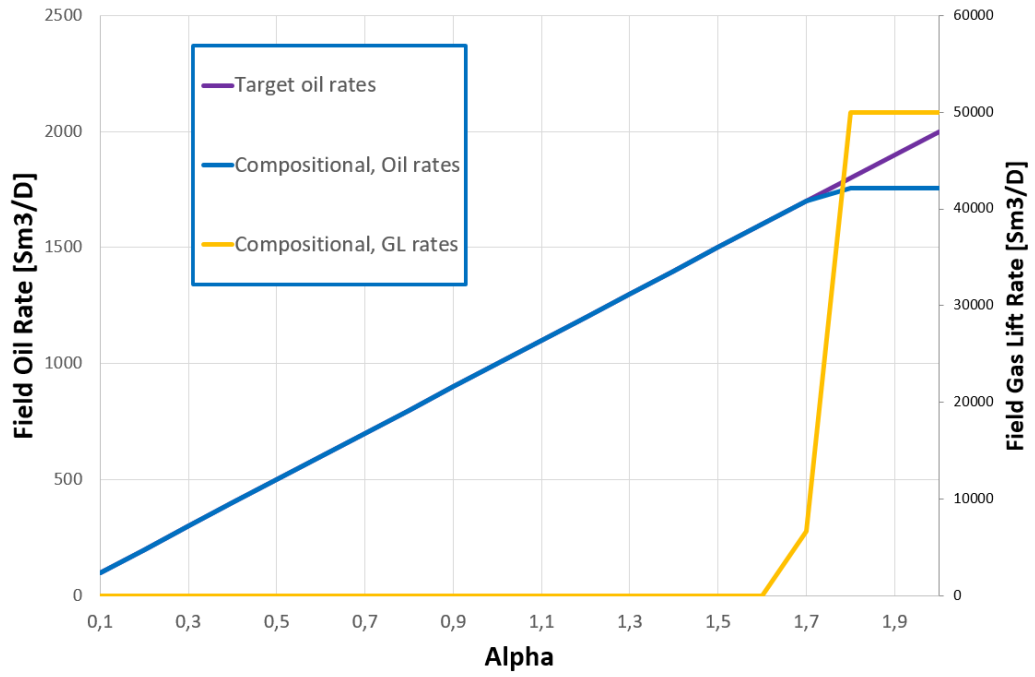
Figure 4.63: Performance of Compositional Model: Field rates.
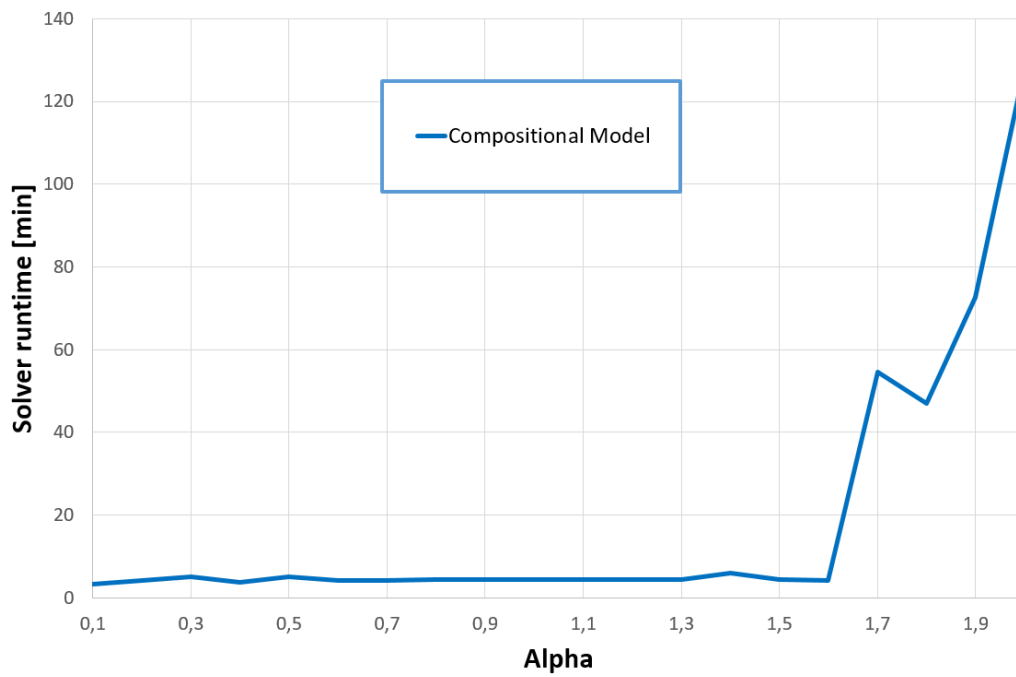
Figure 4.64: Performance of Compositional Model: Solver runtime.

4.6. Material Balance

Setup:

A simple material balance simulation case was created. The procedure of calculating the reservoir pressure is as described in sec. 3.4. No water is produced from the reservoir. The STC-properties (Appendix F) are used. The specific material balance properties are as follows:

Property	Value	Unit
IOIP	$2.5 \cdot 10^6$	Sm^3
IGIP	0	Sm^3
IWIP	15·IOIP	Sm^3
$q_{o, sc}$	500	$\frac{Sm^3}{D}$
C_{res}	$1.45 \cdot 10^{-4}$	Bar^{-1}
C_w	10^{-4}	Bar^{-1}
Prod. Days	350	$Year^{-1}$

Evaluation:

Observations from the graphs are as follows:

- Reservoir pressure decreases with time and production. Initially the choke is partially closed, but as reservoir pressure gradually decreases, the choke opens, and the well needs to be produced with gas lift in stead.

- In the final year the reservoir pressure is too low to produce further. Thus no choking pressure or production rates are found by the Network Solver.

Remarks:

Currently the model assumes that the composition of the reservoir is constant over time. For instance, if the reservoir initially is an undersaturated oil reservoir, and the reservoir pressure goes below the bubble point, the Material Balance Model will still assume an undersaturated oil reservoir. Other simplifications, such as the reservoir temperature being assumed constant over time, makes this Material Balance Model far from ideal. The model also relies heavily on the formation volume factor calculations being accurate, as only this determines the new reservoir pressure. Thus, if a better representation is needed, a more accurate model should be developed.
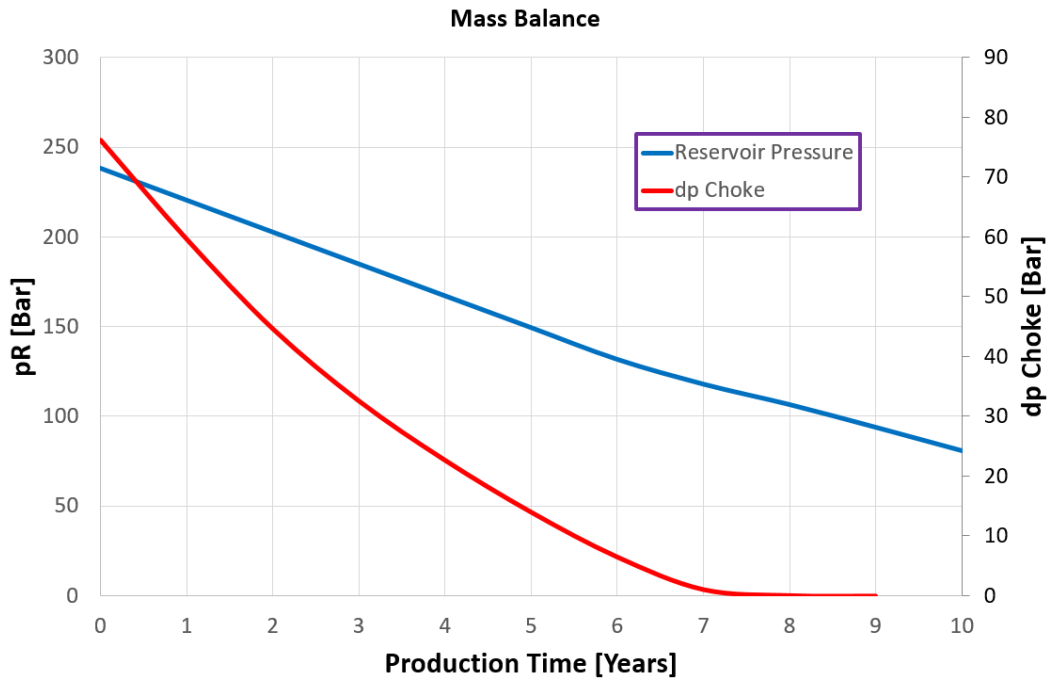
Figure 4.65: Plot of the Reservoir Pressure and the Choking Pressure over time.
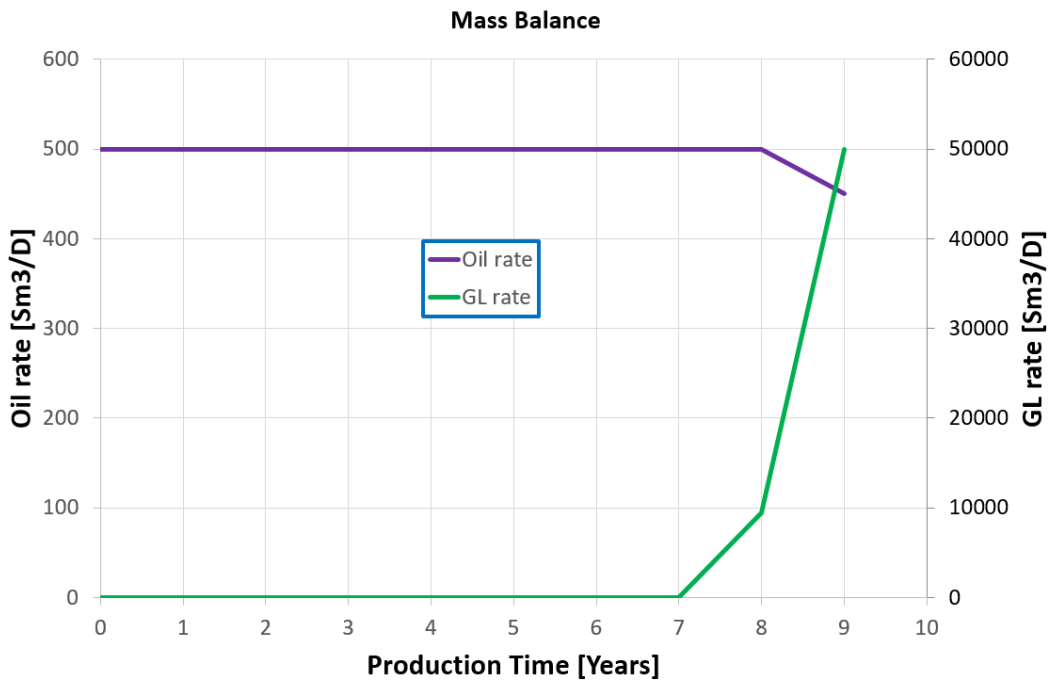
Figure 4.66: Plot of the Oil production rate and the Gas Lift rate over time.

5. Recommendations for further work

1. Further develop the Material Balance Model to be more versatile and precise, as described in the remarks in sec. 4.6.

2. Investigate methods for improving the runtime of the Compositional Model.

3. Implement formulas in the Compositional Model to better estimate the surface tension, the heat capacity and the liquid viscosity, so that they come closer to the results of HYSYS. The Pedersen et Al. (1987,[33]) compositional viscosity correlation may for instance be considered as an alternative to the LBC correlation.

4. Extend the Optimizer and include the possibility of maximizing economical return rather than formation rates.

6. Conclusions

1. The mechanistic approach calculates pressure profiles corresponding well with Pipesim. The pressure drop method returns valid results for several different variations of the network, water cut, GOR and production rate.

2. The temperature calculations seem to be in close correspondence with Pipesim, indicating valid results.

3. The Compositional Model returns good results compared with HYSYS. It is currently too slow to be used efficiently together with the Network Solver.

4. The Material Balance Model is a simple but useful addition to the Network Solver. It has its limitations, but works well together with the Network Solver.

7. References

Note: A lot of the correlations are gathered from the course TPG4245 ("Production Wells"), petrowiki.org and fekete.com [1] and [15], but the correlations are cited with their original source.

References

[1] Fekete.com. *"Oil Correlations"*. URL: http://fekete.com/SAN/TheoryAndEquations/HarmonyTheoryEquations/Content/HTML_Files/Reference_Material/Calculations_and_Correlations/Oil_Correlations.htm

[2] Standing, M.B. 1947. *"A Pressure-Volume-Temperature Correlation for Mixtures of California Oil and Gases"*. New York, New York: Standard Oil Co. of California. URL: https://www.onepetro.org/conference-paper/API-47-275

Fekete.com:
http://fekete.com/SAN/TheoryAndEquations/WellTestTheoryEquations/Standing.htm

[3] Neely, A.B. 1967. *"Use of IPR Curves"*. Houston, Texas: Shell Oil Co.

Petrowiki.org:
http://petrowiki.org/Oil_well_performance

[4] Standing, M.B. and Katz, D.L. 1942. *"Density of Natural Gases"*. Trans., A.I.M.E. URL: https://www.onepetro.org/download/journal-paper/SPE-942140-G?id=journal-paper%2FSPE-942140-G

[5] Sutton, R.P. 1985. *Compressibility Factors for High-Molecular-Weight Reservoir Gases*. Presented at the SPE Annual Technical Conference and Exhibition, Las Vegas, Nevada, USA, 22-26 September. URL: http://dx.doi.org/10.2118/14265-MS

Petrowiki.org:
http://petrowiki.org/Real_gases#cite_note-r4-4

[6] Hall, K.R. and Yarborough, L. 1973. *"A New EOS for Z-factor Calculations"*. Oil and Gas Journal (18. June, p82). URL: https://www.researchgate.net/publication/284299884_A_new_equation_of_state_for_Z-factor_calculations

Course of Curtis H. Whitson, TPG4145:
http://www.ipt.ntnu.no/c̃urtis/courses/PVT-Flow/2013-TPG4145/e-notes/PVT-Papers/SPEPBM-Ch3.pdf

[7] Yarborough, L. and Hall, K.R. 1974. *"How to Solve EOS for Z-factors"*. Oil and gas Journal (18. February, p86).

[8] Vasquez, M.E. and Beggs, H.D. June 1980. *"Correlations for Fluid Physical Property Prediction"*. J Pet Technol Volume 32, issue 06: p 968 - 970. URL: https://www.onepetro.org/journal-paper/SPE-6719-PA

[9] Glasø, Ø. 1980. *"Generalized Pressure-Volume-Temperature Correlations"*. J Pet Technol Volume 32, issue 5: p 785-795. URL: http://dx.doi.org/10.2118/8016-PA

[10] Standing, M.B. 1981. *"Volumetric and Phase Behavior of Oil Field Hydrocarbon Systems"*. Ninth edition. Richardson, Texas: Society of Petroleum Engineers of AIME. URL: http://dl1.ponato.com/eb1/1154__72a63fd.pdf

[11] Chew, J. and Connally, C.A. Jr. 1959. *"A Viscosity Correlation for Gas-Saturated Crude Oils"*. In Transactions of the American Institute of Mining, Metallurgical, and Petroleum Engineers, Vol. 216, 23. Dallas, Texas: Society of Petroleum Engineers of AIME. URL: https://www.onepetro.org/general/SPE-1092-G

[12] Beal, C. 1946. *"The Viscosity of Air, Water, Natural Gas, Crude Oil and Its Associated Gases at Oil Field Temperatures and Pressures"*. No. 3, 114–127. Richardson, Texas: Reprint Series (Oil and Gas Property Evaluation and Reserve Estimates), SPE. URL: https://www.onepetro.org/journal-paper/SPE-946094-G

[13] Carr, N.L., Kobayashi, R., and Burrows, D.B. 1954. *Viscosity of Hydrocarbon Gases Under Pressure*. J Pet Technol, Vul. 6, issue 10, p 47-55. SPE-297-G. URL: http://dx.doi.org/10.2118/297-G

[14] Dempsey, J.R. 1965. *"Computer routine treats gas viscosity as a variable"*. Oil and Gas Journal, Vol. 63, p 141.

[15] Fekete.com. *"Pressure Loss Calculations"*. URL: http://fekete.com/SAN/TheoryAndEquations/HarmonyTheoryEquations/Content/HTML_Files/Reference_Material/Calculations_and_Correlations/Pressure_Loss_Calculations.htm#Beggs_and_Brill_Correlation

[16] Fekete.com. *"Material Balance Analysis Theory"*. URL: http://www.fekete.com/SAN/WebHelp/FeketeHarmony/Harmony_WebHelp/Content/HTML_Files/Referenc

[17] Sintef.no. Url: http://www.sintef.no/projectweb/mrst/

[18] Codas, A.D. March 2016. *Contributions to production optimization of oil reservoirs*. Ph.D.-thesis, NTNU, Trondheim.

[19] Petrowiki. *"Gas lift"*. URL: http://petrowiki.org/Gas_lift

[20] Weinaug, C.F. and Katz, D.L. 1943. *Surface Tensions of Methane-Propane Mixtures*. Ind. & Eng. Chem. (1943) 35, p. 239-246. URL: http://pubs.acs.org/doi/pdf/10.1021/ie50398a028

[21] Katz, D.L. and Saltman, W. 1939. *Surface Tension of Hydrocarbons*. (January 1939) 31, p. 9.-94. URL: http://pubs.acs.org/doi/abs/10.1021/ie50349a019

[22] Shmueli, A. 2010. *Documentation_of_the_multiphase_flow_code*.

[23] Shoham, O. 2006. *Mechanistic Modeling of Gas-Liquid Two-Phase Flow in Pipes*. Chap. 6, p. 297-299.

[24] Sagar, R., Doty, D. R., & Schmidt, Z. (1991, November 1). *Predicting Temperature Profiles in a Flowing Well*. Society of Petroleum Engineers. doi:10.2118/19702-PA. URL: https://www.onepetro.org/journal-paper/SPE-19702-PA

[25] Hasan, A. R., & Kabir, C. S. (1994, August 1). *Aspects of Wellbore Heat Transfer During Two-Phase Flow*. Society of Petroleum Engineers. doi:10.2118/22948-PA. URL: https://www.onepetro.org/journal-paper/SPE-22948-PA

[26] Marius, S. M. December 2015. *Applications of Equations of State in Relief Well Kill Simulation - A preliminary work*. Specialization project.

[27] Flatebakken, V. December 2016. *Standalone Network Solver with gas lift optimization*. Specialization project.

[28] Whitson, C.H., Brulé, M.R. 2000. *PHASE BEHAVIOR*, SPE Monograph, Vol. 20. URL: http://www.ipt.ntnu.no/c̃urtis/courses/PVT-Flow/2017-TPG4145/Monograph/SPE%20Phase%20Behavior%20monograph.pdf

[29] XSteam software. URL: https://se.mathworks.com/matlabcentral/fileexchange/9817-x-steam–thermodynamic-properties-of-water-and-steam

[30] Hysys help guide. URL: http://people.clarkson.edu/ wwilcox/Design/HYSYSpropSelect.pdf

[31] Lohrenz, J., Bray, B.G., and Clark, C.R. October 1964. *Calculating Viscosities of Reservoir Fluids From Their Compositions* 1171; Trans., AIME, 231. URL: https://www.onepetro.org/journal-paper/SPE-915-PA

[32] Lee, A.L., Gonzalez, M.H., and Eakin, B.E. August 1966. *The Viscosity of Natural Gases.* JPT (August 1966) 997; Trans., AIME, 237. URL: https://www.onepetro.org/journal-paper/SPE-1340-PA

[33] Pedersen, K.S. and Fredenslund, A. 1987. *An Improved Corresponding States Model for the Prediction of Oil and Gas Viscosities and Thermal Conductivities.* Chem. Eng. Sci. Vol. 42: p. 182-186. URL: http://www.sciencedirect.com/science/article/pii/0009250987802257

Appendices

A. Fluid property calculation ("local_properties.m")

If the input gas lift rate is greater than zero, this rate is added to the formation gas rate to create a total surface gas rate ($q_{g, tot}$). The GOR (Gas Oil Ratio) and γ_g (specific gas gravity) is updated based on this total rate (note that all properties other than p and T are at surface conditions, and that all correlations are given in SI Units, unless specified otherwise. Also note that all surface densities and specific gravities are given by the user in the "main.m" script):

$$q_{g, tot} = q_{g, formation} + q_{gl} \tag{A.1}$$

$$GOR = \frac{q_{g, tot}}{q_o} \tag{A.2}$$

$$\gamma_{g, tot} = \frac{(q \cdot \gamma)_{g, formation} + (q \cdot \gamma)_{gl}}{q_{g, tot}} \tag{A.3}$$

Further on the notation "g" will indicate the mixture of formation gas and gas lift. The fluid mixture bubble point is then calculated using (Standing, M.B. 1947 [2]) ("bubble_point.m"):

$$p_b = 1.255 \cdot \left(\frac{GOR}{0.0059 \cdot \gamma_g \cdot 10^{2.14/\gamma_o - 0.00198 \cdot T}} \right)^{0.83} - 1.76 \tag{A.4}$$

The Solution Gas Oil Ratio (R_s) is calculated using the same correlation (exchanging GOR for R_s and p_b for p) with $R_s \approx GOR$ for $p \geq p_b$.

Z-factor ("z_Standing.m")

The Z-factor is calculated using the Hall and Yarborough ([6] and [7]) representation of the Standing-Katz (1942, [4]) diagram with the pseudocritical properties of hydrocarbon mixtures from the Sutton (1985, [5]) correlation (in field units):

$$T_{pc} = 169.2 + 349.5 \cdot \gamma_g - 74 \cdot \gamma_g^2 \tag{A.5}$$

$$p_{pc} = 756.8 - 131.07 \cdot \gamma_g - 3.6 \cdot \gamma_g^2 \tag{A.6}$$

$$T_{pr} = \frac{T + 460}{T_{pc}} \tag{A.7}$$

$$p_{pr} = \frac{p}{p_{pc}} \tag{A.8}$$

$$t = \frac{1}{T_{pr}} \tag{A.9}$$

$$a = 0.06125 \cdot t \cdot e^{-1.2 \cdot (1-t)^2} \tag{A.10}$$

$$0 = -a \cdot p_{\text{pr}} + \frac{y + y^2 + y^3 - y^4}{(1-y)^3} - (14.76 \cdot t - 9.76 \cdot t^2$$
$$+ 4.58 \cdot t^3) \cdot y^2 + (90.7 \cdot t - 242.2 \cdot t^2 + 42.4 \cdot t^3) \cdot y^{2.18+2.82 \cdot t} \tag{A.11}$$

$$z = a \cdot \frac{p_{\text{pr}}}{y} \tag{A.12}$$

Where:

- T_{pc} and p_{pc} are the pseudocritical temperature and pressure.

- T_{pr} and p_{pr} are the pseudoreduced temperature and pressure.

- y is the reduced-density parameter (found by a Newton-Raphson scheme).

- z is the resulting z-factor.

Water properties

All water properties, including water density, viscosity and specific heat capacity, are calculated using a free third party matlab script called "XSteam.m", which "provides accurate steam and water properties from 0 - 1000 bar and from 0 - 2000 deg C according to the standard IAPWS IF-97"[29].

Formation Volume Factors ("FVF.m")

Gas FVF is calculated from the Real Gas Law:

$$B_g = \frac{p_{\text{sc}} \cdot T \cdot z}{p \cdot T_{\text{sc}}} \tag{A.13}$$

Oil FVF is calculated for saturated oil in SI units (Standing, M.B. 1947 [2]):

$$B_o = 0.9759 + 0.952 \cdot 10^{-3} \cdot \left[R_s \cdot \left(\frac{\gamma_g}{\gamma_o} \right)^{0.5} + 0.401 \cdot T - 103 \right]^{1.2} \qquad , p \leq p_b \tag{A.14}$$

Oil FVF is calculated for undersaturated oil (Standing, M.B. 1947 [2]) using the Vazquez and Beggs (1980, [8]) correlation for oil compressibility:

$$c_o = 10^{-4} \cdot \frac{2.81 \cdot R_s + 3.10 \cdot T + \frac{171}{\gamma_o} - 118 \cdot \gamma_g - 1102}{p} \tag{A.15}$$

$$B_o = B_{\text{ob}} \cdot e^{-c_o \cdot (p - p_b)} \qquad , p \geq p_b \tag{A.16}$$

Where:

- Where B_{ob} is calculated using (A.14) $\left[\frac{m^3}{Sm^3}\right]$.

- C_o is the oil compressibility $[Bar^{-1}]$.

- p_{sc} and T_{sc} are the pressure and temperature at Standard Conditions.

B_w is calculated from "XSteam.m" [29].

Local fluid rates

The local (in situ) fluid rates are calculated using:

$$q_{g,\,local} = (q_g - R_s \cdot q_o) \cdot B_g \tag{A.17}$$

$$q_{o,\,local} = q_o \cdot B_o + R_s \cdot q_o \cdot B_g \tag{A.18}$$

$$q_{w,\,local} = q_w \cdot B_w \tag{A.19}$$

$$q_{l,\,local} = q_{o,\,local} + q_{w,\,local} \tag{A.20}$$

Local fluid densities

The local (in situ) fluid densities are calculated using:

$$\rho_{g,\,local} = \frac{\rho_g}{B_g} \tag{A.21}$$

$$\rho_{o,\,local} = \frac{\rho_o + \rho_g \cdot R_s}{B_o} \tag{A.22}$$

$$\rho_{w,\,local} = \frac{\rho_o}{B_o} \tag{A.23}$$

$$\rho_{l,\,local} = \frac{\rho_o \cdot q_{o,\,local} + \rho_w \cdot q_{w,\,local}}{q_{l,\,local}} \tag{A.24}$$

Local fluid viscosities ("oil_visc_standing.m" and "gas_visc.m")

Gas viscosity at standard conditions is calculated using the Carr, Kobayashi and Burrows (1954, [13]) correlation (in SI units) ("dead_visc_gas.m"):

$$\mu_g^0 = (3.0764 \cdot 10^{-5} - 3.712 \cdot 10^{-6} \cdot \gamma_g) \cdot (T_{sc} - 256) + 8.188 \cdot 10^{-3} - 6.15 \cdot 10^{-3} \cdot \log_{10}(\gamma_g) \tag{A.25}$$

Carr, Kobayashi and Burrows (1954, [13]) presented a diagram for calculating gas viscosity affected by temperature (i.e. at local conditions). Dempsey (1965, [14]) suggested a mathematical representation of the diagram:

$a_0 = -2.46211820$	$a_4 = 2.80860949$	$a_8 = -0.793385684$	$a_{12} = 8.39387178 \cdot 10^{-2}$
$a_1 = 2.97054714$	$a_5 = -3.49803305$	$a_9 = 1.39643306$	$a_{13} = -0.186408848$
$a_2 = -0.286264054$	$a_6 = 0.360373020$	$a_{10} = -0.149144925$	$a_{14} = 2.03367881 \cdot 10^{-2}$
$a_3 = 8.05420522 \cdot 10^{-3}$	$a_7 = -1.044324 \cdot 10^{-2}$	$a_{11} = 4.41015512 \cdot 10^{-3}$	$a_{15} = -6.09579263 \cdot 10^{-4}$

$$\ln\left[T_{\text{pr}} \cdot \frac{\mu_{\text{g, local}}}{\mu_g^0}\right] = a_0 + a_1 \cdot p_{\text{pr}} + a_2 \cdot p_{\text{pr}}^2 + a_3 \cdot p_{\text{pr}}^3 + T_{\text{pr}} \cdot \left(a_4 + a_5 \cdot p_{\text{pr}} + a_6 \cdot p_{\text{pr}}^2 + a_7 \cdot p_{\text{pr}}^3\right)$$
$$+ T_{\text{pr}}^2 \cdot \left(a_8 + a_9 \cdot p_{\text{pr}} + a_{10} \cdot p_{\text{pr}}^2 + a_{11} \cdot p_{\text{pr}}^3\right) + T_{\text{pr}}^3 \cdot \left(a_{12} + a_{13} \cdot p_{\text{pr}} + a_{14} \cdot p_{\text{pr}}^2 + a_{15} \cdot p_{\text{pr}}^3\right)$$

(A.26)

Dead oil viscosity is calculated using the Glasø (1980, [9]) correlation with field units (°F and cp) ("dead_visc_oil.m"):

$$\mu_{\text{od}} = 3.141 \cdot 10^{10} \cdot T^{-3.444} \cdot \log_{10}(API)^{10.313 \cdot \log_{10}(T) - 36.447}$$

(A.27)

Where:

- API is the "API oil gravity".

- μ_{od} is the dead oil viscosity (free of gas) [cp].

For saturated oil a mathematical representation of Chew and Connally's (1959, [11]) diagram was developed by Standing (1981, [10]) to calculate the viscosity:

$$a = 10^{R_s \cdot (6.9 \cdot 10^{-6} \cdot R_s - 4.2 \cdot 10^{-3})}$$

(A.28)

$$b = 0.68 \cdot 10^{-4.84 \cdot 10^{-4} \cdot R_s} + 0.25 \cdot 10^{-6.18 \cdot 10^{-3} \cdot R_s} + 0.062 \cdot 10^{-2.1 \cdot 10^{-7} \cdot R_s}$$

(A.29)

$$\mu_{\text{o, local}} = a \cdot (\mu_{\text{od}})^b \qquad , p \le p_b$$

(A.30)

For undersaturated oil the Beal (1946, [12]) correlation is used (units in cp and Bar):

$$\mu_{\text{o, local}} = \mu_{\text{ob}} + 10^{-3} + \cdot \left(\mu_{\text{ob}}^{1.6} + 0.55 \cdot \mu_{\text{ob}}^{0.56}\right) \cdot \left(p - p_b\right) \qquad , p \ge p_b$$

(A.31)

Where:

- μ_{ob} is the bubble oil viscosity [cp] calculated using (A.30).

- $\mu_{\text{o, local}}$ is the local oil viscosity [cp].

$\mu_{\text{w, local}}$ is calculated using "XSteam.m" ([29]).

Liquid viscosity is calculated using the same procedure as Hysys [30]:

$$\mu_{\text{l, local}} = \mu_{\text{o}} \cdot e^{3.6 \cdot (1 - f_{\text{o, local}})} = a \qquad\qquad , f_{\text{o, local}} \ge 0.5$$

(A.32)

$$\mu_{\text{l, local}} = \mu_w \cdot \left[1 + 2.5 \cdot f_{\text{o, local}} \cdot \frac{\mu_o + 0.4 \cdot \mu_w}{\mu_o + \mu_w}\right] = b \qquad , f_{\text{o, local}} \le 0.33$$

(A.33)

$$\mu_{\text{l, local}} = \frac{\left(f_{\text{o, local}} - 0.33\right) \cdot a + \left(0.5 - f_{\text{o, local}}\right) \cdot b}{0.5 - 0.33} \qquad , 0.33 < f_{\text{o, local}} < 0.5$$

(A.34)

Where:

- $f_{\text{o, local}} = \frac{q_{\text{o, local}}}{q_{\text{l, local}}}$ is the local oil fraction with respect to liquid.

Local Surface tension

The local surface tension is calculated using:

$$\text{IFT}_{\text{og}} = \left[\frac{567 \cdot (\rho_o - \rho_g) \cdot 0.001}{213} \right]^4 \tag{A.35}$$

$$\text{IFT}_{\text{wg}} = 72.75 \cdot \left[1 - 0.001171 \cdot (T - 60) + 0.000001121 \cdot (T - 60)^2 \right] \tag{A.36}$$

$$\text{ST} = 0.001 \cdot \left[(f_w + 1) \cdot \text{IFT}_{\text{og}} + f_w \cdot \text{IFT}_{\text{wg}} \right] \tag{A.37}$$

Where:

- IFT is the liquid/gas interfacial tension [dyn/cm].

- Densities given in kg/m3, temperature given in °F.

- ST is the surface tension [N/m].

Local Specific Heat Capacity

$$K_{\text{w, oil}} = \frac{T_{\text{b, o}}^{\frac{1}{3}}}{\gamma_o} \tag{A.38}$$

$$K_{\text{w, gas}} = \frac{T_{\text{b, g}}^{\frac{1}{3}}}{\gamma_g} \tag{A.39}$$

$$C_{\text{p, o}} = \left[(0.055 \cdot K_{\text{w, oil}}) + 0.35 \right] \cdot \left\{ \left[0.6811 - (0.308 \cdot \gamma_o) \right] + \left[T \cdot (0.000815 - 0.000306 \cdot \gamma_g) \right] \right\} \cdot 4186.8 \tag{A.40}$$

$$C_{\text{p, g}} = \left(\frac{4 - \gamma_g}{6450} \right) \cdot (T + 670) \cdot \left[(0.12 \cdot K_{\text{w, gas}}) - 0.41 \right] \cdot 4186.8 \tag{A.41}$$

Where:

- C_p is in [J/Kg K].

- T is the temperature in [°F].

- T_b is the boiling temperature in Rankine.

- K_w is the Watson Factor.

$C_{\text{p, w}}$ is calculated from "XSteam.m" [29].

The mixture specific heat capacity is calculated based on a weight average:

$$C_{\text{p, mix}} = \frac{\rho_o \cdot q_o \cdot C_{\text{p, o}} + \rho_w \cdot q_w \cdot C_{\text{p, w}} + \rho_g \cdot q_g \cdot C_{\text{p, g}}}{\rho_l \cdot q_l + \rho_g \cdot q_g} \tag{A.42}$$

B. Pressure drop calculations ("dpBeggs_Brill.m")

The Beggs and Brill method is supposed to be able to calculate pressure gradients in pipes for multiphase flow for all pipe inclinations and flow regimes. The Beggs and Brill model is used in the Remso software and thus also used in this solver in order to get similar results. Note that all rates and properties in this section are local (not surface), and that all units are in SI Units, if not specified otherwise. The entirety of Appendix B eferenced to the pressure loss calculations at fekete.com [15].

Local superficial velocities are defined by:

$$v_{si} = \frac{q_i}{\pi \left(\frac{ID}{2}^2 \right)} \tag{B.1}$$

$$v_m = v_{sl} + v_{sg} \tag{B.2}$$

Where:

- v_{si}, $i \in (g, l)$, is the superficial velocities of gas and liquid [m/s].

- q_i is the (input) local fluid rates [m^3/s].

- ID is the Inner pipe Diameter, specified in the "main.m" script by the user.

The no-slip liquid holdup is then calculated by:

$$\lambda_l = \frac{v_{sl}}{v_m} \tag{B.3}$$

The following parameters are defined and used in the later calculations:

$$N_{fr} = \frac{v_m^2}{g \cdot ID} \tag{B.4}$$

$$L_1 = 316 \cdot \lambda_l^{0.302} \tag{B.5}$$

$$L_2 = 0.0009252 \cdot \lambda_l^{-2.4684} \tag{B.6}$$

$$L_3 = 0.1 \cdot \lambda_l^{-1.4516} \tag{B.7}$$

$$L_4 = 0.5 \cdot \lambda_l^{-6.738} \tag{B.8}$$

Where:

- N_{fr} is the Froude number, a dimensionless number defined as the ratio of the flow inertia to the external field.

- g is the gravitational constant (=9.81 m/s^2).

- $L_{1,2,3,4}$ are parameters used to define the flow regime.

Calculation of the liquid (slip) holdup based on flow regime

The Beggs and Brill method separates the flow into four regimes after the following criteria:

1. **Segregated flow:** $\lambda_l \leq 0.01$ and $N_{fr} < L_1$, or $\lambda_l \geq 0.01$ and $N_{fr} < L_2$

2. **Transitional flow:** $\lambda_l \geq 0.01$ and $L_2 < N_{fr} \leq L_3$

3. **Intermittent flow:** $0.01 \leq \lambda_l < 0.4$ and $L_3 < N_{fr} \leq L_1$, or $\lambda_l \geq 0.4$ and $L_3 < N_{fr} \leq L_4$

4. **Distributed flow:** $\lambda_l < 0.4$ and $N_{fr} \geq L_1$, or $\lambda_l \geq 0.4$ and $N_{fr} > L_4$

For the segregated, transitional and intermittent flow the following formulas may be used:

$$y_{l0} = \frac{a \cdot \lambda_l^b}{N_{fr}^c} \tag{B.9}$$

$$y_{l0} \geq \lambda_l \tag{B.10}$$

$$N_{vl} = 1.938 \cdot v_{sl} \cdot \left(\frac{\rho_l}{\sigma_l}\right)^{\frac{1}{4}} \tag{B.11}$$

$$C = (1 - \lambda_l) \cdot \ln\left(d \cdot \lambda_l^e \cdot N_{vl}^f \cdot N_{fr}^g\right) \tag{B.12}$$

$$\psi = 1 + C\left[\sin(1.8 \cdot \theta) - 1/3 \cdot \sin^3(1.8 \cdot \theta)\right] \tag{B.13}$$

$$y_l = y_{l0} \cdot \psi \tag{B.14}$$

Where:

- y_l is the resulting liquid holdup (with slip).

- σ is the liquid surface tension (=50 Dyn/cm, correlation should be implemented).

- N_{vl} is the liquid velocity number (Field Units used in this formula).

With the constants a, b, c, d, e, f and g given from the following tables:

Flow Regime	a	b	c
Segregated	0.98	0.4846	0.0868
Intermittent	0.845	0.5351	0.0173
Distributed	1.065	0.5824	0.0609

Flow Regime	d	e	f	g
Segregated Uphill	0.011	-3.768	3.539	-1.614
Intermittent Uphill	2.96	0.305	-0.4473	0.0978
Distributed Uphill				
All regimes Downhill	4.70	-0.3692	0.1244	-0.5056

For distributed uphill regime, $C = 0$ and $\psi = 1$. For transitional flow, the liquid holdup is calculated by interpolation of the segregated and intermittent equations:

$$A = \frac{L_3 - N_{\text{fr}}}{L_3 - L_2} \tag{B.15}$$

$$B = 1 - A \tag{B.16}$$

$$y_{\text{l, trans}} = A \cdot y_{\text{l, seg}} + B \cdot y_{\text{l, int}} \tag{B.17}$$

The mixture densities may now be calculated using:

$$\rho_{\text{ns}} = \lambda_l \cdot \rho_l + (1 - \lambda_l) \cdot \rho_g \tag{B.18}$$

$$\rho_{\text{m}} = y_l \cdot \rho_l + (1 - y_l) \cdot \rho_g \tag{B.19}$$

Where:

- ρ_{ns} is the average fluid density (no-slip).

- ρ_{m} is the fluid mixture density (slip).

Calculation of pressure gradients

The total pressure drop gradient for a given point in a pipe is the sum of the frictional, gravitational (potential) and acceleration pressure drop gradients:

$$\frac{\delta p_{\text{tot}}}{\delta L} = \frac{\delta p_{\text{fric}}}{\delta L} + \frac{\delta p_{\text{grav}}}{\delta L} + \frac{\delta p_{\text{acc}}}{\delta L} \tag{B.20}$$

First the no-slip Reynold number is calculated using:

$$\text{Re}_{\text{ns}} = 1000 \cdot \frac{\rho_{\text{ns}} \cdot v_m \cdot \text{ID}}{\mu_{\text{ns}}} \tag{B.21}$$

Where:

- $\mu_{\text{ns}} = \lambda_l \cdot \mu_l + (1 - \lambda_l) \cdot \mu_g$ is the average fluid viscosity (no-slip) [cp].

The no-slip friction factor for a smooth pipe ($\epsilon/\text{ID} = 0$) is then calculated using:

$$f_{\text{ns}} = \frac{1}{\left\{ 2 \cdot \log_{10} \left[\frac{\text{Re}_{\text{ns}}}{4.5223 \cdot \log_{10}(\text{Re}_{\text{ns}}) - 3.8215} \right] \right\}^2} \tag{B.22}$$

Based on experimental data, Beggs and Brill presented a correlation for the ratio of the two-phase friction factor (f_{tp}) and the normalizing (no-slip) friction factor resulting in the following equation:

$$\frac{f_{\text{tp}}}{f_{\text{ns}}} = e^S \tag{B.23}$$

The value of S depends on the no-slip and the actual liquid holdup:

$$x = \frac{\lambda_l}{y_l^2} \qquad \text{(B.24)}$$

$$S = \frac{\ln(x)}{-0.0523 + 3.182 \cdot \ln(x) - 0.8725 \cdot [\ln(x)]^2 + 0.01853 \cdot [\ln(x)]^4} \qquad , x \leq 1 \text{ or } x \geq 1.2 \quad \text{(B.25)}$$

$$S = \ln(2.2 \cdot x - 1.2) \qquad , 1 < x < 1.2 \qquad \text{(B.26)}$$

Finally the frictional and gravitational pressure gradients can be calculated using:

$$\frac{\delta p_{\text{fric}}}{\delta L} = \frac{f_{\text{tp}} \cdot \rho_{\text{ns}} \cdot v_m^2}{2 \cdot \text{ID}} \qquad \text{(B.27)}$$

$$\frac{\delta p_{\text{grav}}}{\delta L} = g \cdot \rho_m \cdot \sin(\theta) \qquad \text{(B.28)}$$

Where:

- θ is the pipe inclination.

No suitable model for the acceleration pressure gradient was found for this model. This gradient is usually very small compared to the other gradients, and ignoring it should not have a major impact on the calculations.

C. Newton-Raphson method

The Newton-Raphson method is used to find the x-value that drives the function f(x) to zero. The method is based on the Taylor series where:

$$f(x + \Delta x) = f(x) + \frac{\delta f(x)}{\delta x} \cdot \Delta x + O(\Delta x^2) \tag{C.1}$$

The objective is to find a Δx that yields $f(x + \Delta x) = 0$, so that:

$$0 = f(x) + \frac{\delta f(x)}{\delta x} \cdot \Delta x + O(\Delta x^2) \tag{C.2}$$

$$\Delta x = -\frac{f(x)}{\left(\frac{\delta f(x)}{\delta x}\right)} + \frac{O(\Delta x^2)}{\left(\frac{\delta f(x)}{\delta x}\right)} \tag{C.3}$$

Omitting the error term and defining $\Delta x = x_{i+1} - x_i$, the Newton-Raphson formula becomes:

$$x_{i+1} = x_i - \frac{f(x_i)}{\left(\frac{\delta f(x_i)}{\delta x_i}\right)} \tag{C.4}$$

For the numerical scheme, δx_i is the Δx of the previous iteration, and $\delta f(x_i)$ is the function values at those x-values.

Similarly for a system of multiple equations $f(x) = [f_1(x) \dots f_N(x)]^T$ and multiple variables $x = [x_1 \dots x_N]^T$:

$$\begin{pmatrix} f_1(x + \Delta x) \\ f_2(x + \Delta x) \\ \vdots \\ f_N(x + \Delta x) \end{pmatrix} \approx \begin{pmatrix} f_1(x) \\ f_2(x) \\ \vdots \\ f_N(x) \end{pmatrix} + \begin{pmatrix} \frac{\delta f_1(x)}{\delta x_1} & \frac{\delta f_1(x)}{\delta x_2} & \cdots & \frac{\delta f_1(x)}{\delta x_N} \\ \frac{\delta f_2(x)}{\delta x_1} & \frac{\delta f_2(x)}{\delta x_2} & \cdots & \frac{\delta f_2(x)}{\delta x_N} \\ \vdots & \vdots & \ddots & \vdots \\ \frac{\delta f_N(x)}{\delta x_1} & \frac{\delta f_N(x)}{\delta x_2} & \cdots & \frac{\delta f_N(x)}{\delta x_N} \end{pmatrix} \cdot \begin{pmatrix} \Delta x_1 \\ \Delta x_2 \\ \vdots \\ \Delta x_N \end{pmatrix} \tag{C.5}$$

$$f(x + \Delta x) \approx f(x) + J_f(x) \cdot \Delta x \tag{C.6}$$

Where $J_f(x)$ is the Jacobian to the system of equations. The Newton-Raphson formula is then:

$$x_{i+1} = x_i - \frac{f(x_i)}{J_{f, i}} \tag{C.7}$$

For this solver, x is the oil or gas lift rate and f(x) is the Δp_{choke}. Multiple equations means that rates for multiple wells are being calculated simultaneously.

D. Optimizer: Sequential approach

The sequential approach first checks if any of the wells have a negative Δp_{choke}. If this is true then the well with the **most negative** Δp_{choke} is recalculated to find rates for this well that yields $\Delta p_{\text{choke, well}} = 0$. Then the next most negative well is corrected, and so on. When rates are changed in one well the Δp_{choke} of other wells will also change. For a standard network with not too high rates the Δp_{choke} of the other wells will increase and decrease with the Δp_{choke} of the well being calculated. Recalculating the well with lowest Δp_{choke} value first, moves the other Δp_{choke} values closer to zero than if any other well was recalculated first. In addition, when the first well has been recalculated, recalculation in other wells will further increase the Δp_{choke} in the well already recalculated. This increase will be as small as possible if the well with lowest Δp_{choke} is recalculated first.

When all Δp_{choke} values are positive, the well with the **most positive** Δp_{choke} that has been recalculated (i.e. has a reduced oil rate and/or a positive gas lift rate) is recalculated again to find $\Delta p_{\text{choke, well}} = 0$. Again, it makes sense starting with the most positive Δp_{choke} because the other wells will be most affected by recalculating this well.

This procedure is repeated until the system converges. When a well is recalculated the Optimizer first puts this well to its initial state with the initial formation rates and no gas lift. Tubing pressure is only changed for the well being recalculated.

As hinted to above, exceptions may occur when the rest of the Δp_{choke} values move in the same direction as the Δp_{choke} being calculated. For example, when the network consists of long horizontal sections (for instance the pipeline) where an increased gas lift rate significantly decreases the fluid density and the tubing head pressure for the well being calculated, but increases the pressure in the pipeline due to the increased fluid velocity. The result may be that Δp_{choke} of the well being calculated moves in the opposite direction of the Δp_{choke} of the other wells.

The procedure for finding the correct rates for a well is the following: First the maximum gas lift rate is tested to find a positive Δp_{choke}. If $\Delta p_{\text{choke}} > 0$, then an upper bound has been found and the Newton-Rahpson method [5] (Appendix C) can be used to find $\Delta p_{\text{choke}} = 0$ (i.e. where the line in figure 2.2 crosses the x-axis). If $q_{\text{gl, max}}$ yields a negative Δp_{choke}, the lift rate is reduced by a factor of 0.65 to check that the initial rate is not on the far right side of the graph in figure 2.2. This procedure is repeated three times. If the Δp_{choke} is still negative, the oil rate is reduced by a factor of 0.9 (to make sure the reduction is stable and will not put the rate on the far left side of figure 2.3) until a positive Δp_{choke} is found. The gas lift rate used further (and kept constant) is either $q_{\text{gl, max}}$ or any of the three reduced gas lift rates that first gave a positive Δp_{choke} with the reduced oil rate. Newton-Raphson is subsequently used to find the correct oil rate between the new-found lower bound and the initial rate.

---

[5]Initially interpolation of the datapoints was considered as a possible method in stead of NR, but this required to constantly keep track of a lot of data; slowing the program and making the code messy.
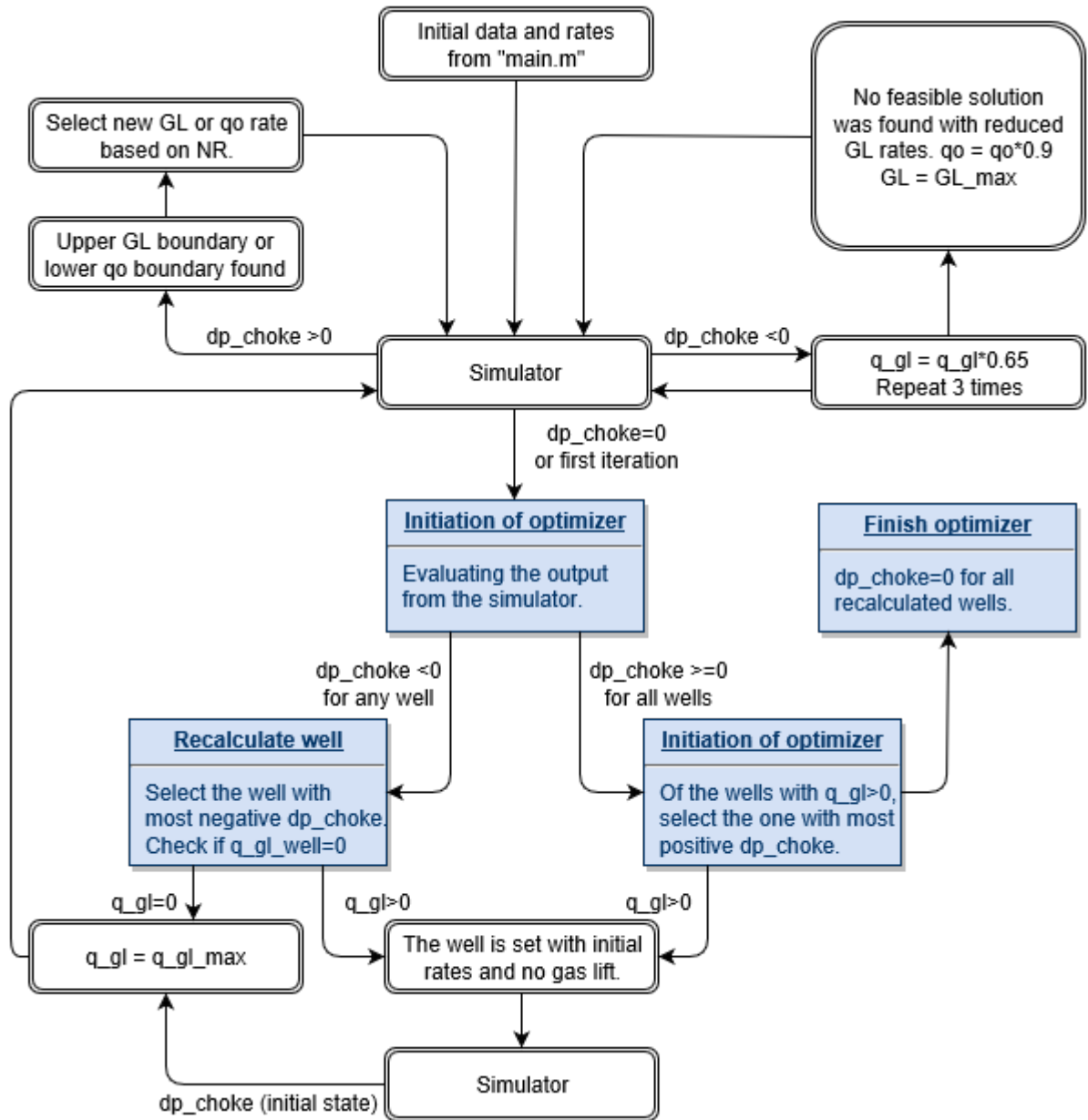
Figure D.1: Simplified flow chart of the Sequential approach ("GL_sequential_NR.m").

E. Optimizer: Parallel approach

The parallel approach has been created with the purpose of being a more formal and theoretical approach than the sequential one, using the Newton-Raphson method (Appendix C) to calculate gas lift rates and formations rate for all wells simultaneously.

In the first iteration the Simulator is run with original formation rates and no gas-lift. If any of the wells have a negative Δp_{choke}, the gas lift rates of these wells are set equal to $q_{\text{gl, max}}$ in the second iteration. The rest of the wells (with positive Δp_{choke}) are deactivated, i.e. excluded from further calculation, because no further changes in rates are to be done for these wells. Including these wells in the calculation would make the Jacobian singular.

For all further iterations the Newton-Raphson method will suggest gas lift rates that are either:

- $q_{\text{gl}} \leq 0$: Because the other wells provide enough total gas lift for this well to have $\Delta p_{\text{choke}} \geq 0$, and this well is then deactivated with $q_{\text{gl}} = 0$ and $q_o = q_{o,\text{init}}$.

- $0 < q_{\text{gl}} < q_{\text{gl, max}}$: An upper bound has been found and the Newton-Raphson method will continue to search for gas lift rates that yields $\Delta p_{\text{choke}} = 0$.

- $q_{\text{gl}} \geq q_{\text{gl, max}}$: I.e. the maximum rate is not high enough to provide a positive Δp_{choke}. The rate is further set to $q_{\text{gl}} = q_{\text{gl, max}}$ and reduced oil rate is found in stead.

When the solver searches for a reduced oil rate, it needs to find a lower bound that yields a positive Δp_{choke}. The first lower bound equals the initial oil rate times a factor of 0.9. Each time the Newton-Raphson formula suggests an oil rate lower than this bound, the lower bound is reduced by a factor of 0.9, and the oil rate is set equal to this value. This procedure is repeated until the Newton-Raphson formula suggests an oil rate that is higher than the previous one, and a valid lower boundary has been found.

Notice that, with this approach, it is possible for the Optimizer to calculate gas lift rates for some wells and reduced oil rates for other wells. The number of functions in the Newton-Raphson regime is always equal to the number of active wells, for instance a three-well network with a Newton-Raphson system with $\Delta p_{\text{choke 1}} = f_1(q_{\text{gl 1}}, q_{\text{o 2}})$, $\Delta p_{\text{choke 2}} = f_2(q_{\text{gl 1}}, q_{\text{o 2}})$ and well 3 is inactive.

For the Optimizer to calculate the Jacobian it needs to calculate the change in Δp_{choke} for all wells while changing the (gas lift or reduced oil) rate of one well, keeping the other wells with their old rates. This must be repeated for all active wells. Finally, the Δp_{choke} of all wells are calculated with all the new rates. This is computational expensive in a large network with many wells.
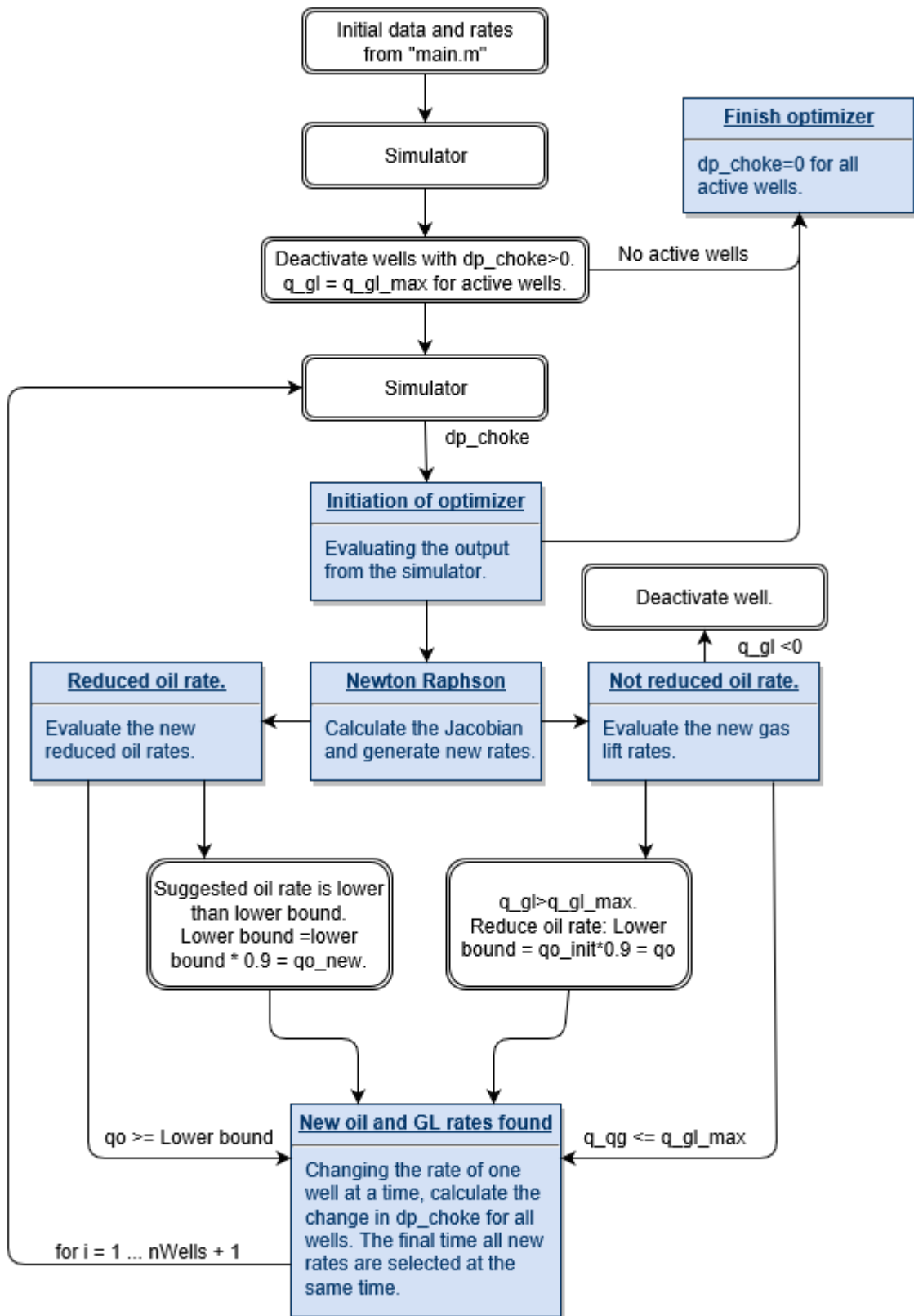
Figure E.1: Simplified flow chart of the Parallel approach ("GL_parallel_NR.m").

F. Standard Testing Conditions

Unless otherwise specified, all solver-examples generated in this report are run with these same conditions (fluid, reservoir and network properties). They are stated in the tables:

Reservoir, formation and network properties:

Property	Value	Unit
p_R	190	Bar
p_{sep}	7	Bar
p_{sc}	1.01325	Bar
T_{sc}	15.56	°C
T_R	100	°C
$q_{gl,\,max}$	$5 \cdot 10^4$	Sm^3/D (per well)
$q_{o,\,min}$	50	Sm^3/D
ID_{tubing}	5	inch
$ID_{flowline}$	$ID_{tubing} \cdot \sqrt{N_{wells\ in\ manifold}}$	inch
$ID_{pipeline\ and\ riser}$	$ID_{tubing} \cdot \sqrt{N_{wells\ in\ total}}$	inch
OD_{tubing}	$ID_{tubing} + 1$	inch
$OD_{flowline}$	$ID_{flowline} + 2$	inch
$OD_{pipeline}$	$ID_{pipeline} + 2.3$	inch
$OD_{ins,\,flowline}$	$OD_{flowline} + 0.066$	m
$OD_{ins,\,pipeline}$	$OD_{pipeline} + 0.066$	m
r_{ci}	$r_{o,\,tubing} + 4$	inch
r_{co}	$r_{co} + 0.8$	inch
r_{wb}	$r_{ci} + 2$	inch
roughness$_{all\ pipes}$	$2.54 \cdot 10^{-5}$	m
h_{sea}	200	$\frac{W}{m^2\,K}$
T_{sea}	6	°C
T_{steel}	43	°C
k_{ann}	0.383	$\frac{Btu}{hr\,ft\,°F}$
$C_{p,\,ann}$	1	$\frac{Btu}{lbm\,°F}$
$\mu_{p,\,ann}$	1	cp
$\rho_{p,\,ann}$	1	$\frac{Kg}{m^3}$
k_e	0.83	$\frac{Btu}{hr\,ft\,°F}$
k_{cas}	21	$\frac{Btu}{hr\,ft\,°F}$
k_{cem}	4.021	$\frac{Btu}{hr\,ft\,°F}$
α (Dif. Earth)	0.04	$\frac{ft^2}{hr}$

Fluid properties:

Property	Value	Unit
ρ_o	780	kg/Sm^3
ρ_w	1000	kg/Sm^3
M_g	19	kg/kg-mole
M_{gl}	25	kg/kg-mole
M_{air}	28.97	kg/kg-mole
h_{oil}	50	$\frac{W}{m^2\,K}$
h_{gas}	11	$\frac{W}{m^2\,K}$
$T_{b,\,oil}$	851	°R
$T_{b,\,gas}$	196.47	°R

Note that the IDs of the pipeline, the riser and the flowline are scaled to include flow from the given amount of wells through those pipes.

The code can easily be tuned to enable different GOR, $q_{gl,\,max}$, fluid properties etc. for individual wells. Multiple PLEMs may also be implemented without much difficulty, in the same manner as the manifolds are implemented.

F.1. Properties specific to Pipesim

Some additional properties are used only in Pipesim, and some properties are either calculated or specified differently in the Network Solver than in Pipesim. The different properties are the following:

Property	Value	Unit
$C_{p,\,earth}$	0.8373574	$\frac{J}{g\,K}$
ρ_{earth}	2242.5844	kg/m^3
$C_{p,\,g}$	2.3027329	$\frac{J}{g\,K}$
$C_{p,\,o}$	1.8840542	$\frac{J}{g\,K}$
$C_{p,\,w}$	4.186787	$\frac{J}{g\,K}$
k_{gas}	0.0345999	$\frac{W}{m\,K}$
k_{oil}	0.1384	$\frac{W}{m\,K}$
k_{water}	0,6054999	$\frac{W}{m\,K}$
Specific Latent heat of evaporation	325.63899	$\frac{J}{g}$

G. Fluid composition

The composition used with the Compositional Model (in molar fractions), along with the associated component specific properties are as follows:

Component	z	M	Pc	Tc	Vc	AF	Tb	Vol.trans.
	Mole Fraction	kg/kmol	bara	K	m3/kmol		Rankine	si=ci/bi
N2	0,0039	28,02	33,99	126,3	0,0901	0,0450	139,3	-0,1927
CO2	0,0206	44,01	73,82	304,2	0,0940	0,2310	350,4	-0,0817
C1	0,281	16,04	46,04	190,6	0,0993	0,0115	201	-0,1595
C2	0,0713	30,07	48,80	305,4	0,1479	0,0908	332,2	-0,1134
C3	0,085	44,09	42,49	369,8	0,2029	0,1454	416	-0,0863
i-C4	0,0307	58,12	36,48	408,2	0,2627	0,1756	470,6	-0,0844
n-C4	0,0304	58,12	37,97	425,2	0,2547	0,1928	490,8	-0,0675
i-C5	0,0225	72,15	33,81	460,4	0,3058	0,2273	541,8	-0,0608
n-C5	0,0203	72,15	33,69	469,7	0,3040	0,2510	556,6	-0,0390
n-C6	0,0345	86,17	30,12	507,4	0,3701	0,2957	615,4	-0,0080
n-C7	0,0498	100,20	27,36	540,3	0,4322	0,3506	668,8	0,0033
n-C8	0,0535	114,20	24,86	568,8	0,4920	0,3978	717,9	0,0314
n-C9	0,0365	128,30	22,89	594,6	0,5477	0,4437	763,1	0,0408
n-C10	0,0203	142,30	20,96	617,7	0,6031	0,4902	805,2	0,0655
C11	0,0195	156,30	19,65	638,9	0,6583	0,5349	844,272015	0,1010
C12	0,0198	170,30	18,2	658,3	0,7155	0,5622	880,970416	0,1149
C13	0,0198	184,40	17,2	675,6	0,7726	0,6231	915,442218	0,1277
C14	0,0153	198,40	16,2	691,7	0,8298	0,6797	947,984436	0,1392
C15	0,0152	221,40	15,2	706,7	0,8869	0,7060	978,78241	0,1563
C16	0,012	226,40	14,2	720,6	0,9441	0,7418	1007,892	0,1597
C17	0,0116	240,50	13,2	733,3	1,0012	0,7699	1035,53822	0,1689
C18	0,0114	254,50	12,1	745,0	1,0583	0,7895	1061,74622	0,1774
C19	0,0102	268,50	13,6	776,1	1,1155	0,8270	1086,83822	0,1854
C20	0,1049	282,60	11,1	767,2	1,1726	0,9070	1110,47223	0,1930

Figure G.1: Fluid composition with associated properties ("FluidProp.xlsx").

H. Computer Specifications

All simulations performed in this Thesis, with the exception of the Pipesim simulations, are done using the same computer. This to ensure that all the runtimes are comparable. The most important computer specifications are:

- Memory: 16 GB of RAM.

- Processor: 3,5 GHz Standard Frequency (Intel Core i5 6600K).